Two-stage Continual Reassessment Method and Patient Heterogeneity for Dose-finding Studies

Xiaoyu Jia

Submitted in partial fulfillment of the
requirements for the degree of
Doctor of Philosophy
under the Executive Committee
of the Graduate School of Arts and Sciences

COLUMBIA UNIVERSITY

2014

ABSTRACT

Two-stage Continual Reassessment Method and Patient Heterogeneity for Dose-finding Studies

Xiaoyu Jia

The continual reassessment method (CRM) is a widely used model-based design in Phase I dose-finding studies. This dissertation examines two extensions of CRM: one is a two-stage method and the other is a method that accounts for patient heterogeneity. Originally proposed in the Bayesian framework, CRM starts by testing the first patient at the prior guess of the maximum tolerated dose (MTD). However, there are safety concerns with this approach as practitioners often prefer to start from the lowest dose level and are reluctant to escalate to higher dose levels without testing the lower ones with a sufficient number of patients. This calls for a two-stage design, where the model-based phase is preceded by a pre-specified dose escalation phase, and the phase transitions when any dose-limiting toxicity (DLT) occurs. In the first part of this dissertation, I propose a theoretical framework to build a two-stage CRM based on the coherence principle and prove the unique existence of the most conservative and coherent initial design. An accompanying calibration algorithm is formulated to facilitate design implementation. We demonstrate that by using real trial examples, the algorithm yields designs with competitive performance compared to the conventional design which uses a much more labor intensive trial-and-error approach. Furthermore, we show that this algorithm can be applied in a timely and reproducible manner.

In addition to the two-stage method, we also take into account of patient's het-

erogeneity in drug metabolism rate that can result in different susceptibility to drug toxicity. This led to a risk-adjusting design for identifying patient-specific MTDs. The existing dose-finding designs which incorporate patient heterogeneity deal either with only categorical risk factor or with continuous risk factor using models based on strong parametric assumptions. We propose a method that uses a flexible semi-parametric model to identify patient-specific MTDs, adjusting for either categorical or continuous risk factor. Initially, our method assigns dose to patients using the aforementioned two-stage CRM ignoring any patient heterogeneity, and tests the risk effect as trial proceeds. It then transitions to a risk-adjusting stage only if sufficient risk effect on toxicity outcome is observed. The performance of this multi-stage design is evaluated under various scenarios, using dosing accuracy measures calculated based on the final model estimate at the end of a trial and on the intra-trial dose allocation. The results are compared to the conventional two-stage CRM without considering patient heterogeneity. Simulation results demonstrate a substantial improvement in dosing accuracy in scenarios where there are true risk effects on toxicity probability; and in situations where risk factors do not have an effect, the performance of the proposed method is also comparable to that of the conventional design.

Table of Contents

List of Figures

List of Tables

Acknowledgments

I like to thank my committee members for their support and help throughout the time period of this dissertation work. I like to thank Dr. Bin Cheng for his critical review and helpful comments. I like to thank Dr. Roger Vaughan and Dr. Shing Lee for their tremendous help, both mentally and academically. I would like to thank Dr. Kathy Panageas, Dr. Glenn Heller, and Dr. Mithat Gonen for their support. I would like to thank Dr. Colin Begg for reviewing partial work of this dissertation and his advice. My deepest appreciation goes to my dissertation advisor Dr. Ken Cheung, for his patience, guidance, and encouragement, and for introducing me to this fascinating research field. My most heartfelt thanks goes to my husband, Hai, for being my strongest ally for over 10 years and continue on.

Dedication text

Chapter 1

Introduction

1.1 Phase I dose-finding study

Clinical trials are controlled experiments conducted on human beings to evaluate the safety and effectiveness of new therapeutic regimen. They usually proceed through several stages: Phase I, II and III, each with a different purpose. Following pre-clinical and animal studies, Phase I trial is the first-in-human experiment, and it primarily focuses on the safety of the drug. Within the trial, a discrete number of doses of the experimental compound is studied, and one is identified as the *most appropriate* dose under the pre-specified toxicity constraint. This is the dose with a toxicity probability closest to the pre-specified target probability. It is also known as the maximum tolerated dose (MTD). The rationale behind this approach is that toxicities may serve as surrogate for tumor shrinkage in a patient undergoing cytotoxic cancer treatment [7]. Such Phase I dose-finding studies usually use sequential designs.

There are two classes of sequential designs: rule-based and model-based. Originally used in oncology clinical trials, rule-based designs, such as "3+3", were widely adopted in Phase I trials. These designs follow a pre-specified rule to assign dose to patients sequentially enrolled into the trial. Although simple enough, these designs are rigid and do not have the flexibility to respond to unexpected addition of pa-

tients or dose assignments. The design's operating characteristics depends arbitrarily on the underlying true dose-toxicity relationship and the MTD thus identified does not correspond to any interpretable quantity upon repeated sampling. While "3+3" method is considered safe, it has been criticized as over-conservative and tend to treat patients excessively on low and inefficacious dose levels.

After O'Quigley [20] proposed the continual reassessment method (CRM), model-based designs gained popularity. CRM approximates the true dose-toxicity relationship through an increasing dose-toxicity function indexed by a single parameter. Dose finding is formulated as a percentile estimation problem, in which, for a pre-specified target toxicity probability, it aims to identify the dose level with an estimated dose toxicity probability closest to this value; this is the dose at which the next patient will be treated. Model based estimate converges fast to MTD, thus treats more patients on the MTD than the "3+3" method. At the end of the trial, the data accumulated throughout will be used to obtain the final estimate on the dose-toxicity curve and the corresponding MTD.

1.2 Clinical Example: NeuSTART trial

The original CRM proposed by O'Quigley et al. in 1990 used the Bayesian framework, and it usually treats the first patient enrolled into a trial on a prior guessed MTD which is not necessarily the lowest dose level, and potentially skipping lower dose levels without testing them. This can raise safety concerns as investigators often prefer to start a trial from the lowest dose level and have a sufficient number of patients tested on each of these lower dose levels before escalating. A two-stage CRM design can be used to satisfy this requirement. In such a design, the trial starts from the lowest dose following a pre-specified dose assignment rule, and then switches to a model-based design using the conventional CRM after the first toxicity occurs. The following real trial example employed a two-stage design.

NeuSTART was a multi-center Phase I dose-finding study. Its objective was to determine the MTD of lovastatin for short-term acute stroke therapy [10]. The target dose toxicity probability was 10%, and there were 5 dose levels. This study enrolled 33 patients with acute ischemic stroke in the trial. Lovastatin was administered in increasing doses from 1 to 10 mg/kg daily for 3 days beginning within 24 hours after symptom onset (Table 1.1). The primary safety event was occurrence of myotoxicity or hepatotoxicity, defined by clinical and laboratory criteria, within a one month period after treatment.

The original trial design used a two-stage CRM. Before any dose limiting toxicities (DLT) occurred, the dose assignment followed a pre-specified dose escalation rule [10]: the first and the second group of 3 patients would be assigned on dose level 1 (1 mg/kg) and 2 (3 mg/kg), respectively, followed by 6 and 9 patients assigned on dose level 3 (6 mg/kg) and 4 (8 mg/kg), respectively. Twelve patients would be treated on the highest dose level 5 (10 mg/kg). The second stage is activated when a primary safety event is observed, at which time, the Bayesian CRM would be used to guide the subsequent dose escalation process. The design parameters used in both stages were determined using a trial-and-error approach described in Chapter 7 of Cheung 2011 [7].

1.3 Clinical Example: An oncology trial

The objective of this Phase I oncology trial was to determine an acceptable dose among the five dose levels for a combination therapy of Gemcitabine, Cabazitaxel and Cisplatin, to treat patients with non-muscle invasive bladder cancer via intravesical administration. Gemcitabine and Cabazitaxel were the standard components and Cisplatin was added as a third and experimental component. The dose of Gemcitabine was fixed at 2g in all five dose levels, and the doses of Cabazitaxel and Cisplatin are listed in Table 1.2. Cisplatin was only added on dose levels 3, 4, and 5. The toxicity

Table 1.1: Dose levels in NeuSTART trial.

Dose level	Lovastatin dose (mg/kg/day)
1	1
2	3
3	6
4	8
5	10

probabilities are expected to increase as dose level increases.

The MTD of this combination therapy is defined as the dose level associated with a target probability of toxicity at 25%. DLT is defined as any grade 3 or 4 systemic toxicity or any grade 3 or 4 hematuria, dysuria, urinary retention, urinary frequency/urgency, or bladder spasms using the NCI CTCAE version 4.0. Even though the three-drug combination regimens are of ultimate interest, and MTD is expected to be one of the three higher dose levels, physicians prefer to start the trial by examining the toxicity tolerance of the standard therapy without Cisplatin, i.e., dose level 1 and 2. This requires conducting a two-stage design.

The above examples illustrate several scenarios where a two-stage design is used in real world clinical studies. The major difference between a two-stage design and the conventional one-stage Bayesian CRM is that the model-based phase is preceded by a pre-specified escalation rule which dictates the initial dose escalation speed. The fact that model based design is postponed after the first DLT is observed provides an opportunity to use maximum likelihood estimation (MLE) rather than Bayesian estimation. While the Bayesian method requires the use of a prior distribution on

Table 1.2: Dose levels in the oncology trial.

Dose level	Cabazitaxel Dose	Cisplatin Dose
1	2.5mg	
2	5mg	
3	5mg	66mg
4	5mg	80mg
5	5mg	100mg

model parameters that may be perceived as subjective and arbitrary, the likelihood method does not have this limitation. However, two-stage designs open up new questions, e.g., how to choose a dose escalation sequence with an appropriate escalation speed before model-based design is activated?

1.4 Clinical Example: Irinotecan individual dosing trial

Conventional dose-finding studies usually identify a common MTD for all enrolled patients and infer that it is the MTD of the target study population. However, many risk factors such as treatment history and demographic characteristics are known to influence the individual patient's susceptibility to drug toxicity. A Phase I dose-finding study that considers additional risk factors and identifies patient-specific MTDs would lead to more accurate dose recommendations for subsequent Phase II and III clinical trials. Such individualized dosing strategy will reduce both over-dosing and under-dosing rates and optimize the drug's therapeutic effect. In addition, us-

ing a sequential design that considers individual differences in drug tolerability can directly benefit the patients participating in the study, as the feedback from the information accumulated during the trial can re-enforce the individualized dosing strategy and yield more accurate dose allocations for subsequently enrolled patients.

Phase I dose-finding oncology studies often recruit end-stage cancer patients who have failed standard therapies. The eligible patients could be fairly mixed in terms of disease status, types of cancer, demographic and pharmacogenetic characteristics. Analyses of multiple early phase clinical trials revealed that various patient characteristics compete with dose as the predictors of the treatment toxicity rate [25]. National Cancer Institute (NCI) accounts for the contribution of prior therapy by establishing separate phase II doses for heavily pre-treated from minimally pre-treated patients. Most clinical trials have already been practicing individualized dosing by administering doses adjusted for body surface area (BSA), a measure associated with weight and height. It was also observed in numerous studies that older patients are more likely to suffer from severe adverse events than younger patients.

Van der Bol et al. reported an individualized dosing trial for the drug irinotecan in cancer patients [30]. The metabolism of irinotecan involves several enzymes and drug transporters including members of the cyto-chrome P450 3A (CYP3A4) and uridine-diphosphate glucuronosyltransferase 1A (UGT1A) families. Both enzymes play an important role in clearing irinotecan, and hence, influence the level of its active form in human body. CYP3A4, in particular, competes with the irinotecan activation pathway and transforms irinotecan into inactive substrates. Meanwhile, UGT1A deactivates the active form of irinotecan. Because the expression and function level of these proteins could be affected by numerous environmental and genetic factors, the pharmacokinetics of irinotecan and its active form could vary greatly among patients. Such large inter-individual variability in the drug's clearance ability may result in over-treatment with unacceptable toxicities in some and under-treatment with diminished therapeutic effects in others. The trial focused on the heterogeneity

of irinotecan clearance and was designed to assess an individualized dosing algorithm based on a few baseline variables associated with irinotecan clearance. Both UTG1A1 genotype and age ($\leq$55 versus >55), as known confounders, were considered as stratifying factors, and patients were matched on the status of these two factors within each treatment group and each participating institution. The dose given to each individual was derived from the predicted irinotecan clearance based on a linear regression model of the historical data:

$$0.0325 \times \text{ midazolam clearance (ml/min)} - 0.0396 \times \gamma - \text{glutamyltransferase (units/L)}$$
$$+27.180 \times \text{ height(m)} - 31.926$$

where midazolam assay directly measures CYP3A4 activity, and γ-glutamyltransferase is a biomarker for liver function. The study was a two-arm randomized study powered by 50% inter-individual variability reduction of irinotecan concentration area under curve (AUC) in the individualized dosing arm compared to the control arm. In the treatment arm, each patient's predicted irinotecan clearance level is calculated using the above equation. And then the respective dose is calculated by multiplying the predicted clearance by 22.157 ($\mu g \times h/mL$), which was the mean concentration AUC of irinotecan observed previously and arbitrarily defined as the target measure of the systemic exposure for this study. Those patients in the control arm were given conventional doses based on BSA alone. Forty patients were randomized. Compared with the conventional dosing arm, the individualized dosing arm decreased the inter-individual variability in the AUC of irinotecan and its active form by 19% and 25%, respectively, but the differences were not significant. The incidence of grades 3 to 4 neutropenia/leukopenia was about 4 folds lower in the individualized dosing arm (p=0.013), and the incidence of grade 3 to 4 diarrhea was equal in both arms (10%). The results show that the baseline CYP3A4 activity, as determined by midazolam clearance, varied widely among enrolled patients: in a range of 203–1257 mL/min with a mean of 698 mL/min (95% confidence interval 609-786 ml/min). The dose range was much broader in the group using the individualized dosing algorithm (380-1060

Table 1.3: Multi-variable analysis on irinotecan data set.

	Any DLT		
Variable	log(OR)	95% CI	p value
Irinotecan clearance	-4.1	(-7.4,-0.8)	0.01
Dose	2.6	(-1.9,7.1)	0.3

vs 480-800 mg).

We pooled data from both arms and analyzed it using multi-variable logistic models. The binary toxicity endpoints include severe neutropenia, severe leukopenia, severe diarrhea and combined endpoint of any severe toxicities (grade ≥ 3). Since the irinotecan doses were determined by the predicted clearance level in half of the patients and by BSA in the other half, neither predicted clearance level and BSA were considered as covariates in the analyses. The variables of interest included in the models are log-transformed dose and log-transformed observed irinotecan clearance (measured by midazolam assay). Irinotecan clearance is significantly associated with the probability of severe leukopenia (p=0.02) and of any severe toxicities (p=0.01, Table 1.3), adjusting for dose. No significant non-linear effect or interaction effect was detected.

While this randomized study demonstrated interesting benefit of individualized dosing, its dose calculation relies on historical data, which may not always align with the data collected from the ongoing prospective study. It would be useful to conduct such trial using sequential design, so that the heterogeneity information on drug toxicity from early enrolled patients can be used to improve the dosing algorithm and yield more accurate dose allocation on subsequently enrolled patients.

As an outline of this dissertation, we will first review the basic components of CRM and the existing dose-finding designs that incorporate patient heterogeneity in Chapter 2. To address the two-stage design problem, in Chapter 3 we propose a theoretical framework based on the coherence principle and characterize each design component under this framework. In Chapter 4, we further derive a semi-automatic calibration algorithm to facilitate the implementation of our method in practical clinical settings and illustrate the application of the algorithm using NeuSTART trial and an oncology trial. Chapter 5 is devoted to address the patient heterogeneity issue in dose-finding studies using sequential designs. We propose a flexible multi-stage design to identify patient-specific MTDs adjusting for either continuous or categorical risk factors. Simulations are performed to illustrate the benefit of using this risk-adjusting design under various scenarios.

Chapter 2

Review of dose finding studies

2.1 Continual reassessment method

CRM was first introduced by O'Quigley et al. [20] as a model-based sequential method for dose finding studies. The basic idea of CRM is to assume a simple one-parameter dose-toxicity model, and repeatedly estimate the dose-toxicity curve with cumulated data collected from sequentially enrolled patients. The method appeals to clinicians because it attempts to treat the next patient at the current best estimate of the target dose [26], and has received much attention in the medical community [24; 18].

2.1.1 Basic components

We first describe the Bayesian version of the method. In a typical dose finding study, we observe a pair of data (x_i, y_i) on the i'th patient enrolled in the trial, for $i = 1, \ldots, N$, where x_i denotes the dose assigned to the patient i, and y_i denotes the binary toxicity indicator of the patient. The choice of dose x_i is confined to a discrete panel of dose levels, $d_1, \ldots, d_K$. Dose finding is often formulated as a percentile estimation problem, that is, for a pre-specified probability θ, we aim to identify $\nu = \arg\min_k |\pi(d_k) - \theta|$, where $\pi(x) = \mathrm{pr}(y_i = 1 \mid x_i = x)$ is the true

probability of toxicity at dose x [7]. CRM approximates $\pi(x)$ through a dose-toxicity function $F(x, \beta)$ indexed by a single parameter β. The main idea of the method is to treat the next patient at a dose with a toxicity probability estimated to be closest to the target θ. Specifically, it sets $x_{i+1} = \arg\min_{d_k} |F(d_k, \hat{\beta}_i^B) - \theta|$, where $\hat{\beta}_i^B$ is the posterior estimate of β based on observations from the first i patients. The process is repeated until a pre-specified sample size N is reached.

An important point about the CRM is that the dose labels $d_1, \ldots, d_K$ are not the actual doses administered, but are values re-scaled to a domain that is compatible with the prior inputs to the model. More precisely, the dose label d_k is obtained by matching an initial guess of toxicity probability p_{0k} for the dose k using the dose-toxicity function $F(x, \beta)$ under the prior model-based estimate $\hat{\beta}_0^B$, that is, setting $p_{0k} = F(d_k, \hat{\beta}_0^B)$ where $\hat{\beta}_0^B$ denotes the prior mean of β. The set of initial guesses $\{p_{0k}\}$ is sometimes called the 'skeleton'. Ideally the skeleton is chosen based on clinical inputs to reflect the initial beliefs of the toxicity probability associated with the test doses. In practice, such information is rarely available from the clinical investigators, and as a result, if we believe ν_0 is the maximum tolerated dose level *a priori*, we will set $p_{0\nu_0} = \theta$, so that the starting dose $x_1 = d_{\nu_0}$ with $F(x_1, \hat{\beta}_0^B) = \theta$. Different skeletons may lead to very different operating characteristics. To avoid the subjectivity in the specification of a particular skeleton, Yin and Yuan [31] proposed specifying multiple skeletons, each representing a set of prior estimates of the toxicity probabilities. Using the Bayesian model averaging to even out the contributions of multiple skeletons into the sequential estimation procedure, this avoids the potential bias caused by only using one specific skeleton. Another pragmatic approach is to treat each p_{0k} as a model parameter and tune it so that CRM will yield good average operating characteristics [7]. However, this tuning problem can be a daunting task as there are K parameters in the skeleton and each has infinitely many possible values.

As an alternative to the Bayesian approach, O'Quigley & Shen proposed using maximum likelihood estimate in conjunction with CRM [21]. The idea is to

treat each subsequent patient at the model-based MTD $x_{i+1} = \hat{\nu}_i$ where $\hat{\nu}_i := \arg\min_{d_k} |F(d_k, \hat{\beta}_i) - \theta|$ and $\hat{\beta}_i$ is the maximizer of the likelihood based on the first i observations. Since the likelihood approach does not require specification of prior distribution of the model parameters, it addresses the perceived subjectivity of its Bayesian counterpart discussed previously. However, for a one-parameter dose-toxicity function F, since $\hat{\beta}_i$ exists if and only if there is heterogeneity in the toxicity outcomes in the first i observations, the trial requires an initial dose escalating sequence $\{x_{i,0}\}$ to determine dose assignments until $\hat{\beta}_i$ exists. Thus, a likelihood approach implies the use of a two-stage design, defined as $x_{i+1} = x_{i+1,0}$ if $Y_j = 0$ for all $j \leq i$, and $x_{i+1} = \hat{\nu}_i$ if $Y_j = 1$ for some $j \leq i$. As a result, a two-stage likelihood design allows starting a trial at the lowest dose level which also addresses the safety concern raised in one-stage Bayesian designs.

The idea of a two-stage design has been examined extensively by simulation [11; 13; 15]. In addition, Shen and O'Quigley [27] studied the large sample properties of the likelihood CRM and showed that it consistently estimates the MTD even when the assumed dose-toxicity model is incorrectly specified. Despite the theoretical advantages, the actual usage of a two-stage likelihood CRM is still quite limited primarily due to its complexity. First, as we no longer have a prior distribution of β, neither $\hat{\beta}_0^B$ nor ν_0 is available in the specification of the dose labels as described in the backward substitution procedure mentioned above. While Cheung 2011 [7] proved that MLE is invariant to the choice of the initial value $\hat{\beta}_0$ for a given dose-toxicity model, the role of the prior maximum tolerated dose ν_0 remains unclear in the likelihood approach. Second, the choice of the initial design sequence $\{x_{i,0}\}$ in practice is often ad hoc and lacks systematic orientation.

In finite sample setting, the choice of CRM design parameters can be crucial to its operating characteristics. First, it is quite plausible to specify a skeleton that can lead to pathological and poor design performance [27; 8]. Second, an unexamined choice of the initial dose sequence will cause dose escalations that are ethically unacceptable

(i.e., incoherent)[6]. Lastly, there is a lack of discussion on how to choose a dose-toxicity function. Overall, we need a systematic exposition on how to determine two-stage CRM design parameters given certain clinical objective and sample size. In the following chapters of this dissertation, in addition to solving the theoretical problems remaining in the two-stage likelihood CRM, we will also propose calibration algorithm to facilitate the choice of the design parameters to achieve satisfying performance.

2.1.2 Indifference interval and calibrated skeleton

CRM is proven to be consistent under certain model mis-specification but not generally. Cheung and Chappell (2002) found that certain models with inappropriate initial guess of dose toxicities can lead to pathological behavior. Suppose dose k is the MTD, an indifference interval associated with this dose level k can be defined as an interval $\theta \pm \delta_k$, within which, the toxicity probability of dose k will eventually fall into when the sample size is sufficiently large (δ_k denotes the half-width of the indifference interval). δ_k specifies the minimal distance in toxicity probability from dose k to its neighboring doses such that the doses can be correctly differentiated given a large enough sample size. For a specific CRM design, the indifference interval δ is defined as the union of the indifference intervals for each of the target doses $\nu \in \{2, \ldots, K-1\}$. CRM is said to have equi-indifference intervals if the length of the indifference interval is the same for all $\nu = 2, \ldots, K-1$.

While tuning for all K parameters p_{0k}'s is quite computationally extensive, Lee and Cheung (2009) developed an algorithm to calibrate the entire skeleton using only two parameters under the Bayesian framework. Given the prior belief that dose level ν_0 is the MTD, thus $p_{0,\nu_0} = \theta$, the algorithm specifies the choice of $\{p_{0k} : k \neq \nu_0\}$ to CRM with equi-indifference interval of δ. Using this algorithm, we only need to specify ν_0 and δ to construct a calibrated skeleton that guarantees the design would eventually select a dose with toxicity probability that falls within the interval of $\theta \pm \delta$. This algorithm reduces the number of model parameters from K to 2 for constructing

the skeleton.

The half-width indifference interval δ indicates the design resolution in large sample setting, i.e., the minimum distance of the target dose from its neighboring doses so that this target dose can be correctly selected as the MTD. This in turn can be used as a design tuning parameter to facilitate the design calibration in finite sample settings. A large δ value defines dose labels that are further apart from each other on the x-axis, hence indicating a working model with a steep slope, while a small δ value corresponds to a flat working model. In the Phase I clinical trial, we can use a series of working model with varying steepness via specifying a range of δ values, evaluate their model performance, and determine the optimal δ value for the given clinical scenario.

2.1.3 Coherence

For a two-stage CRM, the choice of an initial design also impacts the trial behavior. An inappropriately chosen dose-escalating sequence may lead to unethical dose assignment [6], and whether the dose assign is ethical or not is called the design's coherence property [6]. A coherent dose assignment indicates that if the current patient experiences toxicity, the probability of dose escalation on the next patient is zero, i.e., $pr(x_i - x_{i-1} > 0 \mid y_{i-1} = 1) = 0$. Incoherence means the opposite. During the first stage, without toxicity, the dose escalation follows a non-decreasing dose escalation sequence, and thus, is coherent. The model-based dose assignment using CRM is also proven to be coherent [6]. However, Cheung (2005) pointed out that the transition point from first stage to the second stage during a two-stage trial may not be coherent, i.e., the first model-based dose assignment after observing the first toxicity is not necessarily coherent when the initial design is not chosen appropriately. In fact, an overly conservative (slow) initial design will cause incoherence in a two-stage CRM.

Although incoherence in a two-stage design is a single point problem, which can only occur on the first model-based dose assignment upon observing the first toxicity,

the complexity of this problem is that it is unknown where the first toxicity would occur during a dose-finding study using sequential design. If a two-stage trial enrolls a total of N patients, presumably there are up to N different scenarios where the first toxicity could occur, and a two-stage CRM is called coherent only if it is coherent across *all* N scenarios.

The first part of this dissertation is intended to introduce a unified framework to build a coherent two-stage CRM using likelihood approach. A comprehensive calibration algorithm will be proposed and recommendations on design parameters under various clinical scenarios will be made based on this framework.

2.2 Dose finding studies with patient heterogeneity

2.2.1 O'Quigley's two-group CRM

O'Quigley et al. [22; 19] proposed two-parameter CRM models to identify group-specific MTDs for patients belonging to high and low risk groups simultaneously in a single trial. In addition to the parameter indicating the slope of the dose-toxicity curve, another model parameter is introduced to represent the group effect on the dose-toxicity curve. Below is the two-parameter empiric function:

$$F(y_i = 1 | x_i = d_k : z_i) = d_k^{\exp(a+bz_i)}$$

with y_i, x_i, z_i indicating binary toxicity outcome, assigned dose level, and risk group ($z_i = 1$ high risk and $z_i = 0$ low risk for instance) for each patient, respectively. The assigned dose level x_i takes a value of d_k ($k = 1, \ldots, K$). Both groups share the same K dose levels. The group effect is represented by b, and when $b = 0$, it indicates there is no group difference, and all patients in both groups have the same toxicity tolerance and thus share the same MTD. In real trial setting, even though we acknowledge the group difference, we might not know which group has higher tolerance. In their first

paper in 1999, O'Quigley et al. [22] assumed no prior knowledge on the magnitude and direction of the difference between the two risk groups, and employed a two-stage design. An arbitrary initial design was installed to allow independent dose escalation in each group. Once the first toxicity is observed in one group, the usual one-sample CRM $F(y_i = 1|x_i = d_k) = d_k^{\exp(a)}$ will be used to assign the dose to the next patient of the same group, and the dose escalation in the other group will still follow the initial design. Once toxicities are observed in both risk groups, all data are pooled to fit the two-parameter CRM model and model-based dose assignment will proceed within each group.

O'Quigley and Paoletti [19] modified this two-group CRM design by incorporating the prior knowledge on direction of the difference between the two risk groups. First, instead of allowing independent dose escalation between the two risk groups during initial design, the patients belonging to the low risk group are always assigned at a dose level greater than or equal to the current dose level in the high risk group, because low risk group is supposed to have higher drug tolerance level according to the prior knowledge. Such initial design allows skipping doses in one group (low risk group) but not the other (high risk group). However the escalation rule is still arbitrarily determined. Second, Bayesian method was used to estimate parameters a and b, with non-informative prior for a and normal prior for b with mean μ_b and standard error σ_b. μ_b and σ_b can be determined to reflect the uncertainty on the magnitude or even direction of the ordering between the two risk groups.

2.2.2 Bivariate isotonic design

Ivanova and Wang [14] proposed a bivariate isotonic design for ordered risk groups. In addition to satisfy the assumption of non-decreasing dose-toxicity relationship within a group, i.e., $\hat{p_{j1}} \leq \cdots \leq \hat{p_{jK}}$, where $j = 1, 2$ indicating the risk group, the dose-toxicity probability estimates are also subject to between group constraint $\hat{p_{2k}} \leq \hat{p_{1k}}, k = 1, \ldots, K$, if group 2 is believed to have lower toxicity rate than group

1, and vice versa. If no prior knowledge is available on ordering of risk groups, the squared difference between bivariate isotonic estimates and observed dose-toxicity probabilities are computed under both scenarios and the constrained estimator with the smaller squared difference is chosen as the best estimate. For example, the squared difference is

$$M^{(2,1)} \equiv \sum_{j=1}^{2} \sum_{k=1}^{K} (p_{jk}^{(2,1)} - \hat{p_{jk}})^2$$

where $p_{jk}^{(2,1)}$ is the result of bivariate isotonic regression estimate, assuming group 2 has higher tolerance to toxicity. In case $M^{(1,2)} = M^{(2,1)}$, the univariate isotonic estimate of toxicity is obtained from the combined sample. The dose allocation rule for the next patient is as follows: stay on current dose if the estimated toxicity probability of the current dose is within $\theta \pm \Delta$, and escalate/de-escalate if otherwise, where Δ is a design parameter. Without prior knowledge on group orderings, the trial starts with two independent initial designs similar to the one used in O'Quigley et al. 1999 [22]. With known group orderings, the design uses the informative initial design in O'Quigley and Paoletti 2002 [19]. After toxicity is observed, the trial proceeds following the dose allocation rule based on the bi-variate isotonic estimate.

2.2.3 Escalation with overdose control (EWOC)

Babb and Rogatko proposed EWOC method in 1998 [2]. The method controls the overdose probability during the sequential design using CRM. Comparing to the standard CRM which chooses a dose with minimum absolute distance to target toxicity rate, EWOC essentially chooses a dose via minimizing a risk function that has asymmetric weights on overdose and underdose, i.e., a risk function that has more stringent control on overdose probability. In their 2001 paper [3], they extended EWOC to guide individualized dosing for dose-finding study, given continuous risk-modifying factor and continuous dose. In the clinical example illustrated in the paper, the patient's individual tolerance to the experimental drug PNU is modified by endogenous plasma

anti-SEA antibody concentration due to its neutralizing effect on the experimental drug. Higher anti-SEA concentration is associated with higher tolerance and higher dose. A two-parameter logistic model was used to model continuous dose (x) and anti-SEA level (c), in relation to toxicity probability $pr_c(x)$.

$$\text{logit}[pr_c(x)] = \alpha + \beta \ln(x) + \delta \ln(c)$$

It is assumed that $\beta > 0$ and $\delta < 0$, so that the probability of DLT is an increasing function of dose and a decreasing function of anti-SEA concentration. The MTD can be expressed as a function of anti-SEA concentration c and denoted as $\gamma(c)$, which results in toxicity probability equal to $\theta = 0.1$. After observing data from the first i patients, the next optimal dose $x_{i+1}(c)$ is determined such that the overdose probability, i.e., the probability of assigning a dose greater than anti-SEA concentration adjusted MTD, is less than a pre-specified threshold value $1-\omega$. The real trial example designed using this method show that patients with high baseline anti-SEA have robust tolerance to high doses of the experimental drug PNU.

2.2.4 Other model-based designs

Piantadosi and Liu [23] proposed to incorporate the pharmacokinetics parameter in the CRM model to improve the dosing accuracy, and employed a bivariate logistic dose-toxicity model as shown below. In addition to dose, a continuous covariate: Δ_{AUC}, is included into the model. $\Delta_(AUC)$ is the difference between estimated pharmacokinetics parameter area under curve (AUC) and the observed AUC, which is considered ancillary to dose administered.

$$\text{logit}(pr(dose, \Delta_{AUC})) = \beta_0 - \beta_1 \times dose - \beta_2 \times \Delta_{AUC}$$

The method imposes a joint uniform prior distribution on the two parameters. After obtaining their posterior estimates, the optimal dose to be assigned to the next patient can be solved by inserting the parameter estimates into the above formula and setting

the predicted difference (δ_{AUC}) at zero, i.e., $dose_{i+1} = (\hat{\beta_{0i}} - \text{logit}(\pi))/\hat{\beta_{1i}}$, where π is the target toxicity probability.

Thall et al. [29] extended the dose finding method based on toxicity-efficacy trade-off to account for additional covariate effect. The method imposes an informative prior on covariate effect parameters obtained from preliminary fit of historical data and a non-informative prior on dose-toxicity model parameter. Putting aside the model complexity due to bivariate endpoints, the model on the toxicity endpoint for patients observed during the trial is

$$\text{logit}(pr(x, Z)) = f(x, \alpha) + \beta Z + x\gamma_k Z$$

This model is more complex because it not only has the main effect terms of dose $f(x, \alpha)$, covariate βZ, but also the interaction term between dose and covariate $\gamma_k Z$. For cytotoxic agent, the main dose effect can be specified as linear function $f(x, \alpha) = \alpha_0 + \alpha_1 x$ where $\alpha_1 > 0$ indicating that toxicity probability increases as dose x increases. The prior distribution of covariate effect β is obtained from analysis on the historical data. In contrast, the method keeps the prior of $(\alpha_0, \alpha_1, \gamma)$ as non-informative since they are associated with the effects of the experimental dose. In the application example, the authors grouped the continuously measured covariate into high, medium and low risk groups before applying the method.

2.3 Limitations of existing methods

Bayesian approach has many advantages and been widely adopted in clinical trial designs. However it is still perceived as subjective compared to MLE. As illustrated in the papers dealing with two risk group design [21; 22; 14], mis-specified priors on the group ordering parameters may slow down the algorithm convergence, or even lead to incorrectly determined MTD. In more complicated designs such as dose finding with multiple risk groups, more parameters need cautious justification on their prior distributions. The computational complexity is also a prominent issue with Bayesian

method. Non-informative priors are usually considered equivalent to MLE, however, the computation could be much more intensive than MLE.

MLE avoids subjectivity and is often computationally economical, but requires an initial design to specify dose escalation before heterogeneous toxicity outcome occurs and model based method is activated. Dose escalation without observing toxicity outcomes is subject to ethical constraint that has two operationally conflicting guidelines. Escalation is expected to proceed cautiously and not to overshoot the target and put an unacceptably large number of patients at risk for toxic side effects. Meanwhile, it is also desired to avoid treating too many patients at levels so far below the target that the probability of seeing any treatment benefit is almost negligible. The initial designs adopted in the reviewed literature [21; 22; 14] follow an arbitrary escalation rule without sufficient justification from these perspectives.

Bivariate isotonic design is difficult to be extended to deal with continuous risk factor. A more fundamental problem with this type of curve-free design is "rigidity", as pointed out by Cheung [5]. Due to lack of shared information across doses, when target toxicity probability is low, the curve-free design may be confined to a low dose and never escalate no matter how many more non-toxic outcomes observed. A dose-finding study incorporating patient heterogeneity would likely deal with low toxicity rate in one or multiple risk groups, suggesting the curve free method maybe inefficacious for such purpose.

O'Quigley's two-group CRM [22] and Thall's individualized dosing on bivariate outcome [29] deal with the categorical covariates. These methods can be extended to multiple risk groups, which work for risk factors that are naturally measured in discrete form such as heavily pre-treated versus treatment-naive patients. However, it cannot be immediately applied on continuous risk factors as most newly identified laboratory biomarkers through genomic or proteiomic studies. Oftentimes investigators may have knowledge on whether and how a biomarker influences patient drug tolerance but reluctant to group the patients into high risk or low risk groups based

on a specific cut-off value. In small sample study, information preservation by keeping variable continuous and not dichotomizing it could potentially enhance design performance. In such situation, it is desirable to develop a design that has the flexibility to adjust for both continuous and categorical covariates.

Two-parameter EWOC [2] deals with both continuous dose and continuous covariate (anti-SEA concentration) using two-parameter parametric model. However, the method is difficult to be generalized and adopted by other studies as it requires much effort to specify the design parameters for each individual study.

The existing designs reviewed in this chapter deals with the risk factors that are known to have effect on toxicity probability and incorporates this knowledge into the design. However, the designs are less flexible in handling the opposite situation where the risk factor turns out not affect the toxicity outcome in a particular trial. We will propose a multi-stage design that evaluates the effect of risk factor on the toxicity probability as trial goes on, and only allows adjusting individual risk factor when the effect is evident.

Chapter 3

Design components for two-stage Likelihood CRM

To fully specify a two-stage likelihood CRM, we need to determine 1) a dose escalating sequence $\{x_{0,i}\}$ in the first stage (initial design) to dictate the dose assignments for initially enrolled patients before any DLT is observed, and 2) a working model to be used to guide the dose escalation in the second stage, whereas the model parameter β can be repeatedly estimated using accumulated data collected in the sequential experiment to provide updated estimate on dose toxicity probabilities. Furthermore, to fully specify a working model in the second stage, we need to determine, firstly the dose-toxicity function to be used to approximate the true dose-toxicity relationship, along with the initial value for the slope parameter β, i.e., β_0, and the initial estimate of toxicity probability on each dose level, i.e., p_{0k}. With these initial values, the dose labels can be determined using backward substitution and the sequentially collected observed data can be used to obtain the updated model parameter estimate, which then can be further used to obtain the updated model based estimates of dose toxicity probabilities at each dose level.

In this chapter, we will characterize each of the three design components under our proposed framework. We will start from the two design components required in

the second stage model based design: dose-toxicity functions and specification of the initial estimate of the dose toxicity probabilities, and then we will focus on how to choose appropriate initial design. Theoretical results will be derived.

3.1 The Dose-toxicity model

3.1.1 ψ-equivalent functions

The CRM models the dose-toxicity relationship by a one-parameter function $F(.,\beta)$. The two commonly used dose-toxicity models in the CRM literature are the empiric function

$$F(x,\beta) = x^{\exp(\beta)} \text{ for } 0 < x < 1$$

and the one-parameter logistic function

$$F(x,\beta) = \frac{\exp(a_0+\beta x)}{1+\exp(a_0+\beta x)} \text{ for } -\infty < x < \infty$$

with a fixed intercept a_0; see [9; 13; 21] for example. Other functions often considered include a hyperbolic tangent function [20] and a one-parameter logistic function with a fixed slope [27].

Since the use of one-parameter function is not common in other statistical applications, the theory in this area is quite scattered. In this article, we provide a systematic study of the following class of dose-toxicity functions in the context of the CRM:

Consider the class of one-parameter functions

$$F(x,\beta) = \psi\{c(\beta)h(x)\}$$

where ψ, c, h are known functions that are strictly monotone [7].

This class includes the most commonly used dose-toxicity functions such as the empiric function and a one-parameter logistic function in the dose-finding literature [12].

For example, the empiric function can be expressed as $F(x, \beta) = \exp\{\exp(\beta)\log(x)\}$, with $\psi(\cdot) = \exp(\cdot)$, $c(\cdot) = \exp(\cdot)$, and $h(\cdot) = \log(\cdot)$.

Suppose that we can specify a skeleton $\{p_{0k}\}$ and an initial parameter value $\hat{\beta}_0$ so that the dose labels d_ks are obtained by solving $p_{0k} = F(d_k, \hat{\beta}_0) = \psi\{c(\beta)h(x)\}$, and $d_k = h(x) = \psi^{-1}/c(\beta_0)$. Then, the dose-toxicity model can be rewritten as

$$F(d_k, \beta) = F_k(\beta) = \psi\left\{\frac{c(\beta)}{c(\hat{\beta}_0)}\psi^{-1}(p_{0k})\right\} \tag{3.1}$$

which does not depend on the function $h(x)$. Furthermore, Theorem 4.1 in [7] shows that, for a given skeleton $\{p_{0k}\}$, the maximum likelihood CRM is invariant among the dose-toxicity functions represented by the same ψ function, regardless of the choice of $c(\cdot)$ and $\hat{\beta}_0$. Hence, we can arbitrarily set $c(\beta) = \exp(\beta)$ and $\hat{\beta}_0 = 0$ without loss of generality, and the ψ-representation of the dose-toxicity model (3.1) can be simplified as

$$F_k(\beta) = \psi\left\{\exp(\beta)\psi^{-1}(p_{0k})\right\} \tag{3.2}$$

Two dose-toxicity functions are said to be ψ-equivalent if they can be represented by the same ψ. For example, consider one-parameter logistic function with fixed slope a, $F_a(x, \beta) = \{1 + \exp(-\beta - ax)\}^{-1}$. Since the function class $\{F_a(x, \beta) : a > 0\}$ can be represented with $\psi(z) = z/(1 + z)$ that is free of a, all functions in this class are ψ-equivalent. It is immediately clear how the ψ-representation offers great simplification in the model calibration problem; in the above example, for instance, it suffices to consider F_a for a given and arbitrary choice of a. In addition, it allows us to systematically expand the scope of the dose-toxicity functions for the CRM. Other functional forms for modeling binary outcome such as complementary log-log and probit functions can be conveniently summarized using this representation. Table 3.1 lists some commonly used dose-response models.

Table 3.1: Dose-toxicity models generated by some common ψ.

Model	$\psi(z)$	$F_k(\beta)$
Empiric	e^z	$p_{0k}^{\exp(\beta)}$
Complementary log-log		
with intercept a	$1-e^{-\exp(az)}$	$1-e^{-\exp(a+e^{\beta}[\log\{1-\log(1-p_{0k})\}-a])}$
with fixed slope	$1-e^{-z}$	$1-(1-p_{0k})^{\exp(\beta)}$
Logistic		
with intercept a	$(1+e^{-a-z})^{-1}$	$\frac{\exp\left[a+e^{\beta}\{\mathrm{lgt}(p_{0k})-a\}\right]}{1+\exp\left[a+e^{\beta}\{\mathrm{lgt}(p_{0k})-a\}\right]}$
with fixed slope	$(1+z^{-1})^{-1}$	$\frac{\exp(\beta)p_{0k}}{1-p_{0k}+\exp(\beta)p_{0k}}$
Probit		
with intercept a	$\Phi(a+z)$	$\Phi\left[a+\exp(\beta)\{\Phi^{-1}(p_{0k})-a\}\right]$
with fixed slope	$\Phi\{\log(z)\}$	$\Phi\left\{\beta+\Phi^{-1}(p_{0k})\right\}$

$\mathrm{lgt}(p)=\log\{p/(1-p)\}$; Φ is the cumulative distribution function of standard normal.

3.1.2 The skeleton and the irrelevance of ν_0

For a given ψ-class dose-toxicity function with $c(\beta)=\exp(\beta)$ and $\hat{\beta}_0=0$, skeleton $\{p_{0k}\}$ can be specified using an algorithm described in [7]: After specifying ν_0 and δ, set $p_{0\nu_0}=\theta$, p_{0k} can be determined recursively such that the skeleton satisfies

$$\psi^{-1}(p_{0,k+1})\psi^{-1}(\theta-\delta)=\psi^{-1}(p_{0k})\psi^{-1}(\theta+\delta) \text{ for } k=1,\ldots,K-1. \tag{3.3}$$

Since ψ is strictly monotone, the skeleton thus obtained is unique and strictly increasing. Algorithm (3.3) requires the specification of δ, the half-width of the design's indifference interval [8]; that is, the design will converge with probability one to a dose with toxicity probability falling onto the interval $\theta\pm\delta$. While δ, as an asymptotic design resolution, is only interpretable given large sample size, it can also serve as a design parameter in finite sample setting to be tuned to achieve satisfying design operating characteristics. Lee & Cheung [16] propose a numerical algorithm

to calibrate the skeleton p_{0k} via tuning δ under finite sample settings.

In addition to δ, algorithm (3.3) also requires the specification of the prior maximum tolerated dose ν_0. As we attempt to steer away from the Bayesian approach, the choice of ν_0 is artificial at best, and may appear subjective. Importantly, the choice of ν_0 does have an impact on the performance of the Bayesian method [7]. However, the following Theorem holds if using maximum likelihood method.

THEOREM 1. *Suppose that $F(x,\beta)$ and $F^*(x,\phi)$ are ψ-equivalent functions, and that the respective dose-toxicity models are obtained according to (3.2) with skeletons $\{p_{0k}\}$ and $\{p^*_{0k}\}$, that is, $F_k(\beta) = \psi\{c(\beta)\psi^{-1}(p_{0k})\}$ and $F^*_k(\phi) = \psi\{c(\phi)\psi^{-1}(p^*_{0k})\}$. Further assume that both models satisfy the regularity conditions listed in section 3.3.*

(a) If, for some $\lambda > 0$,

$$p^*_{0k} = \psi\{\lambda\psi^{-1}(p_{0k})\} \tag{3.4}$$

then $F_k(\hat{\beta}_i) = F^*_k(\hat{\phi}_i)$ for all k, where $\hat{\beta}_i$ and $\hat{\phi}_i$ be the maximum likelihood estimate of β and ϕ given the observations $\{(x_j, Y_j) : j \le i\}$.

(b) If the skeletons $\{p_{0k}\}$ and $\{p^*_{0k}\}$ are generated using Algorithm (3.3) with (δ, ν_0) and (δ, ν^*_0) respectively, then (3.4) holds.

Theorem 1 implies that the choice of ν_0 is irrelevant in the likelihood estimate and hence the performance of the likelihood CRM if the skeleton is chosen according to Algorithm (3.3); hence, we can arbitrarily set $\nu_0 = 1$.

The proof of Theorem 1 and other theories developed in the following chapters require the regularity conditions on the dose-toxicity model listed in section 3.3.

Proof of Theorem 1. By (3.4), $F^*_k(\phi) = \psi\{c(\phi)\psi^{-1}(p^*_{0k})\} = \psi\{c(\phi)\lambda\psi^{-1}(p_{0k})\}$, whereas $F_k(\beta) = \psi\{c(\beta)\psi^{-1}(p_{0k})\}$. Therefore, the two models represent re-parametrisation of each other with $c(\beta) = \lambda c(\phi)$, and the MLEs are identical, i.e., $\widehat{c(\beta)} = \widehat{\lambda c(\phi)}$. By invariance of maximum likelihood, we also have $c(\hat{\beta}_i) = \lambda c(\hat{\phi}_i)$. The desired result in Theorem 1(a) thus follows, i.e., $F_k(\hat{\beta}_i) = F^*_k(\hat{\phi}_i)$.

To prove Theorem 1(b), consider a given dose level k. By Algorithm (3.3), we have

$$\psi^{-1}(p^*_{0k}) = \left\{\frac{\psi^{-1}(\theta+\delta)}{\psi^{-1}(\theta-\delta)}\right\}^{(k-\nu_0^*)} \psi^{-1}(p_{0\nu_0^*}) \equiv \lambda \left\{\frac{\psi^{-1}(\theta+\delta)}{\psi^{-1}(\theta-\delta)}\right\}^{(k-\nu_0)} \psi^{-1}(p_{0\nu_0}) = \lambda\psi^{-1}(p_{0k}) \tag{3.5}$$

where

$$\lambda = \left\{\frac{\psi^{-1}(\theta+\delta)}{\psi^{-1}(\theta-\delta)}\right\}^{\nu_0-\nu_0^*}.$$

Note the equivalence in 3.5 is due to the fact $\psi^{-1}(p_{0\nu_0}) = \psi^{-1}(p_{0\nu_0^*}) = \psi^{-1}(\theta)$ by definition. Thus, assumption (3.4) holds.

3.2 The initial design

The primary appeal of a two-stage design is that it allows a safe starting dose, which is usually the lowest dose level, that is, $x_{1,0} = d_1$. Also since the initial design does not prescribe de-escalation, that is, $x_{i,0} \leq x_{i+1,0}$, the dose sequence can be equivalently represented by $\mathcal{M}_0 = \{m_{01}, m_{02}, \ldots, m_{0K}\}$, where $m_{0k} = \sum_{i=1}^{N} I(x_{i,0} = d_k)$ is the initial cohort size of dose k and $I(\cdot)$ is an indicator function, such that $\sum_{k=1}^{K} m_{0k} = N$. In practice, it is common to use equal cohort sizes for the non-highest doses, such as, $m_{01} = \cdots = m_{0,K-1} = 3$ with $m_{0K} = N - 3(K-1)$. In order to avoid over-conservative dosing among the earliest patients, Storer [28] suggests that it may be reasonable to escalate relatively quickly at the start and slow down as the trial moves to higher doses. This implies non-decreasing initial cohort sizes, that is,

$$m_{01} \leq m_{02} \leq \cdots \leq m_{0,K-2} \leq m_{0,K-1} \leq m_{0K} \tag{3.6}$$

As a middle ground between equal cohort sizes and the general form of non-decreasing cohort sizes (3.6), we focus our attention to the following class of initial designs that allows at most one cohort size increment:

$$l = m_{01} = m_{02} = \cdots m_{0,j-1} < m_{0,j} = m_{0,j+1} = \cdots m_{0,K-1} = l+s, \text{ and } m_{0,K} = N - m_{+,K-1}, \tag{3.7}$$

where $m_{+,K-1} := \sum_{k=1}^{K-1} m_{0k} = l(K-1)+s(K-j)$ is the number of subjects needed to escalate to the highest dose, and serves as an conservatism index of the initial design. For the moment, assume that N is chosen so that $m_{0,K} \geq l + s$ thus satisfying (3.6). The initial design (3.7), abbreviated as a triple-indexed $\mathcal{D}_0(l, s, j)$, allows an increase in cohort size at most once at a dose level $j \in \{1, \ldots, K-1\}$ by size s, and $l \geq 0$ is the cohort size for doses below j. In case when $j = 1$, $\mathcal{D}_0(l, s, j)$ represents an initial design with equal cohort sizes $l+s$. The design objective is thus to determine (l, s, j). In practice, there is an inclination to choose a conservative initial design, that is, to have a "large" conservative index $m_{+,K-1}$. On the other hand, Cheung [6] shows that an over-conservative initial design causes incoherence in a two-stage CRM. That is, dose escalation occurs on the next patient despite the current patient has developed a toxicity. Therefore, a reasonable design approach is to seek the most conservative $\mathcal{D}_0(l, s, j)$ among all coherent initial designs in class (3.7).

Let $T_0 = \min\{i : Y_i = 1\}$ denote the index for the first patient with a toxicity.

LEMMA. *Suppose that a likelihood CRM is specified with ψ and $\{p_{0k}\}$ generated according to Algorithm (3.3), so that Conditions 1–3 hold. Then if a two-stage CRM with initial design $\mathcal{D}_0(l, s, j)$ is incoherent, an incoherent escalation will occur with probability one on the event $\{T_0 = m_{+,K-1}\}$. That is, $x_{T_0+1} = \hat{\nu}_{T_0} > x_{T_0} = x_{T_0,0}$ when $T_0 = m_{+,K-1}$.*

Lemma holds also for any initial design $\mathcal{M}_0$ satisfying (3.6), and hence holds for more general initial designs than $\mathcal{D}_0$ as described in (3.7).

Proof of Lemma.

Proof of Lemma. Assume without loss of generality that ψ is an increasing function, i.e., $\psi' > 0$, and that $\psi^{-1}(p_{0k}) < 0$ for all k per Condition 2. For brevity, we write $\psi^{-1}(p_{0k})$ as ψ_k^{-1} as shorthand expression, and develop our proof in terms of $\alpha = \exp(\beta)$.

Let $u \leq N - m_{+,K-1}$ so that $x_{u,0} = d_\zeta$ for some $1 \leq \zeta \leq K-1$. It can be verified that $u \leq \sum_{k=1}^{\zeta} m_{0k}$. Suppose that an initial design $\mathcal{M}_0$ satisfying (3.6) induces an

incoherent escalation on $\{T_0 = u\}$, that is, $x_{u+1} = \hat{\nu}_u > x_u = x_{u,0}$ upon observing $x_i = x_{i,0}$ for $i \leq u$ and $Y_1 = \cdots = Y_{u-1} = 0$ and $Y_u = 1$. We will consider two cases in the followings:

Case 1: $u < \sum_{k=1}^{\zeta} m_{0k}$ for $\zeta = 1, \ldots, K-1$

Case 2: $u = \sum_{k=1}^{\zeta} m_{0k}$ for $\zeta = 1, \ldots, K-2$

Under Case 1, we will show that $\mathcal{M}_0$ will induce an incoherent escalation on $\{T_0 = w\}$ for any $w > u$ such that $x_{w,0} = d_\zeta$. Analogously, under Case 2, we will show that $\mathcal{M}_0$ will induce an incoherent escalation on $\{T_0 = \sum_{k=1}^{\zeta+1} m_{k,0}\}$. By applying these results under Cases 1 and 2 deductively, we can then show that $\mathcal{M}_0$ will induce an incoherent escalation on $\{T_0 = m_{+,K-1}\}$ as desired.

First consider Case 1 when $u < \sum_{k=1}^{\zeta} m_{0k}$. The first derivative of log-likelihood with respect to α based on the first u observations given $\{T_0 = u\}$ can be written as

$$\begin{aligned} l_u'(\alpha) &= \sum_{k=1}^{\zeta-1} \left\{ m_{0k} \frac{-\psi'(\alpha\psi_k^{-1})\psi_k^{-1}}{1-\psi(\alpha\psi_k^{-1})} \right\} + (u - \sum_{k=1}^{\zeta-1} m_{0k}) \frac{-\psi'(\alpha\psi_\zeta^{-1})\psi_\zeta^{-1}}{1-\psi(\alpha\psi_\zeta^{-1})} \\ &+ \frac{\psi'(\alpha\psi_\zeta^{-1})\psi_\zeta^{-1}}{\psi(\alpha\psi_\zeta^{-1})\{1-\psi(\alpha\psi_\zeta^{-1})\}} \end{aligned} \tag{3.8}$$

Let $\hat{\alpha}_u$ denote the solution to $l_u'(\alpha) = 0$. Then the assumption that incoherence occurs on $\{T_0 = u\}$ implies $\psi(\hat{\alpha}_u\psi_\zeta^{-1}) + \psi(\hat{\alpha}_u\psi_{\zeta+1}^{-1}) < 2\theta$.

Likewise, we can write the first derivative of the log-likelihood based on the first w observations given $\{T_0 = w\}$, where $w > u$ and $x_{w,0} = d_\zeta$, as follows:

$$\begin{aligned} l_w'(\alpha) &= \sum_{k=1}^{\zeta-1} \left\{ m_{0k} \frac{-\psi'(\alpha\psi_k^{-1})\psi_k^{-1}}{1-\psi(\alpha\psi_k^{-1})} \right\} + (w - \sum_{k=1}^{\zeta-1} m_{0k}) \frac{-\psi'(\alpha\psi_\zeta^{-1})\psi_\zeta^{-1}}{1-\psi(\alpha\psi_\zeta^{-1})} \\ &+ \frac{\psi'(\alpha\psi_\zeta^{-1})\psi_\zeta^{-1}}{\psi(\alpha\psi_\zeta^{-1})\{1-\psi(\alpha\psi_\zeta^{-1})\}} \end{aligned} \tag{3.9}$$

with $\hat{\alpha}_w$ denoted as solution to $l_w'(\alpha) = 0$. Since $\sum_{k=1}^{\zeta-1} m_{0k} < u < w \leq \sum_{k=1}^{\zeta} m_{0k}$, the second term on the right hand side in (3.9) is greater than its counterpart in (3.8), and hence $l_u'(\alpha) < l_w'(\alpha)$. As we can verify that $l_u'(\alpha)$ and $l_w'(\alpha)$ are decreasing in α and have uni-root under Condition 3, we have $\hat{\alpha}_u < \hat{\alpha}_w$. As a result, $\psi(\hat{\alpha}_w\psi_\zeta^{-1}) + \psi(\hat{\alpha}_w\psi_{\zeta+1}^{-1}) < \psi(\hat{\alpha}_u\psi_\zeta^{-1}) + \psi(\hat{\alpha}_u\psi_{\zeta+1}^{-1}) < 2\theta$, that is, incoherence occurs on $\{T_0 = w\}$.

Analogously, under Case 2 when $u = \sum_{k=1}^{\zeta} m_{0k}$, the first derivative of log-likelihood with respect to α based on the first u observations given $\{T_0 = u\}$ can be written as:

$$l_u^{'}(\alpha) = \sum_{k=1}^{\zeta} \left\{ m_{0k} \frac{-\psi^{'}(\alpha\psi_k^{-1})\psi_k^{-1}}{1-\psi(\alpha\psi_k^{-1})} \right\} + \frac{\psi^{'}(\alpha\psi_\zeta^{-1})\psi_\zeta^{-1}}{\psi(\alpha\psi_\zeta^{-1})\{1-\psi(\alpha\psi_\zeta^{-1})\}} \tag{3.10}$$

and that based on the first $w = \sum_{k=1}^{\zeta+1} m_{k,0}$ observations given $\{T_0 = w\}$ as:

$$l_w^{'}(\alpha) = \sum_{k=1}^{\zeta+1} \left\{ m_{0k} \frac{-\psi^{'}(\alpha\psi_k^{-1})\psi_k^{-1}}{1-\psi(\alpha\psi_k^{-1})} \right\} + \frac{\psi^{'}(\alpha\psi_{\zeta+1}^{-1})\psi_{\zeta+1}^{-1}}{\psi(\alpha\psi_{\zeta+1}^{-1})\{1-\psi(\alpha\psi_{\zeta+1}^{-1})\}} \tag{3.11}$$

According to (3.3), we have $\psi_{k+1}^{-1} = r\psi_k^{-1}$ where $r = \psi^{-1}(\theta+\delta)/\psi^{-1}(\theta-\delta) < 1$ under the assumption $\psi^{-1} < 0$. Then we can re-write (3.11) as

$$\begin{aligned}
l_w^{'}(\alpha) &= m_{01} \left\{ \frac{-\psi^{'}(\alpha\psi_1^{-1})\psi_1^{-1}}{1-\psi(\alpha\psi_1^{-1})} \right\} \\
&+ \left[\sum_{k=1}^{\zeta} \left\{ m_{0,k+1} \frac{-\psi^{'}(\alpha r\psi_k^{-1})r\psi_k^{-1}}{1-\psi(\alpha r\psi_k^{-1})} \right\} + \frac{\psi^{'}(\alpha r\psi_\zeta^{-1})r\psi_\zeta^{-1}}{\psi(\alpha r\psi_\zeta^{-1})\{1-\psi(\alpha r\psi_\zeta^{-1})\}} \right] \\
&= m_{01} \left\{ \frac{-\psi^{'}(\alpha\psi_1^{-1})\psi_1^{-1}}{1-\psi(\alpha\psi_1^{-1})} \right\} + \sum_{k=1}^{\zeta} \left\{ (m_{0,k+1} - m_{0k}) \frac{-\psi^{'}(\alpha r\psi_k^{-1})r\psi_k^{-1}}{1-\psi(\alpha r\psi_k^{-1})} \right\} \\
&+ \left[\sum_{k=1}^{\zeta} \left\{ m_{0k} \frac{-\psi^{'}(\alpha r\psi_k^{-1})r\psi_k^{-1}}{1-\psi(\alpha r\psi_k^{-1})} \right\} + \frac{\psi^{'}(\alpha r\psi_\zeta^{-1})r\psi_\zeta^{-1}}{\psi(\alpha r\psi_\zeta^{-1})\{1-\psi(\alpha r\psi_\zeta^{-1})\}} \right] \\
&= m_{01} \left\{ \frac{-\psi^{'}(\alpha\psi_1^{-1})\psi_1^{-1}}{1-\psi(\alpha\psi_1^{-1})} \right\} + \sum_{k=1}^{\zeta} \left\{ (m_{0,k+1} - m_{0k}) \frac{-\psi^{'}(\alpha r\psi_k^{-1})r\psi_k^{-1}}{1-\psi(\alpha r\psi_k^{-1})} \right\} + r l_u^{\prime}(r\alpha) \\
&= A(\alpha) + r l_u^{\prime}(r\alpha)
\end{aligned} \tag{3.12}$$

where

$$A(\alpha) = m_{01} \left\{ \frac{-\psi^{'}(\alpha\psi_1^{-1})\psi_1^{-1}}{1-\psi(\alpha\psi_1^{-1})} \right\} + \sum_{k=1}^{\zeta} \left\{ (m_{0,k+1} - m_{0k}) \frac{-\psi^{'}(\alpha r\psi_k^{-1})r\psi_k^{-1}}{1-\psi(\alpha r\psi_k^{-1})} \right\}$$

Since $\psi^{'} > 0$ and $\psi^{-1}(p_{0k}) < 0$ by assumption, under non-decreasing cohort sizes (3.6) , we have $A(\alpha) > 0$. In addition, $l_w^{'}(\hat{\alpha}_w) = l_u^{'}(\hat{\alpha}_u) = 0$. By (3.12) we have

$$r l_u^{'}(r\hat{\alpha}_w) = l_w^{'}(\hat{\alpha}_w) - A(\hat{\alpha}_w) = -A(\hat{\alpha}_w) < 0 = l_u^{'}(\hat{\alpha}_u) \tag{3.13}$$

Since $0 < r < 1$, $l_u'(\hat{\alpha}_u) > rl_u'(r\hat{\alpha}_w) > l_u'(r\hat{\alpha}_w)$. Since $l_u'(\alpha)$ is decreasing function for α, $\hat{\alpha}_u < r\hat{\alpha}_w$. As a result, $\psi(\hat{\alpha}_w\psi_{\zeta+1}^{-1}) + \psi(\hat{\alpha}_w\psi_{\zeta+2}^{-1}) = \psi(r\hat{\alpha}_w\psi_{\zeta}^{-1}) + \psi(r\hat{\alpha}_w\psi_{\zeta+1}^{-1}) < \psi(\hat{\alpha}_u\psi_{\zeta}^{-1}) + \psi(\hat{\alpha}_u\psi_{\zeta+1}^{-1}) < 2\theta$. Incoherence occurs with probability one on $\{T_0 = w\}$. That is, $x_{w+1} = \hat{\nu}_w > x_w = x_{w,0}$.

The Lemma assumes the skeleton is generated using Lee and Cheung's calibration algorithm 3.3. This Lemma provides a convenient method to check whether a two-stage CRM is coherent for any given initial design in most general form 3.6. Since a two-stage CRM is coherent only if it is coherent across all N scenarios of when the first toxicity occurs, it implies that we need to exhaust all N scenarios to check for coherence before concluding the design is coherent. With this Lemma, this task is further reduced to checking only one scenario when the first toxicity occurs on the last patient assigned on dose level $K-1$, i.e., $\{T_0 = m_{+,K-1}\}$. Following the procedures described in Cheung (2011), for given target toxicity rate θ, number of doses K, dose-toxicity function ψ, and the skeleton generated using Lee and Cheung (2009)'s approach, the likelihood estimate of model parameter $\hat{\beta}$ can be obtained under this specific toxicity outcome, the following inequality will be checked [8]:

$$\psi\{\exp(\hat{\beta})\psi_{K-1}^{-1}\} + \psi\{\exp(\hat{\beta})\psi_{K}^{-1}\} - 2\theta > 0 \tag{3.14}$$

If this inequality holds, the next dose assignment is coherent under this specific toxicity outcome profile, according to the Lemma, the two-stage CRM using this initial design is coherent under any toxicity outcome scenario.

THEOREM 2. *Suppose that the assumptions in the Lemma hold, and Condition 4 also holds.*

(a) For any coherent initial design $\mathcal{D}_0(l, s, j)$, there exists a triplet $(l^*, s^* = 1, j^*)$, such that $\mathcal{D}_0(l^*, s^*, j^*)$ is also coherent, with $l^*(K-1)+s^*(K-j^*) \geq l(K-1)+s(K-j)$.

(b) Among all $\mathcal{D}_0(l^*, s^*, j^*)$ in part (a), there exists a unique triplet that has the largest $m_{+,K-1}$.

Proof of Theorem 2. Similar to the proof of Lemma, we assume without loss of

generality that ψ is an increasing function, i.e., $\psi' > 0$, and that $\psi^{-1}(p_{0k}) < 0$ for all k per Condition 2. For brevity, we write $\psi^{-1}(p_{0k})$ as ψ_k^{-1} as shorthand expression, and develop our proof in terms of $\alpha = \exp(\beta)$.

Suppose an initial design $\mathcal{D}_0(l, s, j)$ is coherent with conservatism index $n_0 = l(K-1)+s(K-j)$, and also that $\mathcal{D}_0(l+1, s, j)$ is coherent with $n_1 = (l+1)(K-1)+s(K-j)$. It is obvious that $n_1 > n_0$. Likewise, suppose that $\mathcal{D}_0(l, s, j-1)$ is coherent with conservatism index $n_2 = l(K-1) + s(K-j+1)$, thus $n_2 > n_0$. To complete the proof of Theorem 2(a), we will only need to consider a "boundary" coherent initial design $\mathcal{D}_0(l, s, j)$ with conservatism index n_0, such that $\mathcal{D}_0(l+1, s, j)$ and $\mathcal{D}_0(l, s, j-1)$ are incoherent; and prove that for this triplet (l, s, j), there exists a coherent $\mathcal{D}_0(l^*, s^* = 1, j^*)$ with

$$n^* = l^*(K-1) + s^*(K-j^*) \geq n_0 \tag{3.15}$$

The proof of Theorem 2(a) can then be completed by induction.

To facilitate the proof, we rewrite the first $K-1$ cohort sizes of an initial design $\mathcal{D}_0(l, s, j)$ under (3.7) as $\bar{\mathcal{D}}_0(l', s', \omega) = \{l' + q_1, l' + q_2, \ldots, l' + q_{K-1}\}$ with $\sum_{k=1}^{K-1} q_k = \omega s'$ and $q_{K-1} - q_1 = s$ or 0. ω and s' are non-negative integers. It is clear that for given (l, s, j), there exists (l', s', ω) so that $\mathcal{D}_0(l, s, j)$ and $\bar{\mathcal{D}}_0(l', s', \omega)$ are identical. Precisely, this can be achieved by letting $l' = l$, $s' = s$, $\omega = K - j$, and $q_1 = q_2 = \ldots = q_{j-1} = 0$ and $q_j = q_{j+1} = \ldots = q_{K-1} = s$.

Now suppose that a boundary sequence $\mathcal{D}_0(l, s, j)$ can be represented as $\bar{\mathcal{D}}_0(l', s', \bar{\omega})$. It implies that $\bar{\mathcal{D}}_0(l', s', \bar{\omega} + 1)$ is incoherent by definition of "boundary" sequence, since $\bar{\mathcal{D}}_0(l', s', \bar{\omega} + 1) = \mathcal{D}_(l, s, j-1)$. For given (l, s), the conservatism index of a boundary sequence $\mathcal{D}_0(l, s, j)$ equals to $n_0 = l'(K-1) + \bar{\omega} s'$. Therefore $\bar{\omega} = \max\{\omega : \bar{\mathcal{D}}_0(l', s', \omega)$ is coherent$\}$.

Next we consider a class of initial design in the form of $\mathcal{E}_0(l', s', \omega) = \{l' + q_1', l' + q_2', \ldots, l' + q_{K-1}'\}$ with $\sum_{k=1}^{K-1} q_k' = \omega s'$ for non-negative integers ω and s' and $q_{K-1}' - q_1' = 1$ or 0. It is easy to see that $\mathcal{E}_0(l', s', \omega)$ belongs to the class of initial design

(3.7) with only cohort size increment 1.

It is clear that $\{\mathcal{E}_0\} \subset \{\bar{\mathcal{D}}_0\}$. Note also that for given $(l^{'}, s^{'}, \omega)$, $\mathcal{E}_0(l^{'}, s^{'}, \omega)$ and $\bar{\mathcal{D}}_0(l^{'}, s^{'}, \omega)$ have the same conservatism index $l^{'}(K-1) + \omega s^{'}$. Define $\omega_1 = \max\{\omega : \mathcal{E}_0(l^{'}, s^{'}, \omega) \text{ is coherent}\}$. Then for given $l^{'}$ and $s^{'}$, if we can show that $\bar{\omega} \leq \omega_1$, it implies that there exists a coherent design $\mathcal{E}_0(l^{'}, s^{'}, \omega_1)$ that is more conservative than $\bar{\mathcal{D}}_0(l^{'}, s^{'}, \bar{\omega})$. Precisely, we will need to prove $\bar{\mathcal{D}}_0(l^{'}, s^{'}, \omega_1 + 1)$ is incoherent, then the desired results follows from the definition of $\bar{\omega}$.

By definition of ω_1 and the Lemma, $\mathcal{E}_0(l^{'}, s^{'}, \omega_1 + 1)$ is incoherent on the event $\{T_0 = m_{+,K-1}\}$. We will proceed the proof under three different cases with $l^{'}$, $s^{'}$ fixed.

Case 1: $\bar{\mathcal{D}}_0(l^{'}, s^{'}, \omega_1 + 1) = \{l^{'} + q_1, \ldots, l^{'} + q_1\}$, i.e., $q_{K-1} - q_1 = 0$. In this case, it is clear that under (3.7) $\mathcal{E}_0(l^{'}, s^{'}, \omega_1 + 1) = \{l^{'} + q_1, \ldots, l^{'} + q_1\} = \mathcal{D}_0(l', s^{'}, \omega_1 + 1)$ because $q^{'}_{K-1} - q^{'}_1 = 1$ or 0. Therefore $\bar{\mathcal{D}}_0(l^{'}, s^{'}, \omega_1 + 1)$ is incoherent.

Case 2: $\bar{\mathcal{D}}_0(l^{'}, s^{'}, \omega_1 + 1) = \{l^{'} + q_1, \ldots, l^{'} + q_{K-1}\}$ with $q_{K-1} - q_1 = 1$.In this case,it can be shown that under (3.7), $\mathcal{E}_0(l^{'}, s^{'}, \omega_1 + 1) = \{l^{'} + q_1, \ldots, l^{'} + q_{K-1}\} = \mathcal{D}_0(l', s^{'}, \omega_1+1)$ because $q^{'}_{K-1} - q^{'}_1 = 1$ or 0.Therefore $\bar{\mathcal{D}}_0(l^{'}, s^{'}, \omega_1+1)$ is also incoherent.

Case 3: Finally, consider the case $\bar{\mathcal{D}}_0(l^{'}, s^{'}, \omega_1 + 1) = \{l^{'} + q_1, \ldots, l^{'} + q_{K-1}\}$ with $q_{K-1} - q_1 = s > 1$. There exists $q^{'}_1, q^{'}_2, \ldots, q^{'}_{K-1}$, such that $\mathcal{E}_0(l^{'}, s', \omega_1 + 1) = \{l^{'} + q'_1, \ldots, l^{'} + q^{'}_{K-1}\}$

$$q_{K-1} - q_1 = \sum_{k=1}^{K-2} q_{k+1} - q_k = s \text{ and } q_{k+1} - q_k \geq 0, 1 \leq k \leq K-2$$

$$q^{'}_{K-1} - q^{'}_1 = \sum_{k=1}^{K-2} q^{'}_{k+1} - q^{'}_k = 1 \text{ and } q^{'}_{k+1} - q^{'}_k \geq 0, 1 \leq k \leq K-2$$

With at most one cohort size increment in both $\bar{\mathcal{D}}_0$ and $\mathcal{E}_0$, there exists a J, such that $q_J - q_{J-1} = s$ and $q_{k+1} - q_k = 0$ for $1 \leq k \leq K-2$ and $k \neq J$. Likewise, there also exits a $J^{'}$, such that $q^{'}_{J'} - q^{'}_{J'-1} = 1$ and $q^{'}_{k+1} - q^{'}_k = 0$ for $1 \leq k \leq K-2$ and $k \neq J^{'}$.

If $q^{'}_1 < q_1$, without loss of generality $q^{'}_1 = q_1 - 1$, then the conservatism index of $\bar{\mathcal{D}}_0(l^{'}, s^{'}, \omega_1+1)$ is $q_1 * (K-1) + s(K - J^{'})$ and the conservatism index of $\mathcal{E}_0(l^{'}, s^{'}, \omega_1+1)$

is $q_1 * (K-1) - (J-1)$, contradicting the fact that their conservatism index are identical. Thus, $q_1^{'} \geq q_1$.

If $q_{K-1}^{'} > q_{K-1}$, without loss of generality $q_{K-1}^{'} = q_{K-1} + 1$, then the conservatism index of $\bar{\mathcal{D}}_0(l^{'}, s^{'}, \omega_1 + 1)$ is $q_{K-1} * (K-1) - s * (J^{'} - 1)$ and the conservatism index of $\mathcal{E}_0(l^{'}, s^{'}, \omega_1 + 1)$ is $q_{K-1} * (K-1) + (K-J)$, contradicting the fact that their conservatism index are identical. Thus, $q_{K-1}^{'} \leq q_{K-1}$.

Since $q_1 \leq q'_1 \leq q'_{K-1} \leq q_{K-1}$, for $1 \leq k \leq K-1$, there exists a k^*, such that $q_k \leq q_k^{'}$ when $1 \leq k < k^*$, and $q_k \geq q_k^{'}$ when $k^* < k \leq K-1$.

Given incoherent $\mathcal{E}_0(l^{'}, s^{'}, \omega_1 + 1)$, the first derivative with respect to α of the log-likelihood function upon $\{T_0 = m_{+,K-1}\}$ is

$$l_{\mathcal{E}_0}^{'}(\alpha) = l^{'} \left\{ \sum_{k=1}^{K-1} \frac{-\psi^{'}(\alpha\psi_k^{-1})\psi_k^{-1}}{1 - \psi(\alpha\psi_k^{-1})} \right\} + \frac{\psi^{'}(\alpha\psi_{K-1}^{-1})\psi_{K-1}^{-1}}{\psi(\alpha\psi_{K-1}^{-1})\{1 - \psi(\alpha\psi_{K-1}^{-1})\}} + A_n$$

where

$$A_n = \sum_{k=1}^{k^*} q_k^{'} \frac{-\psi^{'}(\alpha\psi_k^{-1})\psi_k^{-1}}{1 - \psi(\alpha\psi_k^{-1})} + \sum_{k=k^*+1}^{K-1} q_k^{'} \frac{-\psi^{'}(\alpha\psi_k^{-1})\psi_k^{-1}}{1 - \psi(\alpha\psi_k^{-1})}$$

Define $\hat{\alpha_{\mathcal{E}_0}}$ such that $l_{\mathcal{E}_0}^{'}(\hat{\alpha}_{\mathcal{E}_0}) = 0$, By Lemma, incoherence indicates

$$\psi(\hat{\alpha}_{\mathcal{E}_0}\psi_{K-1}^{-1}) + \psi(\hat{\alpha}_{\mathcal{E}_0}\psi_K^{-1}) < 2\theta$$

Next we examine $\mathcal{D}_0(l^{'}, s^{'}, \omega_1 + 1)$. When the first toxicity occurs on $\{T_0 = m_{+,K-1}\}$,the corresponding score function is

$$l_{\mathcal{D}_0}^{'}(\alpha) = l^{'} \left\{ \sum_{k=1}^{K-1} \frac{-\psi^{'}(\alpha\psi_k^{-1})\psi_k^{-1}}{1 - \psi(\alpha\psi_k^{-1})} \right\} + \frac{\psi^{'}(\alpha\psi_{K-1}^{-1})\psi_{K-1}^{-1}}{\psi(\alpha\psi_{K-1}^{-1})\{1 - \psi(\alpha\psi_{K-1}^{-1})\}} + B_n$$

where

$$B_n = \sum_{k=1}^{k^*} q_k \frac{-\psi^{'}(\alpha\psi_k^{-1})\psi_k^{-1}}{1 - \psi(\alpha\psi_k^{-1})} + \sum_{k=k^*+1}^{K-1} q_k \frac{-\psi^{'}(\alpha\psi_k^{-1})\psi_k^{-1}}{1 - \psi(\alpha\psi_k^{-1})}$$

$$A_n - B_n = \sum_{k=1}^{k^*} (q_k^{'} - q_k) \frac{-\psi^{'}(\alpha\psi_k^{-1})\psi_k^{-1}}{1 - \psi(\alpha\psi_k^{-1})} + \sum_{k=k^*+1}^{K-1} (q_k^{'} - q_k) \frac{-\psi^{'}(\alpha\psi_k^{-1})\psi_k^{-1}}{1 - \psi(\alpha\psi_k^{-1})}$$

Since $\sum_{k=1}^{K-1} q_k = \sum_{k=1}^{K-1} q_k^{'}$, $0 \leq \sum_{k=1}^{k^*} (q_k^{'} - q_k) = -\sum_{k=k^*+1}^{K-1} (q_k^{'} - q_k)$. By the assumptions of $\psi^{'} > 0$ and $\psi_k^{-1} < 0$ for all k. Condition 4 implies

$$\frac{\psi^{'}(\alpha\psi_i^{-1})\psi_i^{-1}}{1-\psi(\alpha\psi_i^{-1})} \leq \frac{\psi^{'}(\alpha\psi_j^{-1})\psi_j^{-1}}{1-\psi(\alpha\psi_j^{-1})} \ , \ 1 \leq j \leq i \leq K$$

Hence $A_n - B_n \leq 0$ and $l_{\mathcal{E}_0}^{'}(\alpha) \leq l_{\bar{\mathcal{D}}_0}^{'}(\alpha)$. In addition, $l_{\bar{\mathcal{D}}_0}^{'}(\hat{\alpha}_{\bar{\mathcal{D}}_0}) = 0 = l_{\mathcal{E}_0}^{'}(\hat{\alpha}_{\mathcal{E}_0}) \leq l_{\bar{\mathcal{D}}_0}^{'}(\hat{\alpha}_{\mathcal{E}_0})$. By Condition 3, each score is a decreasing function of α, $\hat{\alpha}_{\bar{\mathcal{D}}_0} \geq \hat{\alpha_{\mathcal{E}_0}}$. Thus,$\psi(\hat{\alpha}_{\bar{\mathcal{D}}_0}\psi_{K-1}^{-1}) + \psi(\hat{\alpha}_{\bar{\mathcal{D}}_0}\psi_K^{-1}) \leq \psi(\hat{\alpha}_{\mathcal{E}_0}\psi_{K-1}^{-1}) + \psi(\hat{\alpha}_{\mathcal{E}_0}\psi_K^{-1}) < 2\theta$. Therefore, the initial design $\bar{\mathcal{D}}_0(l^{'}, s^{'}, \omega_1 + 1)$ is also incoherent, and $\bar{\omega} \leq \omega_1$, thus $n_0 \leq l^{'}(K-1) + \omega_1 s^{'}$. There exists an initial design $\mathcal{E}_0(l^{'}, s^{'}, \omega_1)$, belong to class (3.7) with $s = 1$ that is more conservative than the "boundary" sequence $\mathcal{D}_0(l, s, j)$.

Next we prove part(b) of Theorem 2. Suppose $\mathcal{D}_0(l^*, s^* = 1, j^*)$ is coherent with $n^* = l^*(K-1) + K - j^* \geq n_0$. if $\mathcal{D}_0(l^*, s^* = 1, j^*)$ is not a boundary sequence, we then check coherence of $\mathcal{D}_0(l^* + 1, s^* = 1, j^*)$ or $\mathcal{D}_0(l^*, s^* = 1, j^* - 1)$ until we identify the boundary sequence. If $\mathcal{D}_0(l^*, s^* = 1, j^*)$ is a boundary sequence,then it is the most conservative and coherent initial design.

Next we show that, given we identify the boundary sequence with the largest conservatism index $n^* = l^*(K-1) + (K - j^*)$, there exists a unique pair (l^*, j^*) such that the boundary sequence $\mathcal{D}_0(l^*, s^* = 1, j^*)$ has conservatism index $n^* = l^*(K-1) + (K - j^*)$. Suppose there are two pairs (l_1^*, j_1^*) and (l_2^*, j_2^*) and both yield the same conservatism index. Without loss of generality, assuming $l_1^* = l_2^* + 1$, we have $l_1^*(K-1) + K - j_1^* = (l_2^*+1)(K-1) + K - j_1^* = l_2^*(K-1) + K - j_2^* + (j_2^* - j_1^* + K - 1)$. Since $1 \leq j_1^*, j_2^* \leq (K-1)$, $1 \leq (j_2^* - j_1^* + K - 1) \leq (2K-3)$, we have $l_1^*(K-1) + K - j_1^* \geq l_2(K-1) + K - j_2^* + 1$, which contradicts the assumption. Therefore, such pair (l^*, j^*) is unique.

Theorem 2 implies the unique existence of a most conservative coherent initial design among all $\mathcal{D}_0(l, s, j)$, for given ψ and $\{p_{0k}\}$. As a consequence of the proof of Theorem 2, this design can be attained by setting $s = 1$ and iterating (l, j) according to the following algorithm:

1. Initialize $l = 0$ and $j = K - 1$.

2. If $\mathcal{D}_0(l, s, j)$ is coherent, update $j = j - 1$ if the current $j > 1$; and set $j = K - 1$ and $l = l + 1$ if the current $j = 1$.

3. If $\mathcal{D}_0(l, s, j)$ is incoherent, stop iterating.

The last coherent $\mathcal{D}_0(l, s, j)$ before stopping the iteration will be the most conservative coherent initial design.

3.3 Regularity conditions

The following assumptions are commonly made for dose-toxicity models used with the CRM, and they can be verified for each ψ considered in Table 3.1 with $\{p_{0k}\}$ generated according to Algorithm (3.3).

Condition 1. $\psi\{\exp(\beta)\psi^{-1}(p_{0k})\}$ is strictly increasing in k for all β.

This is true for all ψ class functions.

Condition 2. $\psi\{\exp(\beta)\psi^{-1}(p_{0k})\}$ is monotone in β in the same direction for all k.

In Table 3.1, empiric/hyperbolic tangent, complementary log-log with sufficiently large positive fixed intercept, logistic with sufficiently large positive fixed intercept, and probit with sufficiently large positive fixed intercept are decreasing in β. The other ψ class functions are increasing in β.

Condition 3. For any given $0 < p < 1$ and k,

$$p\frac{\psi'\{\exp(\beta)\psi^{-1}(p_{0k})\}}{\psi\{\exp(\beta)\psi^{-1}(p_{0k})\}} + (1-p)\frac{-\psi'\{\exp(\beta)\psi^{-1}(p_{0k})\}}{1-\psi\{\exp(\beta)\psi^{-1}(p_{0k})\}}$$

is continuous and strictly monotone in β, where $\psi'\{\exp(\beta)\psi^{-1}(p_{0k})\}$ denotes the derivative of $\psi\{\exp(\beta)\psi^{-1}(p_{0k})\}$ with respect to β.

Let $R(\beta) = F_k'(\beta)\{\frac{p}{F_k(\beta)} - \frac{1-p}{1-F_k(\beta)}\} = F_k'(\beta)\frac{p-F_k(\beta)}{F_k(\beta)\{1-F_k(\beta)\}}$. If $R(\beta)$ is monotone function in β, the function has uni-root at zero. Next we show it is monotone for each ψ class function.

Empiric/hyperbolic tangent: $F_k^{'}(\beta) = F_k(\beta)\exp(\beta)\log(d_k)$. $R(\beta) = \log(d_k)\exp(\beta)\frac{p-F_k(\beta)}{1-F_k(\beta)} = \log(d_k)\exp(\beta)\left\{1-\frac{1-p}{1-F_k(\beta)}\right\}$. Since $F_k(\beta)$ is decreasing on β and $\log(d_k) < 0$, $R(\beta)$ is decreasing on β.

Logistic with fixed intercept a_0: $F_k^{'}(\beta) = F_k(\beta)\{1-F_k(\beta)\}\exp(\beta)d_k < 0$ for sufficiently large positive a_0. $R_(\beta) = \exp(\beta)d_k\{p-F_k(\beta)\}$. Since $F_k(\beta)$ is decreasing on β and $d_k < 0$, $R_(\beta)$ is decreasing on β.

Logistic with fixed slope:$F_k^{'}(\beta) = F_k(\beta)\{1-F_k(\beta)\}$. $R(\beta) = p - F_k(\beta)$. Since $F_k(\beta)$ is increasing on β, $R(\beta)$ is decreasing on β.

Complementary log-log with fixed intercept a_0:$F_k^{'}(\beta) = \{1-F_k(\beta)\}[-\log\{1-F_k(\beta)\}]\exp(\beta)d_k < 0$, with sufficiently large positive a_0 such that $d_k < 0$. $R(\beta) = \frac{\log\{1-F_k(\beta)\}\{p-F_k(\beta)\}}{F_k(\beta)}\exp(\beta)(-d_k) = \log\{1-F_k(\beta)\}\{\frac{p}{F_k(\beta)}-1\}\exp(\beta)(-d_k)$. Since $F_k(\beta)$ is decreasing on β, both $\log\{1-F_k(\beta)\}$ and $\frac{p}{F_k(\beta)}-1$ are increasing functions of β. $-d_k$ is positive. Therefore $R(\beta)$ is increasing on.

Complementary log-log with fixed slope:

Probit with fixed slope:$F_k^{'}(\beta) = \phi\{\beta+\Phi^{-1}(p_{0k})\} > 0.R(\beta) = \frac{\phi(\beta+d_k)(p-\Phi(\beta+d_k)}{\Phi(\beta+d_k)\{1-\Phi(\beta+d_k)\}}$

Condition 4. $\psi^{'}\{\exp(\beta)\psi^{-1}(p_{0k})\}g_{ij}(\beta) \le 0$ for all k and $i > j$, where $g_{ij}(\beta) := \psi^{'}\{\exp(\beta)\psi^{-1}(p_{0j})\}[1-\psi\{\exp(\beta)\psi^{-1}(p_{0i})\}]-\psi^{'}\{\exp(\beta)\psi^{-1}(p_{0i})\}[1-\psi\{\exp(\beta)\psi^{-1}(p_{0j})\}]$.

Empiric/hyperbolic tangent: $F_k^{'}(\beta) = F_k(\beta)\log F_k(\beta) < 0$. $g_{ij}(\beta) = F_j(\beta)\log F_j(\beta)\{1-F_i(\beta)\} - F_i(\beta)\log F_i(\beta)\{1-F_j(\beta)\}$. Suppose $m(x) = \frac{F_\beta(x)}{1-F_\beta(x)}\log F_\beta(x)$, $m^{'}(x) = \frac{F_\beta^{'}(x)\{\log F_\beta(x)+1-F_\beta(x)\}}{(1-F_\beta(x))^2} > 0$. Since $0 < F_\beta(x) < 1$, $\log F_\beta(x) < F_\beta(x)-1$ on interval $0 < F_\beta(x) < 1$. Thus, $m^{'}(x)$ is increasing on x, and $g_{ij}(\beta) > 0$.

Logistic with large positive fixed intercept a_0: $F_k^{'}(\beta) = F_k(\beta)\{1-F_k(\beta)\}\exp(\beta)d_k = F_k(\beta)\{1-F_k(\beta)\}\{\text{logit}F_k(\beta)-a_0\} < 0$. $g_{ij}(\beta) = \{F_j(\beta)\{\text{logit}F_j(\beta)-a_0\}-F_i(\beta)\{\text{logit}F_i(\beta)-a_0\}\}\{1-F_j(\beta)\}\{1-F_i(\beta)\}$. Suppose $m(x) = F_\beta(x)\{\text{logit}F_\beta(x)-a_0\}$. $m^{'}(x) = F_\beta^{'}(x)\{\text{logit}F_\beta(x)+\frac{1}{1-F_\beta(x)}-a_0\}$. Since $F_\beta^{'}(x) > 0$, and when a_0 is sufficiently large,$m^{'}(x) < 0$. Thus, $\{F_j(\beta)\{\text{logit}F_j(\beta)-a_0\}-F_i(\beta)\{\text{logit}F_i(\beta)-a_0\}\} > 0$ for $j < i.g_{ij}(\beta) > 0$.

Logistic with fixed slope has been shown in the Chapter 4 of [7].

Complementary log-log with fixed intercept a_0: $F_k^{'}(\beta) = \{1 - F_k(\beta)\}[-\log\{1 - F_k(\beta)\}](\log[-\log\{1 - F_k(\beta)\}] - a_0) < 0$ for sufficiently large positive a_0. $g_{ij}(\beta) = (\log\{1 - F_i(\beta)\}(\log[-\log\{1 - F_i(\beta)\}] - a_0) - \log\{1 - F_j(\beta)\}(\log[-\log\{1 - F_j(\beta)\}] - a_0))\{1 - F_j(\beta)\}\{1 - F_i(\beta)\}$. Suppose $m(x) = \log\{1 - F_\beta(x)\}(\log[-\log\{1 - F_\beta(x)\}] - a_0)$, $m^{'}(x) = -\frac{F_\beta^{'}(x)}{1-F_\beta(x)}(\log[-\log\{1 - F_\beta(x)\}] - a_0 + 1) > 0$. Thus, $m^{'}(x)$ is increasing on x, and $g_{ij}(\beta) > 0$.

Complementary log-log with fixed slope: $F_k^{'}(\beta) = -\{1 - F_k(\beta)\}\log\{1 - F_k(\beta)\} > 0$. $g_{ij}(\beta) = [\log\{1 - F_i(\beta)\} - \log\{1 - F_j(\beta)\}]\{1 - F_i(\beta)\}\{1 - F_j(\beta)\}$. Since $\log\{1 - F_\beta(x)\}$ is decreasing in x, $g_{ij}(\beta) < 0$.

Probit with fixed slope: $F_k^{'}(\beta) = \phi\{\beta + \Phi^{-1}(p_{0k})\} > 0$. Let the quantiles $z_k = \Phi^{-1}(p_{0k})$ and $z_i > z_j$. $g_{ij}(\beta) = \phi(\beta + z_j)\{1 - \Phi(\beta + z_i)\} - \phi(\beta + z_i)\{1 - \Phi(\beta + z_j)\} = \phi(-\beta - z_j)\Phi(-\beta - z_i) - \phi(-\beta - z_i)\Phi(-\beta - z_j)$. Suppose $m(x) = \frac{\phi(x)}{\Phi(x)}$. $m^{'}(x) = -\frac{\phi(x)\int\Phi(x)\,\mathrm{d}x}{\Phi(x)^2} < 0$. Thus, $g_{ij}(\beta) < 0$.

Probit with fixed intercept a_0: $F_k^{'} = \phi\{a_0 + \exp(\beta)d_k\}\exp(\beta)d_k < 0$, with sufficiently large positive a_0. $g_{ij}(\beta) = \phi\{-(a_0 + e^\beta d_j)\}d_j\Phi\{-(a_0 + e^\beta)\} - \phi\{-(a_0 + e^\beta d_i)\}d_i\Phi\{-(a_0 + e^\beta d_j)\}$. Let $z_i = -(a_0 + e^\beta d_i)$, $z_j = -(a_0 + e^\beta d_j)$, thus $z_i < z_j$. $g_{ij} = \phi(z_j)(-z_j - a_0)\Phi(z_i) - \phi(z_i)(-z_i - a_0)\Phi(z_j) = \phi(z_i)(z_i + a_0)\Phi(z_j) - \phi(z_j)(z_j + a_0)\Phi(z_i)$. Let $m(x) = \frac{\phi(x)(x+a_0)}{\Phi(x)}$,$m^{'}(x) = \frac{\phi(x)\Phi(x)(-x^2 - xa_0 + 1) - \phi(x)^2(x+a_0)}{\Phi(x)^2} < 0$ when a_0 is sufficiently large positive. Hence $m(x)$ is decreasing function of x. Thus, $g_{ij}(\beta) > 0$.

Chapter 4

Design calibration and application

With large sample size, CRM converges to the doses with toxicity probability falling within a window around the target rate θ. The half width of this window is defined as the model sensitivity parameter δ [8]. However, with finite sample size, it is important to calibrate the design parameters to achieve satisfying performance. As discussed in previous Chapter, three design components may influence the design performance of two-stage likelihood CRM: initial design $\mathcal{D}_0$, dose-toxicity function ψ, and initial estimate of the dose toxicity probabilities, "skeleton", (p_{0k}). Theorem 2 reveals that the most conservative and coherent initial design can be determined for given ψ and skeleton. From Theorem 1, skeleton can be determined for given model sensitivity parameter δ. We propose a semi-automatic calibration algorithm which iterates over a range of δ values, for given ψ, and evaluates the performance using average accuracy across a set of true dose-toxicity profiles [16; 7]. This procedure can be repeated for each ψ function to compare across different ψ.

4.1 Calibration algorithm

For given target toxicity rate θ, number of doses K, and total number of patients N, we first specify one of the ψ functions listed in (3.1), then apply the following

calibration algorithm:

- Step 1: Vary δ in a range between 0.01 to $0.7\times\theta$ by step size of 0.01 [16]. For each δ, do step 2-5:
  - Step 2: determine skeleton $\{p_{0k}\}$ using Algorithm (3.3) based on δ and $\nu_0 = 1$.
  - Step 3: Given (ψ, p_{0k}), obtain the most conservative coherent $\mathcal{D}_0(l^*, 1, j^*)$ according to the algorithm in Chapter 3.
  - Step 4: Specify λ and calculate the number of patients to be tested on the highest dose level $m_K = \lambda/\theta$. The initial design obtained in step 3 will be pruned down with respect to is constraints and total sample size N, according to Algorithm 10.2 in [7].
  - Step 5: Simulate 2000 trials with the fully specified two-stage likelihood CRM $(\psi, p_{0k}, \mathcal{D}_0)$, under K dose toxicity scenarios described using the plateau configurations with an odds ratio of 2 [16]. Record the recommended MTD in the end of each trial. Calculate the average probability of correct selection (PCS) across the K scenarios.
- Step 6: Choose the δ value which yields the maximum average PCS. The corresponding design parameters $(p_{0k}, \mathcal{D}_0)$ will be the recommended design parameters, for the specific ψ.

In practice, the number of patients to be reserved on the highest dose level K is usually determined separately as by the time the trial escalates to the highest dose level d_K without observing any toxicity, the highest dose is the one closest to the pre-specified target toxicity rate and it is preferred to test more patients on this dose level before claiming it as MTD. Usually $\lambda = 1, 1.2, 1.5, 2, \ldots$ [7] and its specific value can impact the pruning of the initial design, hence the design performance.

This calibration algorithm can be repeated for each ψ function, and the respective plot of average PCS versus δ can be generated to compare across the ψ functions.

4.2 Redesign the NeuSTART trial

As described in the introduction section, NeuSTART is a dose finding trial that aims to determine the maximum tolerated dose for lovastatin in stroke patients [10] with $\theta = 0.1$ and $K = 5$. The original trial design was the two-stage Bayesian CRM with design parameters described in the introduction Chapter. This design was calibrated by the trial-and-error approach [7].

We re-design NeuSTART using the likelihood CRM with the dose-toxicity functions listed in (3.1). The design parameters are determined based on algorithms described above, as follows. For each ψ, we first calculate the skeleton $\{p_{0k}\}$ using algorithm (3.3) for δ ranging from 0.01 to 0.05 with increment of 0.0025; For each pair (ψ, δ), we obtain the most conservative coherent $\mathcal{D}_0(l^*, 1, j^*)$ according to the algorithm in Chapter 3. In our study design we also set $m_{05} = 12$ with $N = 33$, such that sufficient number of subjects would be tested at the highest dose if there were no toxicity throughout. In order to make the calibrated designs comparable to the original study design, we "prune" $\mathcal{D}_0(l^*, 1, j^*)$ using Algorithm 10.2 in [7] with respect to the constraint $m_{05} = 12$ and $N = 33$ while keeping the pruned design coherent. For each completely specified design $(\psi, \delta, \mathcal{D}_0)$, we ran simulations under K dose toxicity scenarios described as the plateau configurations with an odds ratio of 2 [16]. Table 4.1 gives, for each ψ, the calibrated design that maximises the average probability of correctly selecting ν in the K scenarios. In addition, Figure (4.2) displays the average probability of correct selection by (ψ, δ): the average accuracy reaches maximum either at $\delta = 0.0275$ or at $\delta = 0.0175$; and, the difference in the average accuracy is less than 1% when δ lies between 0.0175 and 0.0275. It gives some assurance that the design performance is insensitive to the choice of δ over this range, thus rendering the choice of "optimal" δ quite robust.

The performance of these calibrated designs are compared to the NeuSTART study design under the toxicity scenarios listed in Table 4.1 using simulation with 5,000 replicates. Table 4.3 shows that all designs give comparable average probability

of correct selection. Also, all the calibrated designs lead to slightly better performance than the NeuSTART design when ν is at the highest dose—a rather common clinical expectation *a priori*. Finally, this simulation study confirms that, for finite sample settings, the CRM is robust against the choice of the dose-toxicity function as long as the design parameters are well calibrated. In particular, it suggests and justifies the use of the most commonly used empiric function.

4.3 Two-stage design for the oncology trial

As described in the introduction, the goal of this oncology trial is to identify MTD among 5 dose levels with either 2-way or 3-way drug combinations of Gemcitabine, Cabazitaxel and Cisplatin, for treating bladder cancer patients. The MTD combination will be estimated using a two-stage Bayesian CRM. In the first stage, a rule based design will be used. Once a DLT is observed, we will switch to the second stage using the CRM. There are several advantages of the CRM compared to conventional designs. First, the CRM has been shown to have better performance than the 3+3 design and treat fewer patients at suboptimal doses. Second, it allows for the specification of a fixed sample size for the trial. Third, it assigns a dose after the outcome of every patient is observed. The advantage of using a two-stage CRM over a one stage-CRM is it starts at the lowest dose, like conventional designs. This is desired because of safety concerns in starting with the combination of all three drugs for intravesical use. Thus, the design is expected to be more conservative than the one stage CRM and outperform the 3+3 design in selecting the correct dose as the MTD.

The specified sample size is 24 patients using a cohort size of one. The first patient will be assigned dose level 1 (2g of Gemcitabine and 2.5mg of CAB). Before a DLT is observed, dose escalation will follow the dose sequence listed in Table 4.4. Once a DLT is observed, dose escalations will be determined using a Bayesian CRM.

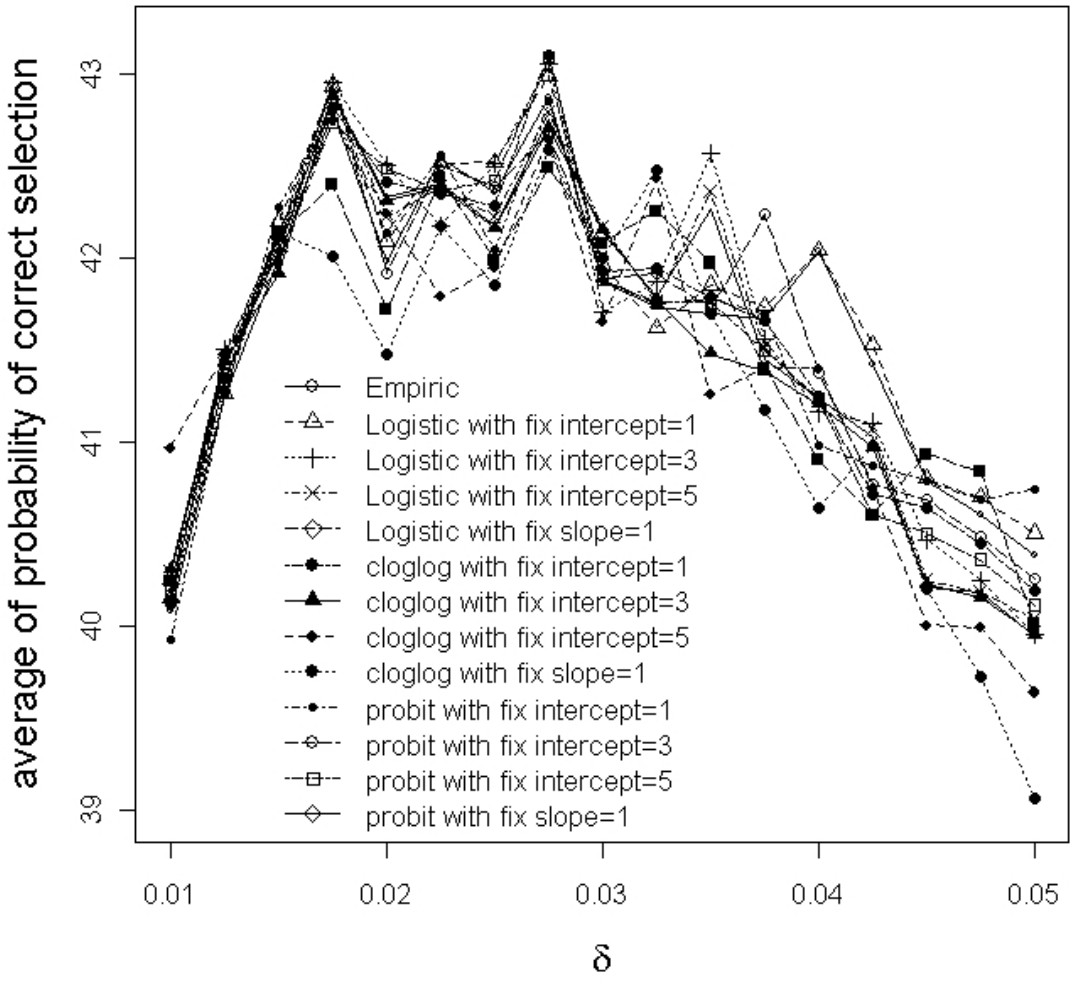

Figure 4.1: Average probability of correct selection versus δ for each ψ-class functional form.

The CRM with an empirical dose-toxicity model and a normal prior distribution on the parameter with mean 0 and variance of 0.55 will be used [17]. The expected MTD is dose level 3. The dose-toxicity model is calibrated such that the method will eventually select a dose that yields between 20% and 30% DLT [16; 8]. The design will not allow for dose skipping and dose escalation immediately after a DLT is observed [6].

The operating characteristics of our design under different various scenarios are displayed in the table 4.5. With 24 patients, the design selects the correct MTD with probabilities over 50% in all five scenarios, outperforming the conventional 3+3 design. The scenarios where selected to have neighborhood doses with DLT rates within 10-15% of the MTD rate. If the neighboring doses have DLT rates significantly different from the target of 25%, the probability of correct selection will be improved. A stopping rule will be implemented whereby if the first two patients experience toxicity the trial will be stopped for toxicity.

4.4 Comprehensive simulation results

Extensive simulations are performed in this section to recommend the optimal design parameter δ under a wide range of clinical scenarios that are commonly encountered in practice [16]. The target toxicity probability considered for typical dose-finding studies are 0.10, 0.20, 0.25, and 0.33, the sample sizes are 25, 30, 35, and 40, and the number of doses ranges from 4 to 7. The dose-toxicity model is assumed to be empiric function. Two thousand simulations were performed under each scenario and no dose skipping during the dose escalation/de-escalation is allowed. The calibration algorithm introduced in the previous section is used to make recommendations on the optimal δ for each scenario. Tables 4.6,4.7,4.8,4.9 display the δ that yields the highest average PCS, the corresponding pruned initial design, and the average PCS. Another design parameter λ is specified at either 1 or 2. For $\theta = 0.10$, these indicates

the number of patients reserved to be tested on the highest dose level is 10 and 20 respectively. Larger λ requires more pruning on the initial design, thus allows more aggressive dose escalation and yields higher accuracy (Table 4.6).

The optimal δ ranges between 0.02 and 0.04 for $\theta = 0.10$, 0.03-0.04 for $\theta = 0.20$, 0.04-0.06 for $\theta = 0.25$, and 0.05-0.07 for $\theta = 0.33$. These results are comparable to the calibration results of one-stage CRM [16]. The optimal δ increases as the target rate increases, and decreases as number of doses increases and number of patients increases.

Table 4.1: Calibrated design parameters for the likelihood CRM for NeuSTART, with $\theta = 0.10$, $K = 5$, $m_{05} = 12$, and $N = 33$.

ψ	δ	Skeleton according to (3.3)					Initial Design, $\mathcal{M}_0$	
		p_{01}	p_{02}	p_{03}	p_{04}	p_{05}	$\mathcal{D}_0(l^*, 1, j^*)$	Pruned
Empiric	.0275	0.10	0.16	0.24	0.33	0.42	6,6,7,7,7	4,5,6,6,12
Complementary log-log								
with fixed intercept=1	.0275	0.10	0.17	0.25	0.34	0.43	6,6,7,7,7	4,5,6,6,12
with fixed intercept=3	.0175	0.10	0.14	0.19	0.25	0.32	4,4,5,5,15	4,4,5,5,15
with fixed intercept=5	.0175	0.10	0.14	0.19	0.26	0.33	4,4,5,5,15	4,4,5,5,15
with fixed slope	.0275	0.10	0.17	0.29	0.47	0.68	6,6,7,7,7	4,5,6,6,12
Logistic								
with fixed intercept=1	.0275	0.10	0.16	0.24	0.31	0.38	6,6,7,7,7	4,5,6,6,12
with fixed intercept=3	.0275	0.10	0.17	0.25	0.35	0.45	6,6,7,7,7	4,5,6,6,12
with fixed intercept=5	.0175	0.10	0.14	0.19	0.25	0.31	4,4,5,5,15	4,4,5,5,15
with fixed slope	.0275	0.10	0.17	0.28	0.42	0.58	6,6,7,7,7	4,5,6,6,12
Probit								
with fixed intercept=1	.0275	0.10	0.16	0.23	0.31	0.38	6,6,7,7,7	4,5,6,6,12
with fixed intercept=3	.0175	0.10	0.14	0.18	0.24	0.29	4,4,4,5,16	4,4,4,5,16
with fixed intercept=5	.0275	0.10	0.17	0.25	0.35	0.45	6,6,7,7,7	4,5,6,6,12
with fixed slope	.0175	0.10	0.14	0.19	0.25	0.32	4,4,5,5,15	4,4,5,5,15

Table 4.2: True dose toxicity probability scenarios for validation in the NeuSTART trial.

Scenarios	Validation sets				
	p_1	p_2	p_3	p_4	p_5
1	.10	.25	.30	.35	.40
2	.04	.10	.25	.30	.35
3	.01	.04	.10	.25	.30
4	.01	.01	.04	.10	.25
5	.01	.01	.01	.04	.10

Table 4.3: Operating characteristics of the calibrated designs and NeuSTART design under the scenarios in Table 4.2.

Designs	PCS (%) for each scenario					
	1	2	3	4	5	Average
NeuSTART						
Bayesian	88	54	55	53	65	63.00
Likelihood	86	52	54	54	67	62.66
Empiric	87	53	56	45	73	62.67
Complementary log-log						
fixed intercept=1	87	53	54	47	72	62.63
fixed intercept=3	87	44	45	47	75	59.75
fixed intercept=5	87	46	46	43	76	59.66
with fixed slope	89	51	48	46	71	61.06
Logistic						
fixed intercept=1	86	54	56	46	73	62.82
fixed intercept=3	87	53	53	46	73	62.31
fixed intercept=5	87	45	45	47	75	59.79
with fixed slope	89	51	49	47	71	61.27
Probit						
fixed intercept=1	86	54	56	46	72	62.94
fixed intercept=3	86	46	47	49	73	60.18
fixed intercept=5	87	53	54	47	72	62.45
with fixed slope	87	45	45	47	75	59.79

PCS is probability of correct selection

Table 4.4: Calibrated initial design for the oncology trial.

Patient Number	Cabazitaxel Dose	Cisplatin Dose
1,2	2.5mg	
3,4	5mg	
5,6	5mg	66mg
7,8	5mg	80mg
9 to 24	5mg	100mg

Table 4.5: Operating characteristics of the calibrated design for the oncology trial.

Method	MTD below level 1	1	2	3	4	5
		0.25	0.35	0.50	0.65	0.80
3+3 Design	0.44	**0.36**	0.18	0.02	0.00	0.00
Two-Stage CRM	0.07	**0.60**	0.30	0.03	0.00	0.00
		0.15	**0.25**	0.40	0.55	0.70
3+3 Design	0.21	0.34	**0.33**	0.11	0.01	0.00
Two-Stage CRM	0.03	0.22	**0.53**	0.21	0.01	0.00
		0.10	0.15	**0.25**	0.40	0.55
3+3 Design	0.10	0.19	0.30	**0.30**	0.10	0.02
Two-Stage CRM	0.01	0.03	0.25	**0.51**	0.19	0.01
		0.03	0.07	0.15	**0.25**	0.40
3+3 Design	0.01	0.06	0.17	0.36	**0.29**	0.10
Two-Stage CRM	0.00	0.00	0.03	0.27	**0.52**	0.19
		0.01	0.03	0.07	0.15	**0.25**
3+3 Design	0.00	0.01	0.05	0.17	0.32	**0.46**
Two-Stage CRM	0.00	0.00	0.00	0.05	0.31	**0.65**

Table 4.6: Recommended design parameters for $OR = 2$ and $\theta = 0.10$.

K	N	λ	δ	pruned $\mathcal{D}_0$	average PCS
4	25	1	0.03	(4,5,6,10)	45.95
		2	0.04	(1,2,2,20)	46.94
	30	1	0.02	(5,5,6,14)	47.38
		2	0.03	(2,4,4,20)	48.75
	35	1	0.02	(5,5,6,19)	49.59
		2	0.03	(4,5,6,20)	50.54
	40	1	0.02	(5,5,6,24)	52.3
		2	0.02	(5,5,6,24)	52.3
5	25	1	0.03	(3,3,4,5,10)	40.11
		2	0.03	(1,1,1,2,20)	41.04
	30	1	0.03	(4,5,5,6,10)	41.16
		2	0.04	(2,2,3,3,20)	43.19
	35	1	0.02	(5,5,5,5,15)	43.38
		2	0.04	(3,3,4,5,20)	45.19
	40	1	0.02	(5,5,5,5,20)	45.71
		2	0.03	(4,5,5,6,20)	45.72
6	25	1	0.04	(2,2,3,4,4,10)	36.6
		2	0.03	(1,1,1,1,1,20)	36.88
	30	1	0.02	(3,3,4,5,5,10)	37.38
		2	0.04	(1,1,2,3,3,20)	39.77
	35	1	0.02	(4,4,4,5,5,13)	39.16
		2	0.02	(2,2,3,4,4,20)	41.23
	40	1	0.02	(4,4,4,5,5,18)	41.43
		2	0.02	(3,3,4,5,5,20)	42.43
7	25	1	0.04	(2,2,2,2,3,4,10)	33.53
		2*	–	–	–
	30	1	0.04	(3,3,3,3,4,4,10)	33.54
		2	0.04	(1,1,1,1,3,3,20)	36.31
	35	1	0.02	(3,4,4,4,5,5,10)	35.71
		2	0.03	(2,2,2,3,3,3,20)	37.67
	40	1	0.02	(4,4,4,4,5,5,14)	37.29
		2	0.02	(3,3,3,3,4,4,20)	38.7

*:Non-valid initial designs under all δ values.

Table 4.7: Recommended design parameters for $OR = 2$ and $\theta = 0.20$.

K	N	λ	δ	pruned $\mathcal{D}_0$	average PCS
4	25	1	0.04	(2,3,3,17)	54.45
		2	0.04	(2,3,3,17)	54.45
	30	1	0.04	(2,3,3,22)	57.05
		2	0.04	(2,3,3,22)	57.05
	35	1	0.04	(2,3,3,27)	60.18
		2	0.04	(2,3,3,27)	60.18
	40	1	0.04	(2,3,3,32)	62.9
		2	0.04	(2,3,3,32)	62.9
5	25	1	0.04	(2,2,2,3,16)	48.45
		2	0.04	(2,2,2,3,16)	48.45
	30	1	0.04	(2,2,2,3,21)	50.8
		2	0.04	(2,2,2,3,21)	50.8
	35	1	0.04	(2,2,2,3,26)	53.9
		2	0.04	(2,2,2,3,26)	53.9
	40	1	0.04	(2,2,2,3,31)	56.61
		2	0.04	(2,2,2,3,31)	56.61
6	25	1	0.03	(1,2,2,2,2,16)	44.13
		2	0.03	(1,2,2,2,2,16)	44.13
	30	1	0.03	(1,2,2,2,2,21)	46.74
		2	0.03	(1,2,2,2,2,21)	46.74
	35	1	0.03	(1,2,2,2,2,26)	50.02
		2	0.03	(1,2,2,2,2,26)	50.02
	40	1	0.03	(1,2,2,2,31)	52.7
		2	0.03	(1,2,2,2,31)	52.7
7	25	1	0.03	(1,1,1,2,2,2,16)	40.71
		2	0.03	(1,1,1,2,2,2,16)	40.71
	30	1	0.03	(1,1,1,2,2,2,21)	43.81
		2	0.03	(1,1,1,2,2,2,21)	43.81
	35	1	0.03	(1,1,1,2,2,2,26)	46.74
		2	0.03	(1,1,1,2,2,2,26)	46.74
	40	1	0.03	(1,1,1,2,2,2,31)	49.93
		2	0.03	(1,1,1,2,2,2,31)	49.93

Table 4.8: Recommended design parameters for $OR = 2$ and $\theta = 0.25$.

K	N	λ	δ	pruned $\mathcal{D}_0$	average PCS
4	25	1	0.06	(2,2,3,18)	56.14
		2	0.06	(2,2,3,18)	56.14
	30	1	0.04	(2,2,2,24)	59.91
		2	0.04	(2,2,2,24)	59.91
	35	1	0.05	(2,2,2,29)	62.76
		2	0.05	(2,2,2,29)	62.76
	40	1	0.04	(2,2,2,34)	64.93
		2	0.04	(2,2,2,34)	64.93
5	25	1	0.04	(1,1,2,2,19)	51.19
		2	0.04	(1,1,2,2,19)	51.19
	30	1	0.04	(1,1,2,2,24)	55.02
		2	0.04	(1,1,2,2,24)	55.02
	35	1	0.04	(1,1,2,2,29)	57.76
		2	0.04	(1,1,2,2,29)	57.76
	40	1	0.04	(1,1,2,2,34)	60.52
		2	0.04	(1,1,2,2,34)	60.52
6	25	1	0.04	(1,1,1,2,2,18)	46.71
		2	0.04	(1,1,1,2,2,18)	46.71
	30	1	0.04	(1,1,1,2,2,23)	50.84
		2	0.04	(1,1,1,2,2,23)	50.84
	35	1	0.04	(1,1,1,2,2,28)	53.97
		2	0.04	(1,1,1,2,2,28)	53.97
	40	1	0.04	(1,1,1,2,2,28)	56.1
		2	0.04	(1,1,1,2,2,28)	56.1
7	25	1	0.04	(1,1,1,1,2,2,17)	42.89
		2	0.04	(1,1,1,1,2,2,17)	42.89
	30	1	0.04	(1,1,1,1,2,2,22)	47.19
		2	0.04	(1,1,1,1,2,2,22)	47.19
	35	1	0.04	(1,1,1,1,2,2,27)	49.99
		2	0.04	(1,1,1,1,2,2,27)	49.99
	40	1	0.04	(1,1,1,1,2,2,32)	52.24
		2	0.04	(1,1,1,1,2,2,32)	52.24

Table 4.9: Recommended design parameters for $OR = 2$ and $\theta = 0.33$.

K	N	λ	δ	pruned $\mathcal{D}_0$	average PCS
4	25	1	0.06	(1,1,2,21)	59.91
		2	0.06	(1,1,2,21)	59.91
	30	1	0.07	(1,2,2,25)	63.69
		2	0.07	(1,2,2,25)	63.69
	35	1	0.06	(1,1,2,31)	66.04
		2	0.06	(1,1,2,31)	66.04
	40	1	0.05	(1,1,2,36)	68.14
		2	0.05	(1,1,2,36)	68.14
5	25	1	0.07	(1,1,2,2,19)	53.73
		2	0.07	(1,1,2,2,19)	53.73
	30	1	0.06	(1,1,1,2,25)	57.38
		2	0.06	(1,1,1,2,25)	57.38
	35	1	0.05	(1,1,1,1,31)	60.58
		2	0.05	(1,1,1,1,31)	60.58
	40	1	0.05	(1,1,1,1,36)	62.84
		2	0.05	(1,1,1,1,36)	62.84
6	25	1	0.05	(1,1,1,1,1,20)	49
		2	0.05	(1,1,1,1,1,20)	49
	30	1	0.06	(1,1,1,1,2,24)	52.44
		2	0.06	(1,1,1,1,2,24)	52.44
	35	1	0.06	(1,1,1,1,2,29)	55.68
		2	0.06	(1,1,1,1,2,29)	55.68
	40	1	0.05	(1,1,1,1,1,35)	58.29
		2	0.05	(1,1,1,1,1,35)	58.29
7	25	1	0.05	(1,1,1,1,1,1,19)	45.04
		2	0.05	(1,1,1,1,1,1,19)	45.04
	30	1	0.05	(1,1,1,1,1,1,24)	48.11
		2	0.05	(1,1,1,1,1,1,24)	48.11
	35	1	0.05	(1,1,1,1,1,1,29)	51.69
		2	0.05	(1,1,1,1,1,1,29)	51.69
	40	1	0.05	(1,1,1,1,1,1,34)	54.27
		2	0.05	(1,1,1,1,1,1,34)	54.27

Chapter 5

CRM with continuous risk factor

The study objective of conventional dose-finding design is usually to identify a common MTD associated with per-specified target toxicity rate for all patients. In such studies we may run into the problem of substantial patient heterogeneity. A typical example in cancer studies is that heavily pre-treated patients tend to have less tolerance to drug toxicity, compared to treatment naive patients. Extensions of standard design have been proposed to deal with heterogeneity: some sought to identify MTD for discrete number of risk groups [21; 22; 14], others used fully parameterized models to identify patient specific MTD for continuous risk factor, but the methods are difficult to generalize and adapt to a different trial. We propose a risk adjusting design using a flexible multi-parameter model to identify patient specific MTD among a discrete set of doses, and the patient heterogeneity can be indicated by either continuous or discrete risk factor. The method in the following sections is developed for continuous risk factor, but can be conveniently applied on discrete risk factor.

5.1 Design objective

The design objective is to evaluate the effect of a risk factor (continuous or discrete) on dose toxicity probabilities, and when the effect is evident, the trial will adjust for the risk factor in dose allocation and identify the patient-specific MTD: $\nu(z) = \underset{k}{\text{argmin}}|F(d_k, z) - \theta|$, $\{k : k = 1, \ldots, K\}$. where z denotes the continuous risk factor.

The following notations will be used throughout this chapter to describe the clinical setting and statistical models: Suppose a dose-finding trial has K dose levels and enrolls N patients sequentially. For the i'th patient enrolled in the trial, x_i is the dose assignment and y_i is the binary toxicity outcome. Specifically, x_i is confined to a discrete set of values, $x_i = d_k$, $k = 1, \ldots, K$, and d_k indicates the k'th dose level. The patient's risk factor value is represented using z_i, with z_0 a specified reference level for this continuous risk factor. Model parameter γ indicates the effect size of the risk factor on toxicity probability. Model parameter α_k is the intercept of the covariate-toxicity curve at the reference covariate value z_0, for the k'th dose level.

The true covariate-toxicity relationship is represented using the the most common logistic regression model, with a single continuous risk factor z and k dose levels. We assume a linear function for covariate effect and non-parametric form for dose effect, except that the toxicity probabilities are non-decreasing with dose levels for given covariate z. Assuming there is no interaction effect between covariate z and dose level d_k, this model can be represented using the following $K + 1$-parameter model.

$$\text{logit}\{F_k(z|\alpha_k, , \gamma)\} = \{\alpha_k + \gamma(z - z_0)\} \tag{5.1}$$

where $\alpha_1 \leq \alpha_2 \ldots \leq \alpha_K$. $F_k(z)$ is the toxicity probability given dose level k and z.

When the patient population are homogeneous, because either all patients have the same covariate value or the risk factor z does not have modifying effect on toxicity probability ($\gamma = 0$), the product term on the right hand side of the equation becomes

a constant, the model reduces to

$$\text{logit}\{F_k(z|\alpha_k)\} = \alpha_k \tag{5.2}$$

The $k+1$-parameter model (5.1) can be viewed as K parallel covariate-toxicity curves, and each curve has a common "slope" γ and different "intercept" α_k.

This true regression model (5.1) is also the working model to be used in the trial design in the following sections.

5.2 Trial design

Presumably a risk-adjusting design is preferred when there is a plausible biological mechanism for patient heterogeneity in drug tolerance. For example, CYP3A4 metabolises irinotecan, hence varying level of CYP3A4 activity modifies the individual's toxicity probability. However, we do not expect such effect to be prominent in every trial; thus, one should not assume the risk adjusting design is necessary at the beginning of a trial. Instead, it would be useful to evaluate the risk effect using the initially accumulated data, and only incorporate the individual risk level into the dose allocation when the risk effect becomes evident in the patients enrolled in this specific trial. If there is a lack of the risk effect during the trial, a conventional design is sufficient to serve the purpose.

To achieve such flexibility in dealing with patient heterogeneity, the trial will proceed in two stages: In the beginning, the trial will be conducted using the conventional design as if all patients are exchangeable in terms of risk in developing DLT. When sufficient data are available, a testing procedure will be used to examine the effect of risk factor z on toxicity probabilities. When the risk effect is significant enough and exceeds a pre-specified threshold, the second stage, risk adjusting stage, will be activated. During the risk adjusting stage, the $K+1$-parameter model (5.1) will be fitted using all data after each new patient is treated, and the parameter estimates

will be updated to guide the risk adjusted dose assignment for the next patient.

Exchangeable stage: We use the two-stage likelihood CRM developed in chapter 3 during this stage. While all patients enrolled in the trial are treated exchangeably in terms of individual susceptibility to drug toxicity, the trial will start from the lowest dose level and the initial dose escalation follows a pre-specified rule (initial design $\mathcal{D}_0$). Upon observing the first DLT, model based design will be activated and the dose assignments will follow a conventional one-parameter CRM model with a single parameter β modeling the dose-toxicity relationship, such as the one-parameter logistic function.

Using ψ representation, the working model is

$$\text{logit}\{F_k(\beta)\} = \{\exp(\beta)/\exp(\beta_0)\text{logit}(p_{0k})\} \tag{5.3}$$

MLE will be used to obtain the parameter estimate $\hat{\beta}$. Therefore initial values of design parameters do not impact the design performance [7]. β_0 can be set to 0 and p_{0k} can be determined by the algorithm (3.3) given a design parameter δ. Using the calibration algorithm in chapter 4, the design parameters in this stage including model sensitivity parameter δ and the most conservative and coherent initial design $\mathcal{D}_0$ can be determined given the clinical parameters. The dose assignment for the next patient enrolled in the trial is determined using the formula

$$\hat{x}_i = \underset{k}{\text{argmin}} \left| \frac{\exp(\hat{\beta})\text{logit}(p_{0k})}{1+\exp(\hat{\beta})\text{logit}(p_{0k})} - \theta \right| \tag{5.4}$$

For ethical reason, we allow no more than one dose level escalation or de-escalation at any time during the exchangeable stage.

Switching condition: As more data are cumulated during the exchangeable stage, we may be able to start to test the presence of the patient heterogeneity by fitting $k+1$-parameter model 5.1 on the data, and evaluate the risk effect estimate $\hat{\gamma}$ and the significance level. However, certain conditions are required to obtain a valid estimate of $\hat{\gamma}$ using the $k+1$-parameter model.

Condition 1: Toxicity outcome heterogeneity is observed on at least one dose level.

Condition 2: Among the dose levels that satisfy condition 1, there exists non-perfect partition of covariate z by toxicity outcome on at least one of them.

If we denote m_k as the number of patients who are treated on dose level k and t_k as the number of them develop toxicity, then condition 1 is equivalent to that there exists at least a k, $k \in \{k : m_k > 0\}$, such that $0 < t_k < m_k$. Condition 2 is equivalent to that among all the dose levels that satisfy condition 1, there exists at least a k, such that $\min\{z_i : x_i = d_k, y_i = 1\} < \max\{z_i : x_i = d_k, y_i = 0\}$, **a**nd $\min\{z_i : x_i = d_k, y_i = 0\} < \max\{z_i : x_i = d_k, y_i = 1\}$, $i = 1, \ldots, N$.

Once these two conditions are met, we will fit the $k+1$-parameter model to obtain $\hat{\gamma}$ and determine if the effect is strong enough to switch to the next stage, risk-adjusting design. Assuming $i-1$ patients have been treated in the exchangeable stage, and both conditions are met, we can obtain $\hat{\gamma}$ by maximizing the conditional likelihood function [4]. Let j be the running index to denote the j'th patient from the total of $i-1$ patients treated thus far, and $I(.)$ be an indicator function, the full likelihood is

$$\mathcal{L}(\gamma, \alpha_1, \ldots, \alpha_K) = \frac{exp[\sum_{k=1}^{K} \sum_{j=1}^{i-1} y_j I(x_j = d_k)\{\alpha_k + \gamma(z_j - z_0)\}]}{\prod_{k=1}^{K} \prod_{j=1}^{i-1} [1 + \exp\{\alpha_k + \gamma(z_j - z_0)\}]^{I(x_j = d_k)}}$$

The sufficient statistics for α_k is $\sum_{j=1}^{i-1} y_j I(x_j = d_k)$, for $k = 1, \ldots, K$. The sufficient statistics for γ is $\sum_{k=1}^{K} \sum_{j=1}^{i-1} y_j (z_j - z_0) I(x_j = d_k)$.

Let $t_{k,i-1} = \sum_{j=1}^{i-1} y_j I(x_j = d_k)$, which indicates the total number of toxicities occurred on dose level k after $i-1$ patients are treated. The conditional likelihood function (conditioning on $t_{k,i-1}$, the sufficient statistics for α_k) is

$$\mathcal{L}(\gamma | t_{k,i-1}) = \prod_{k=1}^{K} \frac{exp\{\sum_{j=1}^{i-1} (z_j - z_0) y_j I(x_j = d_k)\gamma\}}{\sum_{s(t_{k,i-1})} exp\{\sum_{j=1}^{i-1} (z_j - z_0) y_j I(x_j = d_k)\gamma\}} \tag{5.5}$$

where $\sum_{s(t_{k,i-1})}$ indicates summation of the summand over all the possible sets $\{y_j : \sum_{j=1}^{i-1} y_j I(x_j = d_k) = t_{k,i-1}\}$.

$\hat{\gamma}$ is estimated by maximizing the conditional likelihood (5.5). However, this estimate may be highly variable due to small number of patients tested at the beginning of a trial, thus lead to a large p value. To conduct such a risk-adjusting dose-finding study, we often have some knowledge about the covariate effect while planning for the trial, where at least we could anticipate the direction of the effect estimate. Therefore we adopt one-sided test instead of two-sided test to evaluate the strength of the risk effect on toxicity probability. If the one-sided p value is sufficiently small and less than a pre-specified threshold p^*, the trial will switch to the risk-adjusting stage where the subsequent dosing algorithm will take into account the individual risk z. Otherwise, the trial proceeds in exchangeable stage, where $\hat{\beta}$ in the regular one-parameter model (5.3) will be updated using the $i-1$ patients and dosing algorithm (5.4) will be used to determine the dose level for the next patient. Meanwhile, $k+1$-parameter model will be re-fitted to obtain $\hat{\gamma}$ each time a new patient is enrolled and treated, and the switching condition will be re-examined to determine when the trial will switch to the next stage.

We use Wald test statistic based on the asymptotic normality of $\hat{\gamma}$ to derive the one-sided p value. A trial would switch to the risk-adjusting stage only if the observed covariate effect aligns with the prior knowledge and is evident enough. When an opposite effect is observed, the trial will continue in the exchangeable stage because of the uncertainty of the risk effect due to the conflict with the prior knowledge.

Risk-adjusting stage: When the switching condition is satisfied, i.e., the one-sided p value drops below a threshold value p^*, the trial will switch to the next stage and adjust for the individual risk factor. At this point, toxicity outcome heterogeneity has been observed on at least one dose level, and possibly on multiple dose levels. While it is possible that higher dose level(s) have not yet been assigned with any patients, each of the lower dose levels should have been assigned with at least one patient, due to the no dose skipping rule from the exchangeable stage. In other words, we expect to test at least one patient on each of the consecutive dose levels starting

from the lowest one.

For these consecutive dose levels each with at least one assigned patient, the corresponding covariate-toxicity curve intercept α_k can be estimated given the recently updated $\hat{\gamma}$. Assuming a total of $i-1$ patients enrolled and treated after entering the risk adjusting stage, the full likelihood is

$$\mathcal{L}(\gamma, \alpha_1, \ldots, \alpha_K) = \frac{exp[\sum_{k=1}^{K}\sum_{j=1}^{i-1} y_j I(x_j = d_k)\{\alpha_k + \hat{\gamma}(z_j - z_0)\}]}{\prod_{k=1}^{K}\prod_{j=1}^{i-1}[1 + \exp\{\alpha_k + \hat{\gamma}(z_j - z_0)\}]^{I(x_j = d_k)}}$$

We can set the following score functions to be zero

$$\frac{\partial log\mathcal{L}}{\partial \alpha_k} = \sum_{j=1}^{i-1} I(x_j = d_k)\left[y_j - \frac{exp\{\alpha_k + \hat{\gamma}(z_j - z_0)\}}{1 + exp\{\alpha_k + \hat{\gamma}(z_j - z_0)\}}\right] = 0 \tag{5.6}$$

where $k \in \{k : 0 < m_k, k = 1, \ldots, K\}$, and $m_k = \sum_{j=1}^{i-1} I(x_j = d_k)$ and $\hat{\gamma}$ is the solution that maximizes the conditional likelihood (5.5).

To obtain the estimates of α_k under the non-decreasing constraint, we first obtain $\tilde{\alpha}_k$, which are the solutions to the equations (5.6). Specifically, $\tilde{\alpha}_k$ equals to a finite value when heterogeneous toxicity outcomes are observed on k'th dose level, i.e., $k \in \{k : 0 < m_k, k = 1, \ldots, K, \text{ and } 0 < t_k < m_k\}$; $\tilde{\alpha}_k$ equals to $-\infty$ when no patient developed toxicity on this dose level, i.e., $k \in \{k : 0 < m_k, k = 1, \ldots, K; \text{ and } t_k = 0\}$; $\tilde{\alpha}_k$ equals to ∞ when all patients developed toxicities on this dose level, i.e., $\{k : 0 < m_k, k = 1, \ldots, K \text{ and } t_k = m_k\}$.

The solutions $\tilde{\alpha}_k$ will be examined for violations of the non-decreasing constraint between any neighboring pairs. When a violation occurs, we will apply the pool-adjacent-violator algorithm (PAVA) [1] iteratively, until the updated estimate $\hat{\alpha}_k$ satisfies the non-decreasing constraint, i.e., $\hat{\alpha}_1 \leq \hat{\alpha}_2 \leq \ldots \leq \hat{\alpha}_K$, where $\{k : 0 < m_k, k = 1, \ldots, K\}$.

To illustrate the calculation of $\hat{\alpha_k}$ following the aforementioned procedure, a snapshot of patient level data at the end of a simulated trial with $K = 5$ and $N = 40$ is listed in Table 5.1. The data are grouped by dose levels, and both the covariate value and toxicity outcome for each patient is listed. Through maximizing the conditional

likelihood on this set of data, we obtain $\hat{\gamma} = -3.5$ and the associated one-sided p value 0.027. Table 5.2 lists summary statistics for the patient level data in Table 5.1: number of assigned patients m_k and observed toxicities t_k on each dose level; the corresponding raw estimate ($\tilde{\alpha}$) and the constraint estimate ($\hat{\alpha}$). Since zero toxicity occurs on dose level 1 and 5, $\tilde{\alpha}_1 = \tilde{\alpha}_5 = -\infty$; the estimates on the rest of the dose levels take finite values due to the heterogeneous outcome. Because $\tilde{\alpha}_4 > \tilde{\alpha}_5$, violating the non-decreasing constraint, the patient level data on these two dose levels were pooled together to obtain the updated estimates $\hat{\alpha}_4 = \hat{\alpha}_5 = -0.86$. Since there is no further violation of the constraint among the updated estimate, they serve as the final estimate of the intercept parameters.

Dose assignment algorithm: Similar to the dose assignment algorithm in the exchangeable stage, the dose with toxicity probability closest to the target rate will be assigned to the next patient in the risk adjusting stage. However, the dose toxicity probabilities not only vary by doses but also depend on patient specific risk level, the one dimensional search problem becomes two dimensional, with an additional factor z. $\nu(z) = \underset{k}{\operatorname{argmin}} |F(d_k, z) - \theta|$, $\{k : k = 1, \ldots, K\}$.

After estimating the parameters $\hat{\gamma}$ and $\hat{\alpha}_k$, the entire covariate-toxicity curve can be constructed by inserting these estimates into the $k+1$-parameter model (5.1) for each of the consecutively tested dose levels $\{k : 0 < m_k, k = 1, \ldots, K\}$. The toxicity probability at covariate z on dose level k is estimated as $\hat{F}_k(z|\hat{\gamma}, \hat{\alpha}_k) = \frac{\exp\{\hat{\alpha}_k + \hat{\gamma}(z - z_0)\}}{1 + \exp\{\hat{\alpha}_k + \hat{\gamma}(z - z_0)\}}$. To determine the optimal dose for a newly enrolled i'th patient with covariate z_i, a set dose toxicity probability estimates can be read off the estimated covariate-toxicity curves at $z = z_i$, : $\{\hat{p}_k(z = z_i), k = 1, \ldots, K\}$. To determine the dose assignment for this specific patient with covariate z_i, we only need to concern this panel of cross-sectional values instead of the entire covariate-toxicity curves, and the decision becomes a one-dimensional problem.

However, the covariate-toxicity curves for some dose levels may not be distinguishable or even available, if the trial has not proceeded far enough to collect sufficient

data. Particularly, two or more adjacent dose levels will have identical estimated covariate-toxicity curves after applying PAVA. When there are multiple doses with risk adjusted toxicity probability equally close to the target toxicity rate θ, denoted as $\mathcal{C}_i = \{k : |\hat{p}_k(z) - \theta| \leq |\hat{p}_j - \theta|, j \neq k, j, k \in 1, \ldots, K\}$ and the estimated toxicity probability $\hat{p}_k(z)$ for this set is higher than the target toxicity rate θ, we would consider the lowest dose in this set to be the most "likely" correct dose, because potentially the lower dose may be differentiated from the rest and be the single dose that is closest to the target rate should more data be collected. Likewise, we consider the highest dose in this set to be the more "likely" correct dose when the estimated probability $\hat{p}_k(z)$ is lower than θ. In summary, the most "likely" dose is defined as below, for the

$$\hat{\nu}(z_i) = \begin{cases} \min\{\mathcal{C}_i(z_i)\} & \text{if } \hat{p}_{\mathcal{C}_i(z_i)} \geq \theta, \\ \max\{\mathcal{C}_i(z_i)\} & \text{if } \hat{p}_{\mathcal{C}_i(z_i)} < \theta \end{cases} \tag{5.7}$$

Figure 5.1 demonstrates an example where dose 1 and 2 share the same estimated covariate-toxicity curve, dose 3 and 4 share the same covariate-toxicity curve, and estimate on dose 5 is not available as trial has not escalated to the highest dose level yet. With any given covariate z value, the set of point estimates on these curves at z can be extracted and plotted separately as a function of dose. For a finite number of doses, a dose-toxicity curve appears as a step function with at most K steps if the estimates on all dose levels are available and distinguishable. As shown in Figure 5.2, the step function has only two steps as there are only two distinguishable dose toxicity estimates from the five dose levels. The fifth dose level is not estimable and indicated with a circle and labelled as"NA" on the step function. Since the cross-sectional estimate of dose toxicity probabilities is also a function of covariate value z, the position of the dose-toxicity curve (the step function) relative to the same target toxicity rate θ vary depends on the input of z. If the newly enrolled i'th patient has a relatively low tolerance level due to the low expression level of the metabolic enzyme, i.e., $z_i = 3.35$ as shown in the upper left graph of Figure 5.2, dose 1 and 2 are the

closest to the target rate. As both doses still appear more toxic than expected as they yield higher toxicity probability than the target rate θ, according to the algorithm 5.7, dose 1 will be assigned to this patient. With higher covariate value, a patient is able to tolerate higher dose level. Consequently, dose level 2 and 3 would be assigned if z is sufficiently large (the upper right and middle left graphs in Figure 5.2).

Table 5.1: Simulated patient data on each dose level in a single trial.

Dose level 1																								
y	0																							
z	3.31																							
Dose level 2																								
y	0	0	0	0	0	0	0	0	0	0	0	0	1	0										
z	3.69	3.2	3.53	3.42	3.99	3.41	3.24	3.38	3.58	3.78	3.75	3.02	3.19											
Dose level 3																								
y	0	1	0	1	1	1	0	0	1	0	0	0	0	0	1	0	0	0	0	1				
z	3.53	3.69	3.31	3.09	3.41	3.51	3.42	3.88	2.9	3.64	3.29	3.86	3.34	3.86	3.46	2.87	3.31	2.91	3.5	4.04	2.74			
Dose level 4																								
y	0	1	0																					
z	3.23	3.52	3.75																					
Dose level 5																								
y	0	0																						
z	4.01	3.88																						

Table 5.2: Estimating α using simulated data in 5.1 with $N = 40$,K=5, $z_0 = 3.44$, and $\gamma = -4$. The conditional logistic regression yields $\hat{\gamma} = -3.5$ and p=0.027.

n_k	1	12	14	2	2
t_k	0	1	7	1	0
$\tilde{\alpha}_k$	$-\infty$	-2.74	-1.04	-0.61	$-\infty$
$\hat{\alpha}_k$	$-\infty$	-2.74	-1.04	-0.86	-0.86

The dose assignment algorithm is more complicated for patient tolerating higher doses (high z value) as the decision may involve dose level(s) with unavailable toxicity estimate. As shown in Figure 5.1, dose 5 is not available because either the trial has not escalated to it or the dose is too toxic and the trial had finished at a lower dose. This is problematic when both dose 3 and 4 are the closest doses to θ and their estimate is below θ. According to definition 5.7, dose 4 should be the recommended dose. However, we cannot rule out the possibility that dose level 5 is the most "likely" dose just because data is not available to estimate its toxicity probability. There is a higher chance that dose level 5 is the most "likely" one if the estimate $\hat{p}(z)_3 = \hat{p}(z)_4$ is too far below θ. We further incorporate "acceptable probability range" to facilitate the decision making in such situations. The recommended dose from the estimable set by definition 5.7 remain the most "likely" dose if the estimated toxicity probability falls within an symmetric window around target rate $[\theta - h, \theta + h]$; otherwise, the immediate next dose level outside the estimable set is the most "likely" dose. Suppose $h = 0.05$, the middle right and bottom left graphs in Figure 5.2 illustrate that patients with relatively large covariate values $z = 3.80$ and $z = 3.95$ are assigned dose levels 4 and 5, respectively, using this "acceptable probability range" approach. This dosing algorithm provides another level of flexibility and allows dispersion in dose assignment to explore the more toxic doses.

Furthermore, a map can be generated to illustrate the one-to-one correspondence

between risk factor level z and MTD. This map summarizes the dose assignment decisions across a wide range of covariate z values, and it again appears to be a step function (Figure 5.3). Instead of generating an individual graph for each specific z value as in Figure 5.2, this map shows dose assignment for continuously changing z values. One can easily identify the next optimal dose level by drawing a vertical line with x-axis at z and the assigned dose level $\hat{\nu}(z)$ would be the one that the line crosses. Such map is particularly useful in the end of a trial as the final product of dosing guidance to help physicians make a decision according to each patient's specific risk level.

5.3 Simulation

5.3.1 True scenarios

The true risk effect on toxicity probability γ is chosen based on Irinotecan data analysis in the introduction section. The multi-variable analysis on composite DLT endpoint (grade ≥ 3 neutropenia, leukopenia or diarrhea) suggests the effect estimate of baseline clearance level (largely determined by CYP3A4 activity level) on toxicity is -4.07, i.e., one unit increase in log transformed baseline clearance level decreases the odds of having any DLT by 98%. Since -4 indicates a rather steep slope of the covariate-toxicity curve, to evaluate the design performance under varying extent of risk effect, the true γ takes one of the following three values: -4, -2, and 0. Particularly, $\gamma = 0$ represents no covariate effect on toxicity probability and flat covariate-toxicity curves, for which the conventional dose-finding study for homogeneous patient population is deemed to be sufficient. In addition to the slope parameter (γ), the true "intercepts" α_k's are determined via specifying the true dose toxicity probabilities at the reference covariate value $z = z_0$. For each γ value, K true dose toxicity profiles at $z = z_0$ were generated to cover from the most toxic scenario (dose level 1 has target toxicity probability) to the least toxic scenario (dose level K has the target toxicity

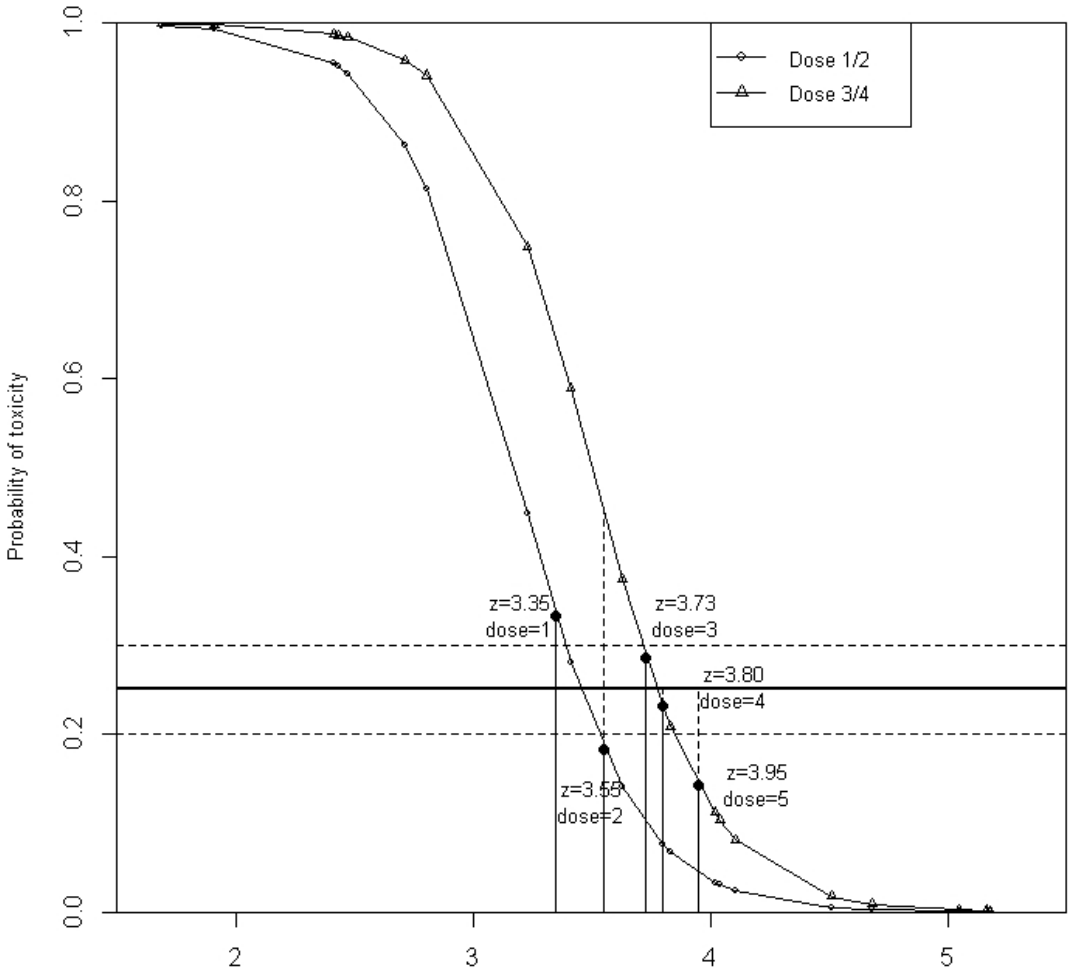

Figure 5.1: An example of estimated covariate-toxicity curves: dose 1 and 2 share the same curve; dose 3 and 4 share the same curve; dose 5 is not available. The covariate value and the corresponding risk-adjusted MTD for 5 example patients are labelled.

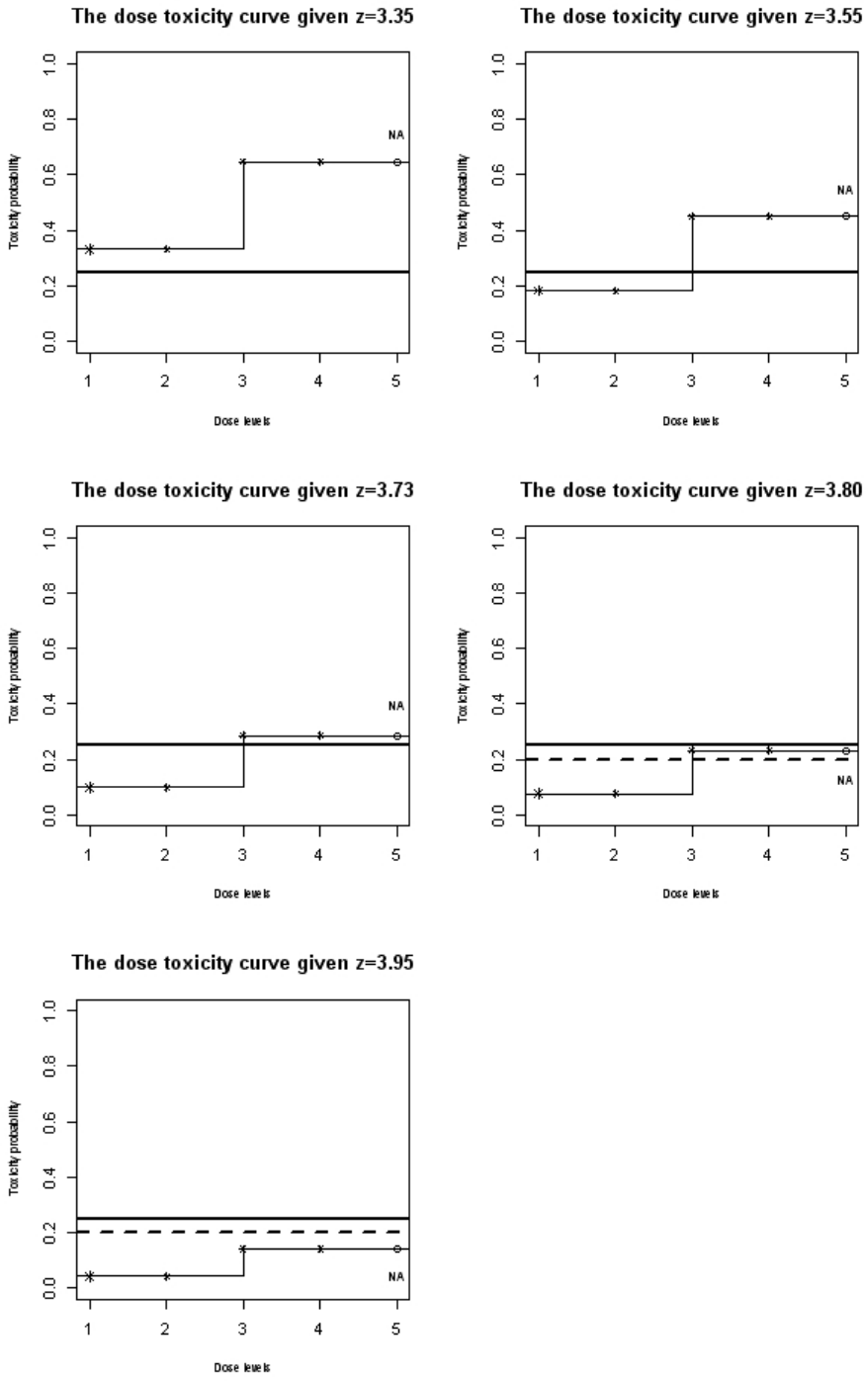

Figure 5.2: The estimated dose-toxicity curves given the estimated covariate-toxicity curves in figure 5.1, for $z = 3.35$,$z = 3.55$,$z = 3.73$,$z = 3.80$ and $z = 3.95$. The risk-adjusted dose for each of these z values is dose level 1, 2, 3, 4, and 5, respectively.

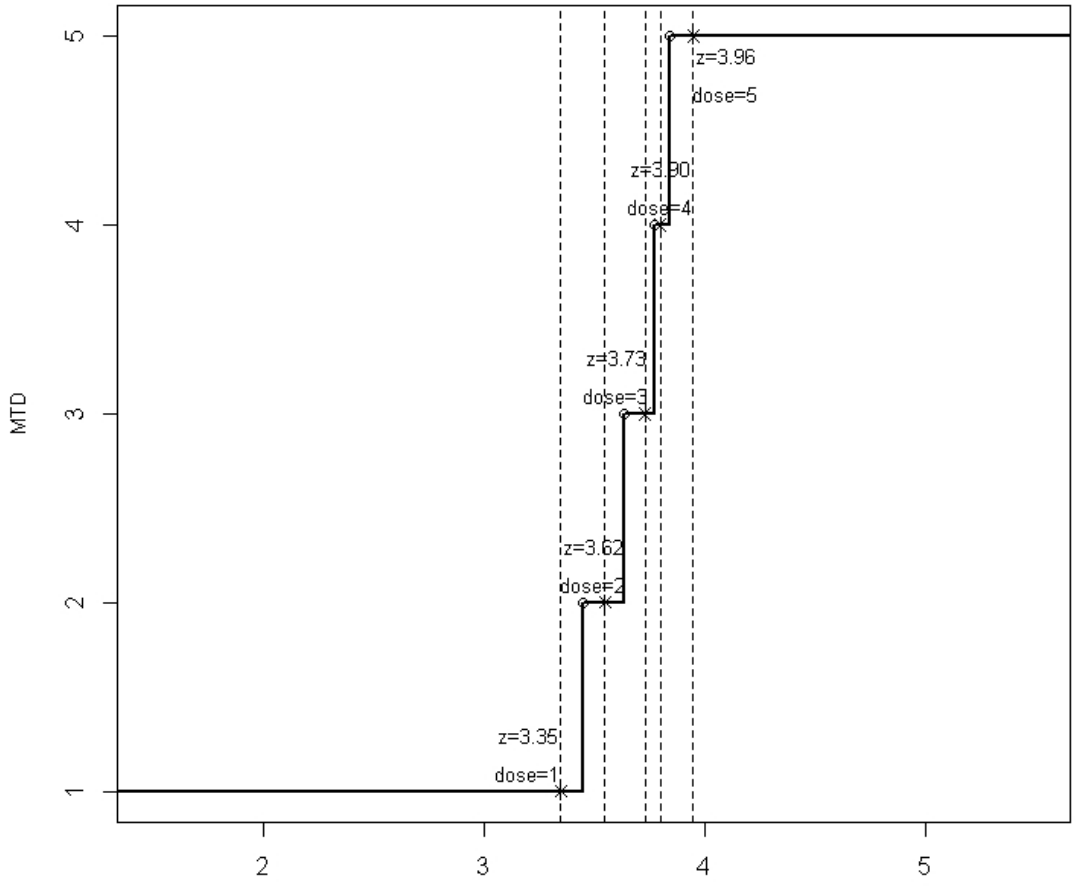

Figure 5.3: The step function to map the covariate range and risk-adjusted MTD, with the same 5 examples labelled on the map.

probability). The target toxicity rate is $\theta = 25\%$.

All fifteen true scenarios (3 γ values and $K = 5$ sets of dose toxicity profiles) are illustrated in Figures 5.4,5.5,5.6. In each figure, $K = 5$ scenarios were generated by setting the toxicity probabilities given $z = z_0$ as {0.25,0.4,0.45,0.55,0.55}, {0.05, 0.25, 0.4, 0.45, 0.55},{0.05,0.05, 0.25, 0.45, 0.55}, {0.05,0.05,0.08,0.25,0.45},{0.05,0.05,0.08,0.12,0.25} [16]. The true α_k's are derived as $\alpha_k = \log\{p_k/(1-p_k)\}$, where p_k is the k'th dose toxicity probability. Larger γ indicates steeper covariate-toxicity curves and stronger risk effect on toxicity probability. Consequently, a relatively small change in covariate z would cause shift in MTD.

5.3.2 Trial simulation and conduct

With target toxicity rate $\theta = 0.25$ and $K = 5$, for each trial, we specify the total number of patients to be enrolled $N = 40$, the same sample size as the Irinotecan trial[30]. The patient level data in each trial are simulated sequentially, with the covariate value $z_i \sim N(3.44, 0.31)$ and toxicity tolerance score $u_i \sim U(0, 1)$. The mean and standard deviation of the covariate distribution are estimated based on the distribution of the natural log transformed baseline clearance level in the Irinotecan data set [30]. The individual true toxicity probability at any covariate z_i can be calculated using $\pi(d_k, z) = \frac{\exp\{\alpha_k+\gamma(z_i-z_0)\}}{1+\exp\{\alpha_k+\gamma(z_i-z_0)\}}$, where α_k is the corresponding true intercept value at dose level d_k in the specified true scenarios. If u_i is less than the true toxicity probability $\pi(d_k, z)$, the patient will experience DLT and y_i=1, otherwise y_i=0.

Based on Table 4.8 in chapter 4, the design parameters in the exchangeable stage are determined as follows: one-parameter logistic dose-toxicity function, half width of the indifference interval δ=0.04, and the most conservative and coherent initial design $\mathcal{D}_0 = \{1, 1, 2, 2, 34\}$. Each simulated trial starts using the same two-stage likelihood CRM design and the trial will either switch to risk-adjusting stage or remain in the exchangeable stage depending on whether the switching condition is met. As

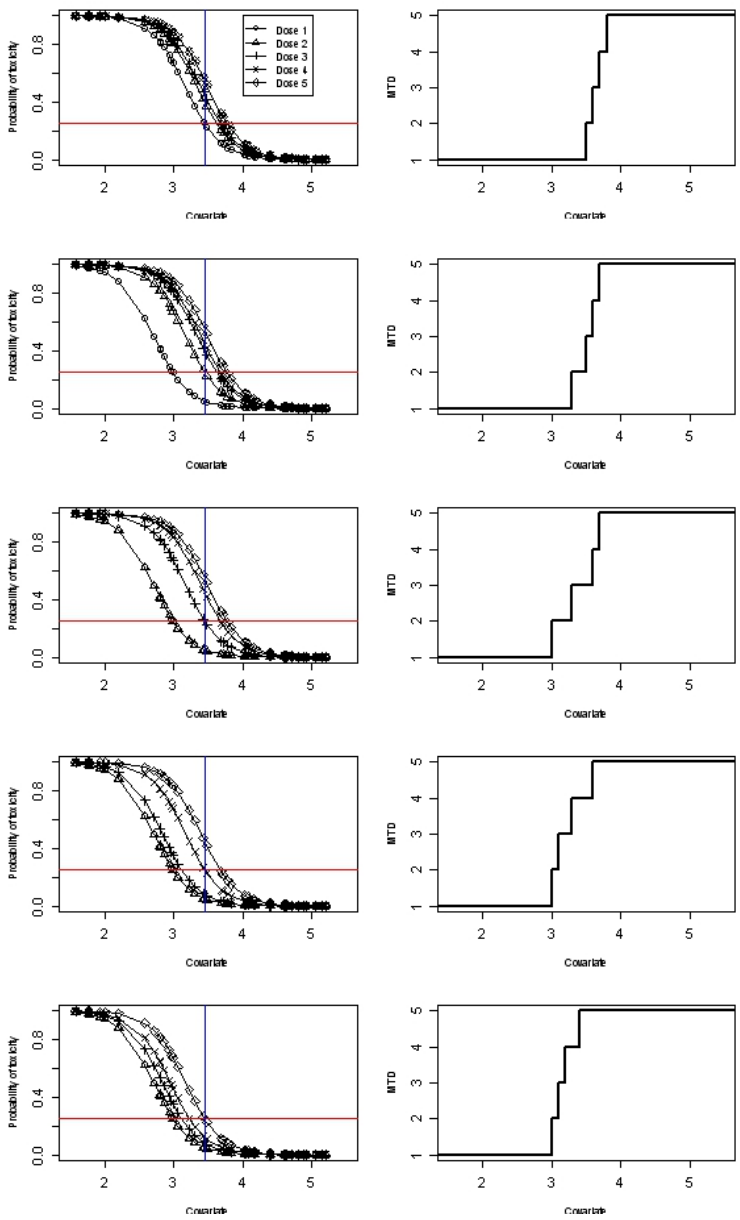

Figure 5.4: True toxicity scenarios with $\gamma = -4$, K=5, θ=0.25 (horizontal reference line). From top to bottom on the left-hand side, the 5 true covariate-toxicity graphs represent most toxic scenario (dose level 1 has target toxicity rate of 25% at $z_0 = 3.45$) to the least toxic scenario (dose level 5 has target toxicity rate of 25% at $z_0 = 3.45$). The reference covariate value $z_0 = 3.45$ is labelled using a vertical reference line. From top to bottom on the right-hand side, the step function to map covariate range and the true risk-adjusted MTD for each scenario.

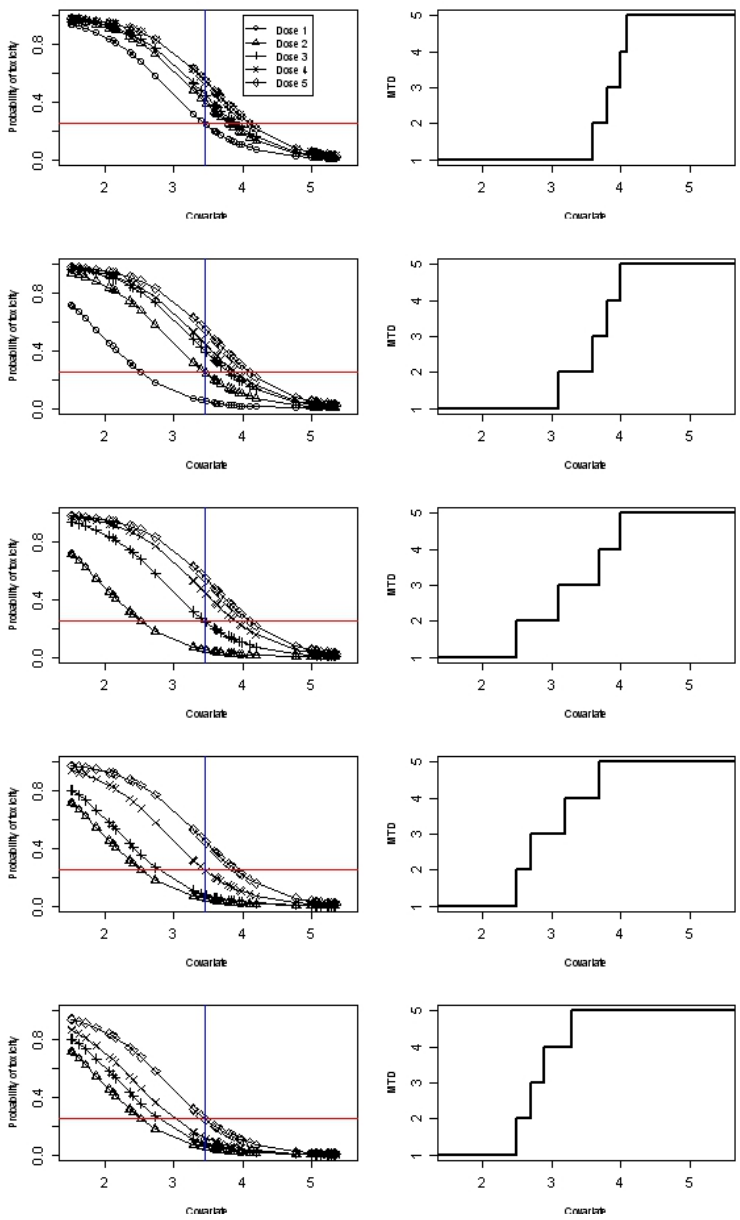

Figure 5.5: True toxicity scenarios with $\gamma = -2$, K=5, θ=0.25 (horizontal reference line). From top to bottom on the left-hand side, the 5 true covariate-toxicity graphs represent most toxic scenario (dose level 1 has target toxicity rate of 25% at $z_0 = 3.45$) to the least toxic scenario (dose level 5 has target toxicity rate of 25% at $z_0 = 3.45$). The reference covariate value $z_0 = 3.45$ is labelled using a vertical reference line. From top to bottom on the right-hand side, the step function to map covariate range and the true risk-adjusted MTD for each scenario.

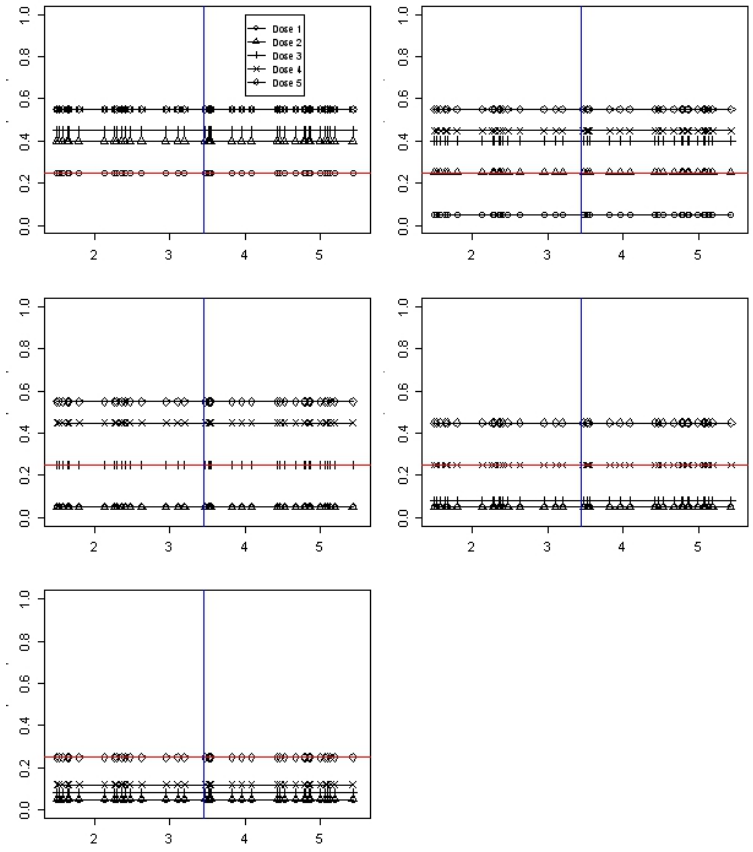

Figure 5.6: True toxicity scenarios with $\gamma = 0$, K=5, θ=0.25 (horizontal reference line). The 5 true covariate-toxicity graphs represent most toxic scenario (dose level 1 has target toxicity rate of 25% at $z_0 = 3.45$) to the least toxic scenario (dose level 5 has target toxicity rate of 25% at $z_0 = 3.45$). The reference covariate value $z_0 = 3.45$ is labelled using a vertical reference line.

part of the switching criteria, we specify the threshold for one-sided p value range among 0,0.01,0.05,0.1,0.2, 0.5 and 0.75, to reflect an increasingly flexible control on entering the risk adjusting stage. Particularly, the p value threshold 0 allows no transition into risk-adjusting stage, hence the entire trial is carried out using the two-stage likelihood design to identify a common MTD for homogenous study population. Different dosing algorithm is used in different stages as described previously. When expanding to the unexplored high dose levels during the risk-adjusting stage, the half width of the "acceptable probability window" $h = 0.05$, indicating the dose with estimated toxicity probability within $\theta \pm$ 5%, i.e., $[20\%, 30\%]$, is "acceptable".

All dose assignments and toxicity outcomes for patients enrolled during the trial are recorded. If a trial stays within the exchangeable stage at the end of the simulation, the final recommended MTD is recorded. Otherwise, a final set of estimates $\hat{\gamma}$ and $\hat{\alpha}_k$ will be obtained using records of all $N = 40$ patients.

5.3.3 Simulation results

Under each of the 15 true scenarios and each p threshold value, two thousand trials were simulated. Table 5.3 lists the number of trials remaining at the exchangeable stage or entered the risk-adjusting stage in the end. With very strong risk effect on toxicity, larger proportion of trials switched to risk-adjusting stage. Trials also have higher chance to enter the risk-adjusting stage under more toxic scenario (scenario 1) compared to less toxic scenario (scenario 5). As the design parameter p threshold increases, an increasing number of trials is allowed to switch to the risk-adjusting stage.

With $\gamma = 0$, i.e., no risk effect on toxicity outcome and patients are homogeneous in terms of probability of developing toxicity, the proportion of trials ended in risk-adjusting stage are the false positive trials. The bottom panel in Table 5.4 shows the design's false positive rate increases as p value threshold increases. With non-zero risk effect ($\gamma = -4$ or -2), the proportion of trials remaining at exchangeable stage

are the false negative trials. Apparently the false negative proportion depends on the risk effect size. The top two panels in Table 5.4 show that the false negative rate decreases as p value threshold becomes large. For the true effect size $\gamma = -4$, the design with $p = 0.05$ yields 6-15% false negative rates and around 7-11% false positive rates across scenarios.

Table 5.3: Summary of the final status of 2000 simulated trials.

γ=-4	p=0		p=0.01		p=0.05		p=0.10		p=0.20		p=0.50		p=0.75	
	Exch	Risk-adj	Exch	Risk-adj	Exch	Risk-adj	Exch	Risk-adj	Exch	Risk-adj	Exch	Risk-adj	Exch	Risk-adj
Scenario 1	2000	0	720	1280	128	1872	44	1956	16	1984	0	2000	0	2000
Scenario 2	2000	0	1210	790	251	1749	108	1892	28	1972	7	1993	7	1993
Scenario 3	2000	0	1340	660	280	1720	118	1882	36	1964	7	1993	7	1993
Scenario 4	2000	0	1323	677	294	1706	112	1888	42	1958	8	1992	5	1995
Scenario 5	2000	0	1366	634	311	1689	131	1869	42	1958	11	1989	10	1990
γ=-2														
Scenario 1	2000	0	1665	335	806	1194	457	1543	190	1810	17	1983	1	1999
Scenario 2	2000	0	1814	186	1023	977	579	1421	245	1755	32	1968	2	1998
Scenario 3	2000	0	1847	153	1051	949	607	1393	271	1729	34	1966	3	1997
Scenario 4	2000	0	1853	147	1041	959	586	1414	249	1751	43	1957	7	1993
Scenario 5	2000	0	1832	168	1069	931	636	1364	287	1713	39	1961	5	1995
γ=0														
Scenario 1	2000	0	1983	17	1789	211	1528	472	1026	974	313	1687	68	1932
Scenario 2	2000	0	1991	7	1829	171	1532	468	1072	928	319	1681	81	1919
Scenario 3	2000	0	1990	10	1846	154	1572	428	1105	895	375	1625	71	1929
Scenario 4	2000	0	1994	6	1827	173	1540	460	1091	909	372	1628	87	1913
Scenario 5	2000	0	1996	4	1833	167	1580	420	1131	869	383	1617	83	1917

Table 5.4: False negative and false positive rates based on 2000 simulated trials.

γ=-4	p=0	p=0.01	p=0.05	p=0.10	p=0.20	p=0.50	p=0.75
%	FN	FN	FN	FN	FN	FN	FN
Scenario 1	100	36	6.4	2.2	0.8	0	0
Scenario 2	100	60.5	12.6	5.4	1.4	0.35	0.35
Scenario 3	100	67	14	5.9	1.8	0.35	0.35
Scenario 4	100	66.2	14.7	5.6	2.1	0.4	0.25
Scenario 5	100	68.3	15.6	6.6	2.1	0.55	0.5
γ=-2							
%	FN	FN	FN	FN	FN	FN	FN
Scenario 1	100	83.3	40.3	22.9	9.5	0.85	0.0
Scenario 2	100	90.7	51.2	29.0	12.3	1.6	0.1
Scenario 3	100	92.4	52.6	30.4	13.6	1.7	0.15
Scenario 4	100	92.7	52.1	29.3	12.5	2.2	0.35
Scenario 5	100	91.6	53.5	31.8	14.4	1.2	0.25
γ=0							
%	FP	FP	FP	FP	FP	FP	FP
Scenario 1	0	0.85	10.55	23.6	48.7	84.35	96.6
Scenario 2	0	0.4	8.55	23.4	46.4	84.05	95.95
Scenario 3	0	0.5	7.7	21.4	44.75	81.25	96.45
Scenario 4	0	0.35	8.65	23	45.45	81.4	95.65
Scenario 5	0	0.2	8.35	21	43.45	80.85	95.85

To evaluate the benefit of using risk-adjusting design, we use two different approaches to summarize the results: 1) intra-trial dose allocation. 2) probability of correct dosing, under-dosing and over-dosing based on the final model estimate in the end of the trial.

Intra-trial dose allocation: The model based sequential design repeatedly updates the dose-toxicity model based on the available data to treat the next enrolled patient on the current best estimate of the MTD. This characteristic suggests that its advantage is not only to obtain more accurate dose recommendation in the end of a trial, but also to maximize the chance of receiving correct dose for the patients participating the trial. Risk-adjusting design directly incorporates individual drug tolerability when assigning doses to patients enrolled in a trial, thus enhancing the dosing accuracy for each individual patient, which is desirable feature from an ethical perspective. We evaluate the intra-trial dose allocation of risk-adjusting design and make comparison with conventional design under various scenarios using simulated data.

We denote the assigned dose for the i'th patient with covariate z following the risk-adjusting design as $\hat{x}_i(z)$, and the dose which should have been received according to the simulated true tolerability, $x_i(z)$. Tables 5.5, 5.6, and 5.7 list the cross tabulations of x_i and $\hat{x}_i$ divided by the number of simulated trials two thousand, under specific scenarios defined by risk effect size, toxicity profile, and p threshold. The number listed in the i'th row and j'th column in each square represents the percentage of patients who should have received dose i while actually received dose j, $j, i = 1, \ldots, K$. The sum of the each $K \times K$ square equal to 100.

Since the patient-specific risk factor z is simulated using a normal distribution that samples more patients with covariate values around the mean z_0, a majority of patients is expected to receive the lowest dose under the most toxic scenario (scenario 1), and the highest dose under the least toxic scenario (scenario 5). Therefore, the highest row percentage in each square shifts from dose 1 to dose 5, and within that

row most patients are assigned on the correct dose ($j = i$) or neighboring doses.

Each square can be further summarized using the proportion of correct dosing, under dosing and over dosing, which are the total proportions fall on, below and above the diagonal line. These summaries are listed in Table 5.8. When there is a strong risk effect ($\gamma = -4$ or $\gamma = -2$), the conventional design without adjusting for risk factor (p threshold equals to 0) is least desirable, as it yields the lowest correct dosing proportion. The dosing accuracy increases as the p threshold increases to 0.20, and levels off as p continues to increase. Meanwhile, using risk-adjusting design by relaxing p value threshold effectively reducing both over dosing and under dosing proportions. Specifically, compared to the conventional design (p=0), using risk-adjusting design with p threshold 0.20 increases the correct dosing proportion from 33.2% to 42.1% (a relative increase of 27%) for $\gamma = -4$, and increases from 43.4% to 46.3% (a relative increase of 6.7%) for $\gamma = -2$. However, when there is no risk effect ($\gamma = 0$), the conventional design (p=0) remains the most suitable design and yields the highest correct dosing proportion and lowest under/over dosing proportions. However, even in the least favorable scenarios for using risk-adjusting design($\gamma = 0$), the risk-adjusting design seems fairly robust and does not lose much dosing accuracy, compared to the conventional design, as the difference in correct dosing proportion using these two designs (p=0 vs. p=0.20) is only 2%.

Table 5.5: Summary of intra-trial dose allocation, γ=**-4**.

scenario 1

	p=0					p=0.01					p=0.05					p=0.10					p=0.20					p=0.50					p=0.75				
truth	1	2	3	4	5	1	2	3	4	5	1	2	3	4	5	1	2	3	4	5	1	2	3	4	5	1	2	3	4	5	1	2	3	4	5
1	48.8	8.1	3.3	1.2	0.5	48.3	8.3	3.4	1.3	0.6	47.7	8.3	3.7	1.5	0.7	47.6	8.3	3.9	1.5	0.7	47.4	8.2	4.0	1.5	0.7	47.1	8.3	4.2	1.6	0.7	46.9	8.5	4.3	1.6	0.7
2	9.6	1.5	0.7	0.2	0.1	8.7	1.9	0.9	0.4	0.3	7.1	0.6	1.4	0.6	0.4	6.6	2.7	1.5	0.8	0.5	6.2	2.9	1.6	0.8	0.6	6.1	2.9	1.6	0.9	0.6	6.1	3	1.6	0.9	0.6
3	5.6	1	0.4	0.1	0.1	5	1.2	0.6	0.3	0.2	3.8	1.7	0.9	0.5	0.4	3.4	1.8	1.0	0.5	0.5	3.1	1.8	1.1	0.6	0.6	3	1.9	1.1	0.6	0.6	3	1.9	1.1	0.6	0.6
4	3.2	0.5	0.2	0.1	0	2.8	0.6	0.3	0.2	0.1	2.0	0.9	0.5	0.3	0.2	1.8	1.0	0.6	0.4	0.3	1.6	1.0	0.6	0.4	0.4	1.6	1	0.6	0.4	0.4	1.6	1	0.6	0.4	0.4
5	11.6	1.9	0.9	0.3	0.1	10.2	2.3	1.2	0.6	0.4	7.3	3.2	1.8	1.2	1.3	6.2	3.3	2.2	1.5	1.6	5.4	3.5	2.4	1.6	1.9	5.2	3.6	2.4	1.6	2	5.2	3.6	2.4	1.6	1.9

scenario 2

	p=0					p=0.01					p=0.05					p=0.10					p=0.20					p=0.50					p=0.75				
truth	1	2	3	4	5	1	2	3	4	5	1	2	3	4	5	1	2	3	4	5	1	2	3	4	5	1	2	3	4	5	1	2	3	4	5
1	8.9	12.7	4.6	1.5	0.6	9.5	12.2	4.5	1.5	0.6	12.9	9.7	3.8	1.4	0.6	14.5	8.8	3.3	1.3	0.5	15.5	8.3	2.9	1.2	0.5	47.1	8.3	4.2	1.6	0.7	16	7.8	2.9	1.2	0.4
2	10.7	15	5.4	1.8	0.7	10.4	14.9	5.5	1.9	0.8	9.8	14.8	5.8	2.2	0.9	9.6	14.7	5.9	2.4	1.0	9.6	14.7	5.8	2.5	1	16	8	2.9	1.1	0.4	10	14.4	5.8	2.4	0.9
3	3.8	5.4	2	0.6	0.3	3.6	5.2	2.1	0.8	0.4	2.9	4.7	2.5	1.3	0.7	2.6	4.5	2.7	1.5	0.8	2.3	4.6	2.8	1.5	0.9	9.8	14.6	5.8	2.4	0.9	2.5	4.5	2.7	1.6	0.9
4	2.3	3.1	1.3	0.4	0.1	2.2	3	1.3	0.5	0.2	1.7	2.6	1.5	0.9	0.6	1.5	2.5	1.6	1.0	0.7	1.4	2.4	1.7	1	0.8	2.4	4.6	2.7	1.6	0.9	1.4	2.4	1.6	1	0.8
5	5.9	8.4	3	1	0.4	5.6	8.1	3.1	1.3	0.7	4.4	6.5	3.6	2.3	2.0	3.7	6.0	3.8	2.8	2.5	3.2	5.7	3.8	2.9	3.1	1.4	2.4	1.6	1.1	0.8	3.4	5.8	3.7	2.8	3.1

scenario 3

	p=0					p=0.01					p=0.05					p=0.10					p=0.20					p=0.50					p=0.75				
truth	1	2	3	4	5	1	2	3	4	5	1	2	3	4	5	1	2	3	4	5	1	2	3	4	5	1	2	3	4	5	1	2	3	4	5
1	0.5	1.9	3	1	0.3	0.6	2	2.9	1	0.3	1.3	2.4	2.1	0.8	0.3	1.6	2.6	1.7	0.7	0.2	1.9	2.7	1.4	0.5	0.2	1.9	2.8	1.3	0.5	0.2	1.9	2.8	1.3	0.5	0.2
2	1.6	6.2	10	3	0.8	1.7	6.4	9.8	2.9	0.8	2.3	8.1	7.9	2.5	0.8	2.7	8.8	7.1	2.2	0.7	3	9.5	6.5	1.9	0.6	3.1	9.9	6.3	1.8	0.5	3	10	6.2	1.8	0.6
3	2.9	10.7	17.2	5	1.4	2.9	10.5	17.1	5.2	1.5	2.9	9.6	17.2	5.9	1.8	2.8	9.4	17.2	6.0	1.9	2.7	9.5	17	6.1	1.9	2.7	10.1	16.7	5.9	1.8	2.8	10.2	16.6	5.8	1.8
4	1.2	4.5	7	2.2	0.6	1.2	4.3	6.8	2.4	0.8	1.1	3.3	6.1	3.4	1.6	1.1	2.9	6.0	3.8	1.9	1	2.6	5.9	3.9	2.1	1	2.7	5.8	4	2.1	1	2.9	5.7	3.9	2.1
5	1.4	5.4	8.6	2.5	0.7	1.4	5.2	8.3	2.7	1.1	1.3	4.0	6.8	3.7	3.0	1.3	3.3	6.2	4.3	3.8	1.2	2.9	5.8	4.5	4.3	1.1	3	5.7	4.4	4.5	1.2	3.2	5.7	4.3	4.4

scenario 4

	p=0					p=0.01					p=0.05					p=0.10					p=0.20					p=0.50					p=0.75				
truth	1	2	3	4	5	1	2	3	4	5	1	2	3	4	5	1	2	3	4	5	1	2	3	4	5	1	2	3	4	5	1	2	3	4	5
1	0.4	0.6	2	2.7	1.1	0.5	0.7	2	2.6	1.1	0.9	1.1	2.1	1.9	0.9	1.1	1.3	2.2	1.5	0.7	1.3	1.5	2.2	1.2	0.6	1.3	1.5	2.3	1.1	0.5	1.3	1.5	2.2	1.2	0.5
2	0.2	0.3	1	1.3	0.5	0.2	0.3	1	1.3	0.5	0.3	0.5	1.1	1.0	0.4	0.4	0.6	1.1	0.8	0.4	0.4	0.6	1.2	0.7	0.3	0.5	0.7	1.1	0.7	0.3	0.5	0.7	1.2	0.7	0.3
3	1.3	1.9	6.8	9	3.6	1.3	2	7	8.7	3.6	1.6	2.5	8.0	7.4	3.1	1.8	2.8	8.6	6.7	2.7	1.9	3.2	8.8	6.3	2.2	2	3.4	8.9	6.2	2	2	3.4	8.9	6.2	2
4	2	2.9	9.9	13	5.3	1.9	2.8	9.7	13.1	5.5	1.9	2.7	8.8	13.5	6.1	1.9	2.6	8.7	13.8	6.1	1.9	2.7	8.6	14	5.9	2	2.8	8.7	13.9	5.6	2	2.9	8.8	13.8	5.5
5	2	3	10.3	13.7	5.4	2	2.9	9.9	13.3	6.2	1.9	2.6	7.6	11.7	10.6	1.9	2.4	6.6	11.2	12.3	1.8	2.3	5.9	11.1	13.2	1.9	2.5	5.8	11	13.2	2	2.6	6.1	11.1	12.7

scenario 5

	p=0					p=0.01					p=0.05					p=0.10					p=0.20					p=0.50					p=0.75				
truth	1	2	3	4	5	1	2	3	4	5	1	2	3	4	5	1	2	3	4	5	1	2	3	4	5	1	2	3	4	5	1	2	3	4	5
1	0.4	0.5	1	1.8	3.1	0.4	0.5	1	1.8	3	0.7	0.8	1.3	1.7	2.1	0.9	1.0	1.5	1.7	1.6	1.1	1.1	1.6	1.7	1.3	1.2	1.2	1.6	1.7	1.1	1.2	1.2	1.6	1.7	1.1
2	0.2	0.2	0.4	0.9	1.5	0.2	0.3	0.5	0.9	1.4	0.3	0.4	0.7	0.9	1.1	0.3	0.4	0.7	1.0	0.8	0.4	0.5	0.8	1	0.7	0.4	0.5	0.8	0.9	0.6	0.4	0.5	0.8	0.9	0.6
3	0.4	0.6	1.2	2.3	3.9	0.4	0.6	1.3	2.3	3.8	0.6	0.8	1.7	2.5	2.8	0.7	1.0	2.0	2.6	2.3	0.8	1.1	2.1	2.6	1.8	0.9	1.2	2.1	2.6	1.7	0.9	1.2	2.1	2.6	1.7
4	1.1	1.3	2.6	5.2	8.7	1.1	1.3	2.6	5.3	8.5	1.2	1.5	3.1	5.9	7.2	1.2	1.6	3.4	6.3	6.4	1.3	1.8	3.5	6.5	5.7	1.4	2	3.7	6.5	5.3	1.4	2	3.7	6.6	5.3
5	3.5	4.5	8.8	17.1	28.8	3.5	4.4	8.6	16.6	29.5	3.4	4.2	7.6	14.1	33.2	3.4	4.0	7.2	13.3	34.6	3.4	4.1	6.9	13.2	35	3.6	4.5	7.1	13.3	34.1	3.6	4.7	7.6	13.6	33.1

Table 5.6: Summary of intra-trial dose allocation, γ=**-2**.

scenario 1

	p=0					p=0.01					p=0.05					p=0.10					p=0.20					p=0.50					p=0.75				
truth	1	2	3	4	5	1	2	3	4	5	1	2	3	4	5	1	2	3	4	5	1	2	3	4	5	1	2	3	4	5	1	2	3	4	5
1	54.5	11.7	4.4	1.6	0.7	54.2	11.8	4.4	1.6	0.7	53.3	12	4.9	1.8	0.8	52.4	12.4	5.2	2	0.8	51.4	12.9	5.5	2.2	0.9	50.6	13	6.2	2.3	0.9	50	13.2	6.4	2.4	0.9
2	12.9	2.8	1.1	0.3	0.2	12.6	2.9	1.1	0.4	0.2	10.8	3.6	1.6	0.7	0.4	9.7	4.1	2	0.9	0.6	8.8	4.5	2.3	1	0.6	8.4	4.5	2.5	1.2	0.7	8.5	4.5	2.5	1.2	0.6
3	4.6	1	0.4	0.1	0	4.5	1.1	0.4	0.2	0.1	3.7	1.3	0.7	0.3	0.2	3.2	1.5	0.8	0.4	0.3	2.8	1.7	0.9	0.5	0.4	2.7	1.6	1	0.5	0.4	2.7	1.7	0.9	0.5	0.4
4	1.4	0.3	0.1	0	0	1.4	0.3	0.1	0.1	0	1.1	0.4	0.2	0.1	0.1	1	0.4	0.2	0.2	0.1	0.8	0.5	0.3	0.2	0.1	0.8	0.5	0.3	0.2	0.2	0.8	0.5	0.3	0.2	0.1
5	1.3	0.3	0.1	0	0	1.3	0.3	0.1	0	0	1.1	0.3	0.2	0.1	0.1	0.9	0.4	0.2	0.1	0.1	0.7	0.4	0.3	0.2	0.1	0.7	0.4	0.3	0.2	0.2	0.7	0.4	0.3	0.2	0.2

scenario 2

	p=0					p=0.01					p=0.05					p=0.10					p=0.20					p=0.50					p=0.75				
truth	1	2	3	4	5	1	2	3	4	5	1	2	3	4	5	1	2	3	4	5	1	2	3	4	5	1	2	3	4	5	1	2	3	4	5
1	3	6	2.5	0.8	0.3	3	6	2.5	0.8	0.3	4	5.3	2.2	0.8	0.3	4.8	4.8	2	0.7	0.3	5.6	4.4	1.7	0.7	0.3	5.9	4.2	1.6	0.7	0.2	5.8	4.1	1.7	0.8	0.3
2	14.1	28.7	12.2	3.8	1.6	14.1	28.6	12.2	3.8	1.6	14.2	27.8	12.2	4.3	1.7	14.3	27.6	12.1	4.5	1.8	14.6	27.2	11.8	4.8	1.8	15.3	26.4	11.9	5	1.7	15.8	25.9	11.8	5.1	1.6
3	4.1	8.1	3.5	1.1	0.4	4.1	8	3.5	1.1	0.4	3.7	7.3	3.8	1.6	0.8	3.3	6.8	4.1	2	1	2.9	6.5	4.2	2.4	1.2	3	6.4	4.1	2.5	1.3	3.2	6.4	4.1	2.4	1.2
4	1.5	3	1.2	0.4	0.2	1.5	2.9	1.3	0.4	0.2	1.3	2.6	1.3	0.6	0.4	1.2	2.4	1.4	0.7	0.6	1	2.2	1.4	0.9	0.7	1	2.1	1.4	1	0.7	1.1	2.1	1.3	1	0.7
5	0.9	1.7	0.7	0.2	0.1	0.9	1.7	0.7	0.2	0.1	0.8	1.5	0.8	0.4	0.3	0.7	1.3	0.8	0.5	0.4	0.6	1.2	0.8	0.6	0.5	0.6	1.1	0.8	0.6	0.5	0.6	1.1	0.8	0.6	0.5

scenario 3

	p=0					p=0.01					p=0.05					p=0.10					p=0.20					p=0.50					p=0.75				
truth	1	2	3	4	5	1	2	3	4	5	1	2	3	4	5	1	2	3	4	5	1	2	3	4	5	1	2	3	4	5	1	2	3	4	5
1	0	0	0.1	0	0	0	0	0.1	0	0	0	0	0.1	0	0	0	0	0.1	0	0	0	0.1	0	0	0	0	0.1	0	0	0	0	0.1	0	0	0
2	0.6	2.8	6.2	2.2	0.6	0.7	2.8	6.2	2.2	0.6	0.9	3.6	5.4	2	0.6	1.1	4.2	4.9	1.8	0.5	1.3	4.7	4.4	1.5	0.5	1.4	5	4.2	1.4	0.4	1.4	4.9	4.2	1.5	0.5
3	3.4	14.9	33	11.8	3.1	3.4	14.9	32.9	11.9	3.1	3.5	14.8	32.1	12.3	3.4	3.6	14.7	31.8	12.5	3.6	3.6	14.8	31.8	12.3	3.6	3.9	16	30.8	12	3.4	3.9	16.4	30.7	11.8	3.3
4	0.9	4	8.7	3.1	0.8	0.9	4	8.7	3.1	0.9	0.9	3.6	7.7	3.8	1.6	0.8	3.1	7.2	4.4	2	0.8	2.6	6.9	4.8	2.5	0.9	2.7	6.7	4.8	2.5	0.9	3	6.7	4.6	2.3
5	0.2	0.9	1.8	0.6	0.2	0.2	0.8	1.8	0.6	0.2	0.2	0.8	1.6	0.7	0.4	0.2	0.7	1.4	0.8	0.6	0.2	0.5	1.3	0.9	0.7	0.2	0.6	1.2	1	0.8	0.2	0.7	1.2	0.9	0.7

scenario 4

	p=0					p=0.01					p=0.05					p=0.10					p=0.20					p=0.50					p=0.75				
truth	1	2	3	4	5	1	2	3	4	5	1	2	3	4	5	1	2	3	4	5	1	2	3	4	5	1	2	3	4	5	1	2	3	4	5
1	0	0	0	0.1	0	0	0	0	0.1	0	0	0	0	0.1	0	0	0	0	0.1	0	0	0	0.1	0	0	0	0	0.1	0	0	0	0	0.1	0	0
2	0	0	0.1	0.2	0.1	0	0	0.1	0.2	0.1	0	0	0.1	0.1	0.1	0	0	0.2	0.1	0.1	0.1	0.1	0.2	0.1	0.1	0.1	0.1	0.2	0.1	0	0.1	0.1	0.2	0.1	0.1
3	0.7	1	4.4	8	3.7	0.7	1	4.4	7.9	3.6	0.8	1.3	5	7.1	3.4	1	1.6	5.7	6.5	2.9	1.1	1.9	6.1	6.2	2.4	1.3	2.1	6.5	5.9	2	1.3	2.1	6.4	5.8	2
4	2.6	3.6	14.5	27.1	12.7	2.6	3.6	14.5	27.1	12.8	2.6	3.6	14.2	26.8	13.4	2.6	3.6	13.9	27.1	13.3	2.7	3.8	13.7	27.2	13.1	3.1	4.2	14.5	26.9	11.8	3.2	4.3	15.2	26.5	11.2
5	0.9	1.2	5.3	9.5	4.4	0.9	1.2	5.2	9.4	4.5	0.9	1.2	4.6	8.5	6	0.9	1.2	4	8	7.2	0.9	1.1	3.5	7.6	8.2	1	1.2	3.5	7.6	7.9	1	1.4	3.9	7.6	7.4

scenario 5

	p=0					p=0.01					p=0.05					p=0.10					p=0.20					p=0.50					p=0.75				
truth	1	2	3	4	5	1	2	3	4	5	1	2	3	4	5	1	2	3	4	5	1	2	3	4	5	1	2	3	4	5	1	2	3	4	5
1	0	0	0	0	0.1	0	0	0	0	0.1	0	0	0	0	0.1	0	0	0	0	0.1	0	0	0	0	0	0	0	0	0	0	0	0	0	0	0
2	0	0	0	0.1	0.3	0	0	0.1	0.1	0.3	0	0	0.1	0.1	0.2	0	0	0.1	0.1	0.2	0.1	0	0.1	0.1	0.1	0.1	0	0.1	0.1	0.1	0.1	0	0.1	0.1	0.1
3	0.2	0.1	0.3	0.7	1.8	0.2	0.1	0.3	0.7	1.8	0.2	0.2	0.4	0.8	1.6	0.2	0.2	0.5	0.9	1.3	0.3	0.3	0.6	1	1	0.3	0.4	0.6	1	0.8	0.3	0.4	0.6	1	0.8
4	0.9	1.1	2.2	5	13.1	0.9	1.1	2.3	5	13	1	1.2	2.8	5.8	11.6	1.1	1.4	3.2	6.4	10.3	1.2	1.7	3.5	7	8.9	1.4	1.9	3.8	7.4	7.8	1.4	2	3.8	7.5	7.7
5	3.1	3.7	7.3	16.6	43.3	3.1	3.7	7.2	16.4	43.5	3.1	3.7	7.1	15.8	44.2	3.1	3.7	7	15.4	44.7	3.2	3.8	7.1	15.4	44.4	3.5	4.4	7.5	16.7	41.7	3.7	4.6	8.1	17.8	39.7

Table 5.7: Summary of intra-trial dose allocation, γ=**0**.

scenario 1

	p=0					p=0.01					p=0.05					p=0.10					p=0.20					p=0.50					p=0.75				
truth	1	2	3	4	5	1	2	3	4	5	1	2	3	4	5	1	2	3	4	5	1	2	3	4	5	1	2	3	4	5	1	2	3	4	5
1	71.2	18.7	7.0	2.3	0.9	71.2	18.7	7.0	2.3	0.9	70.6	18.9	7.2	2.4	0.9	69.6	19.2	7.7	2.6	1.0	67.7	19.9	8.4	2.9	1.1	64.4	21.1	10.1	3.4	1.1	62.3	21.8	11.0	3.7	1.2

scenario 2

	p=0					p=0.01					p=0.05					p=0.10					p=0.20					p=0.50					p=0.75				
truth	1	2	3	4	5	1	2	3	4	5	1	2	3	4	5	1	2	3	4	5	1	2	3	4	5	1	2	3	4	5	1	2	3	4	5
2	21.0	47.5	22.4	6.8	2.4	21.0	47.5	22.4	6.8	2.4	21.1	47.0	22.4	7.0	2.5	21.3	46.3	22.3	7.4	2.7	21.5	45.7	21.9	8.0	2.9	22.6	44.2	21.4	8.9	2.9	23.3	42.5	21.8	9.5	3.0

scenario 3

	p=0					p=0.01					p=0.05					p=0.10					p=0.20					p=0.50					p=0.75				
truth	1	2	3	4	5	1	2	3	4	5	1	2	3	4	5	1	2	3	4	5	1	2	3	4	5	1	2	3	4	5	1	2	3	4	5
3	4.6	19.8	51.2	19.5	4.9	4.6	19.8	51.1	19.5	4.9	4.7	19.9	50.7	19.7	5.1	4.7	20.0	50.0	19.9	5.3	4.8	20.2	49.1	20.2	5.6	5.2	21.3	48.0	20.0	5.4	5.5	22.2	47.0	20.0	5.4

scenario 4

	p=0					p=0.01					p=0.05					p=0.10					p=0.20					p=0.50					p=0.75				
truth	1	2	3	4	5	1	2	3	4	5	1	2	3	4	5	1	2	3	4	5	1	2	3	4	5	1	2	3	4	5	1	2	3	4	5
4	3.8	5.1	21.6	46.4	23.1	3.8	5.1	21.6	46.4	23.1	3.8	5.1	21.8	46.0	23.3	3.9	5.2	21.7	45.8	23.3	4.0	5.4	21.7	46.2	22.6	4.5	6.1	23.5	45.6	20.3	4.7	6.5	24.5	45.4	18.9

scenario 5

	p=0					p=0.01					p=0.05					p=0.10					p=0.20					p=0.50					p=0.75				
truth	1	2	3	4	5	1	2	3	4	5	1	2	3	4	5	1	2	3	4	5	1	2	3	4	5	1	2	3	4	5	1	2	3	4	5
5	3.8	4.3	8.1	19.7	64.2	3.8	4.3	8.1	19.7	64.2	3.8	4.3	8.2	19.8	64.0	3.8	4.3	8.4	20.1	63.3	3.9	4.5	8.9	21.3	61.4	4.4	5.4	9.8	24.4	56.1	4.6	5.7	10.4	26.3	52.9

Table 5.8: Summary of intra-trial dose allocation across scenarios.

	true γ=-4																	
	p=0			p=0.01			p=0.05			p=0.10			p=0.20			p=0.50			p=0.75		
Scenarios	correct	over	under	correct	over	under	correct	over	under	correct	over	under	correct	over	under	correct	over	under	correct	over	under
1	50.9	14.4	34.7	51.4	15.7	32.9	52.8	17.8	29.5	53.3	18.5	28.1	53.7	19.1	27.2	53.6	19.5	26.9	53.3	19.7	27.0
2	26.7	28.4	44.9	27.7	28.5	43.8	33.2	26.9	39.9	35.4	26.1	38.5	37.0	25.4	37.6	37.6	24.8	37.7	37.2	24.7	38.1
3	26.8	27.1	46.0	27.7	27.2	45.1	33.0	25.9	41.1	35.2	25.0	39.8	36.7	24.2	39.2	37.1	23.2	39.7	36.8	23.2	40.0
4	25.9	27.0	47.1	27.1	26.8	46.1	33.4	25.0	41.6	36.3	23.5	40.1	37.9	22.2	40.0	38.0	21.3	40.7	37.4	21.2	41.4
5	35.9	24.1	40.0	36.8	23.8	39.4	42.0	21.2	36.8	44.2	19.6	36.2	45.2	18.3	36.5	44.5	17.5	38.1	43.5	17.4	39.1
Average	33.2	24.2	42.6	34.1	24.4	41.5	38.9	23.4	37.8	40.9	22.5	36.5	42.1	21.8	36.1	42.1	21.2	36.6	41.6	21.2	37.1
	true γ=-2																	
	p=0			p=0.01			p=0.05			p=0.10			p=0.20			p=0.50			p=0.75		
Scenarios	correct	over	under	correct	over	under	correct	over	under	correct	over	under	correct	over	under	correct	over	under	correct	over	under
1	57.7	20.2	22.1	57.7	20.6	21.7	57.8	23.0	19.2	57.6	24.8	17.6	57.1	26.5	16.4	56.5	27.7	15.9	55.8	28.2	16.0
2	35.6	28.8	35.6	35.6	28.9	35.5	36.4	29.8	33.8	37.6	29.9	32.6	38.5	29.8	31.7	37.9	29.8	32.3	37.3	29.6	33.1
3	39.1	24.8	36.1	39.1	25.0	36.0	40.0	25.5	34.6	41.0	25.5	33.5	42.0	25.0	32.9	41.4	24.1	34.5	41.0	23.7	35.3
4	35.9	24.9	39.3	36.0	24.9	39.1	37.8	24.4	37.8	40.0	23.3	36.7	41.6	22.1	36.3	41.4	20.1	38.5	40.4	19.6	40.0
5	48.6	16.3	35.1	48.8	16.2	35.0	50.4	14.4	35.1	51.7	13.0	35.3	52.1	11.4	36.5	49.9	10.1	40.0	47.9	10.1	42.1
Average	43.4	23.0	33.6	43.4	23.1	33.5	44.5	23.4	32.1	45.5	23.3	31.2	46.3	23.0	30.8	45.4	22.3	32.2	44.5	22.2	33.3
	true γ=0																	
	p=0			p=0.01			p=0.05			p=0.10			p=0.20			p=0.50			p=0.75		
Scenarios	correct	over	under	correct	over	under	correct	over	under	correct	over	under	correct	over	under	correct	over	under	correct	over	under
1	71.2	28.8	0.0	71.2	28.8	0.0	70.6	29.4	0.0	69.6	30.4	0.0	67.7	32.3	0.0	64.4	35.6	0.0	62.3	37.7	0.0
2	47.5	31.5	21.0	47.5	31.5	21.0	47.0	31.9	21.1	46.3	32.3	21.3	45.7	32.8	21.5	44.2	33.3	22.6	42.5	34.2	23.3
3	51.2	24.4	24.4	51.1	24.4	24.4	50.7	24.8	24.5	50.0	25.3	24.8	49.1	25.8	25.0	48.0	25.5	26.5	47.0	25.4	27.6
4	46.4	23.1	30.6	46.4	23.1	30.6	46.0	23.3	30.7	45.8	23.3	30.8	46.2	22.6	31.2	45.6	20.3	34.1	45.4	18.9	35.7
5	64.2	0.0	35.8	64.2	0.0	35.8	64.0	0.0	36.0	63.3	0.0	36.7	61.4	0.0	38.6	56.1	0.0	43.9	52.9	0.0	47.1
Average	56.1	21.6	22.4	56.1	21.6	22.4	55.6	21.9	22.5	55.0	22.3	22.7	54.0	22.7	23.3	51.7	22.9	25.4	50.0	23.2	26.7

Dosing accuracy based on the final model estimate: As an end product of the phase I dose finding trial, the dosing algorithm and its accuracy in predicting the dose assignment of a future patient is of most interest. In the end of a risk-adjusting design, the $K+1$-parameter model will be fitted on all patients enrolled in the entire trial to obtain the final model estimate $\hat{\alpha}_k$ and $\hat{\gamma}$. Covariate-toxicity curves can be constructed using these estimates and used to guide the dose assignment for future patients. A map can also be generated between covariate value and the corresponding risk-adjusted MTD using the same dosing algorithm described in the earlier sections. On the x-axis of this map, covariate z is divided into consecutive intervals, with each interval corresponding to an assigned dose level. There are up to K consecutive intervals: and their corresponding MTDs are $1, \ldots, K$ respectively. Similar map and covariate intervals can be obtained based on the γ and α_k's values specified in the true scenarios (right hand side graphs in Figures 5.4, 5.5, and 5.6: Oftentimes these two sets of intervals do not align with each other perfectly. An extreme case would be the design regards all patients exchangeable and recommends a common MTD in the end, whereas these patients should have received different MTD's according to their individual risk levels, or vice versa. We further compare the dosing intervals at the end of each simulated trial with the dosing intervals under the true scenarios, and define the correct, over and under dosing intervals to be the covariate regions where the estimated risk-adjusted MTD is the same as, above or below the true MTD. We use $\mathcal{C}$,$\mathcal{O}$, and $\mathcal{U}$ to represent the union of the intervals on the real line that falls in one of the three categories. $\mathcal{C} = \{z : \hat{x}(z) = x(z)\} = \cup_{k=1}^{K}\{z : \hat{x}(z) = x(z) = k\}$, $\mathcal{O} = \{z : \hat{x}(z) > x(z)\}$, and $\mathcal{U} = \{z : \hat{x}(z) < x(z)\}$. $\hat{x}(z)$ indicates the estimated MTD at covariate z based on the model and $x(z)$ indicates the true MTD at covariate z based on the true scenario. The probabilities of correct dosing, under dosing and over dosing can be calculated as the total sampling probabilities over each of these three sets of intervals on the real line.

Since we use normal distribution with mean $z_0 = 3.45$ and standard deviation

$\sigma = 0.31$ to simulate the covariate z, this is also the sampling distribution in the probability calculation.

$$Prob_{correct} = \int_{\mathcal{C}} \frac{1}{\sigma\sqrt{2\pi}} \exp^{-\frac{(z-z_0)^2}{2\sigma^2}} \, \mathrm{d}z$$

$$Prob_{over} = \int_{\mathcal{O}} \frac{1}{\sigma\sqrt{2\pi}} \exp^{-\frac{(z-z_0)^2}{2\sigma^2}} \, \mathrm{d}z$$

$$Prob_{under} = \int_{\mathcal{U}} \frac{1}{\sigma\sqrt{2\pi}} \exp^{-\frac{(z-z_0)^2}{2\sigma^2}} \, \mathrm{d}z$$

We further average the probabilities over K toxicity scenarios to obtain an average performance in terms of correct dosing, over dosing and under dosing for each true γ value and design parameter p threshold. The average performance is listed at the bottom of the table 5.9. Note that the sum of the three probabilities is 1. The three summary probabilities are plotted against the p value threshold in Figure 5.7. In the top left graph, the correct dosing probabilities are plotted against the p value threshold from 0 to 0.75, with each line representing a different true γ value. The graphs for over dosing probabilities and under dosing probabilities are generated in a similar manner. As demonstrated in the graph, when there is a very strong risk effect ($\gamma = -4$), the correct dosing probability increases from 38.2% using the conventional design (p=0) to 56.5% using the risk adjusting design with p value threshold 0.10, representing a 48% relative increase in correct dosing. As the p value continues to increase, the correct dosing accuracy plateaus and remains at a high level. The similar gain in correct dosing probability is also observed when there is a relatively strong risk effect ($\gamma = -2$), that the probability increases from 54% using conventional design (p=0) to 59.8% using risk-adjusting design with p value 0.10, representing a 11% relative increase. On the contrary, when there is no risk effect ($\gamma = 0$), the conventional design is the most suitable design and yields the highest accuracy with correct dosing probability 74%, and this probability tend to decline slowly as p threshold increases as more trials would enter the risk-adjusting stage by chance.

These graphs may be used to guide the choice of the design parameters if such risk-adjusting design is of consideration. For example, to conduct a trial to identify the individual MTD for patients treated with irinotecan, we probably can choose a design with p threshold around 0.10 as it yields the highest correct dosing probability under both true scenarios with strong risk effects. Meanwhile, even if the baseline clearance level turns out not to relate with the toxicity outcome as much as expected, using the risk-adjusting design suffers minor loss in dosing accuracy compared to the conventional design as the probability of correct dosing only decreases from 74% to 71.7%, a roughly 2.3% decrease.

The rest of the graphs suggests that the risk-adjusting design not only increases correct dosing probability, but also decreases both over dosing and under dosing simultaneously, when there is true risk effect. Therefore the risk adjusting design effectively increases the dosing accuracy by correctly allocating the patients to their respective MTD according to their individual risk level.

Table 5.9: Summary of dosing accuracy based on the final model estimate.

true $\gamma = -4$	p=0			p=0.01			p=0.05			p=0.10			p=0.20			p=0.50			p=0.75		
Scenarios	correct	over	under	correct	over	under	correct	over	under	correct	over	under	correct	over	under	correct	over	under	correct	over	under
1	57.9	5.2	36.9	60.9	10.9	28.2	63.2	11.7	25.1	63.4	11.8	24.8	63.5	11.8	24.7	63.4	11.5	25.1	63.3	11.5	25.2
2	29.7	26.1	44.2	39.4	24.1	36.5	50.3	18.8	30.9	51.4	17.4	31.2	51.8	16.6	31.6	51.3	15.6	33	50.8	15.5	33.7
3	31.4	26.1	42.5	39.4	25.1	35.5	50.9	18.9	30.2	51.9	17.6	30.5	51.9	16.5	31.6	50.7	15.7	33.7	50.1	15.5	34.4
4	29.1	27.5	43.4	39.9	25.6	34.5	53.3	19	27.8	54.3	17.1	28.6	53.2	16	30.8	51.8	15.5	32.7	51	15.4	33.6
5	43.1	28.7	28.2	51.3	25.3	23.4	61.6	18	20.4	61.5	16.5	22	60.2	15.4	24.5	57.9	14.8	27.3	56.8	14.8	28.5
Average	38.2	22.7	39.0	46.2	22.2	31.6	55.8	17.3	26.9	56.5	16.1	27.4	56.1	15.2	28.6	55.0	14.6	30.4	54.4	14.5	31.1
	true $\gamma = -2$																				
	p=0			p=0.01			p=0.05			p=0.10			p=0.20			p=0.50			p=0.75		
Scenarios	correct	over	under	correct	over	under	correct	over	under	correct	over	under	correct	over	under	correct	over	under	correct	over	under
1	65.8	9.3	24.9	65.6	11.9	22.5	67	15.3	17.7	67.4	16.2	16.4	67	17.3	15.8	66	18.2	15.8	65.7	18.4	15.9
2	45.2	22.4	32.4	45.6	23.4	31	48.9	24	27.1	51	23.2	25.8	51	22.6	26.4	49	21.8	29.2	47.7	21.6	30.7
3	51.4	19.1	29.5	51.5	19.9	28.6	54.5	19.6	25.9	56.4	18.6	25	57.3	17.3	25.4	54.1	16.6	29.3	53	16.1	30.9
4	46.7	22.7	30.6	47.9	22.8	29.3	54.3	19.5	26.2	57.1	17	25.9	57.5	15.4	27.1	55.1	14.1	30.8	53.7	13.8	32.6
5	60.8	20.6	18.7	62.1	19.3	18.6	65.8	14	20.1	67.2	11.7	21.1	66.1	10.2	23.7	61.8	9.1	29.1	59.6	8.9	31.5
Average	54.0	18.8	27.2	54.5	19.4	26.0	58.1	18.5	23.4	59.8	17.3	22.9	59.8	16.5	23.7	57.2	16.0	26.8	55.9	15.8	28.3
	true $\gamma = 0$																				
	p=0			p=0.01			p=0.05			p=0.10			p=0.20			p=0.50			p=0.75		
Scenarios	correct	over	under	correct	over	under	correct	over	under	correct	over	under	correct	over	under	correct	over	under	correct	over	under
1	82.2	17.7	0	82.1	17.9	0	80.7	19.3	0	79.9	20.1	0	77.7	22.3	0	73.7	26.3	0	71.7	28.3	0
2	66	22.4	11.5	65.8	22.6	11.6	64.3	23.4	12.3	63.2	24	12.9	62.6	24.1	13.3	57.7	25.5	16.8	54.5	26.4	19.1
3	71.7	15	13.2	71.6	15.1	13.3	70.4	15.6	14	69.3	16.1	14.6	68.5	16.5	14.9	65.4	15.9	18.6	61.9	16.8	21.3
4	68.2	15.3	16.4	68.2	15.3	16.5	67.2	15.7	17.2	67	15.3	17.7	66.7	14.6	18.7	63.4	12.4	24.1	61.6	11.4	26.9
5	81.6	0	18.4	81.6	0	18.4	80.3	0	19.7	79	0	21	75.7	0	24.3	67.3	0	32.7	63	0	37
Average	74.0	14.1	11.9	73.8	14.2	12.0	72.6	14.8	12.6	71.7	15.1	13.2	70.2	15.5	14.2	65.5	16.0	18.4	62.5	16.6	20.9

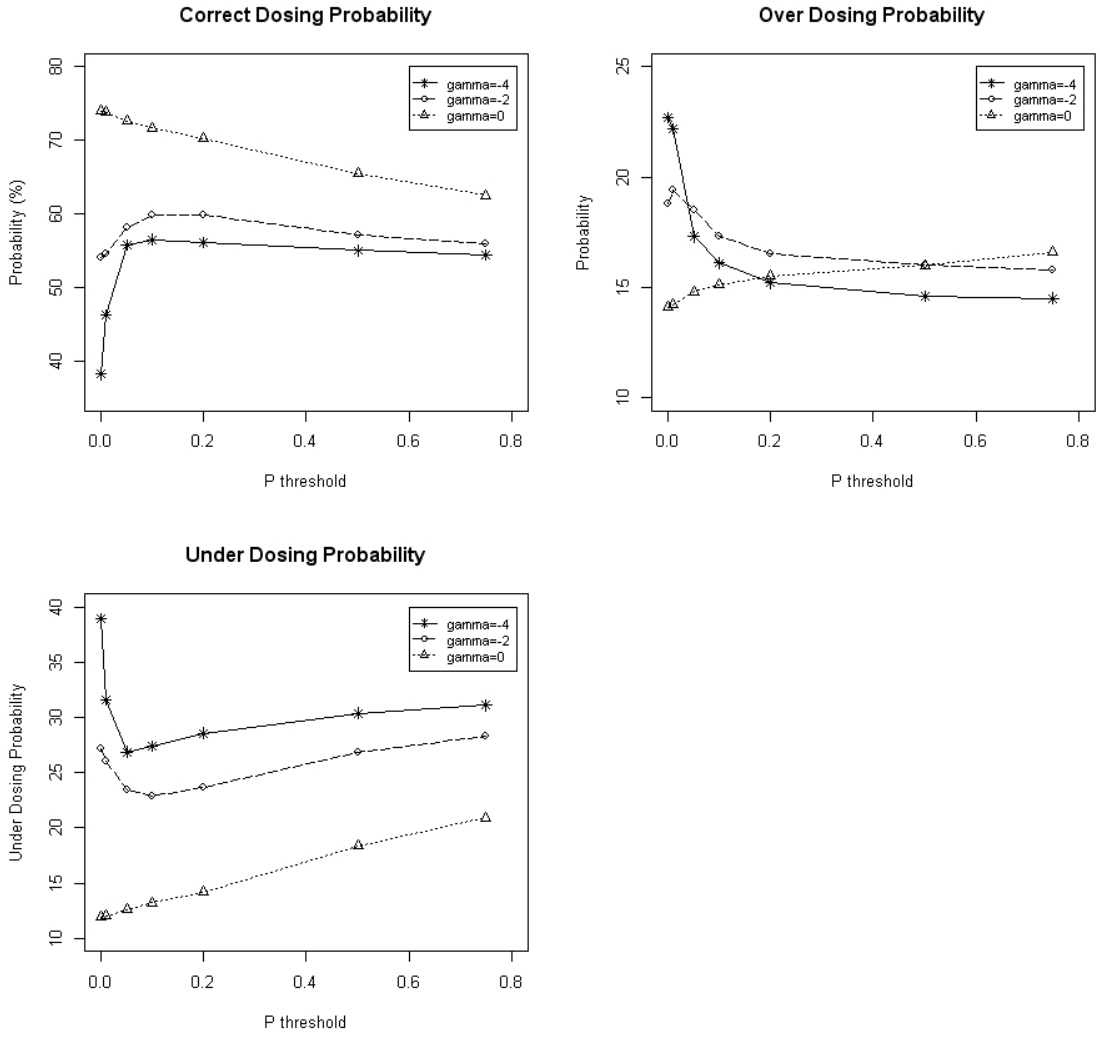

Figure 5.7: Correct, over and under dosing probabilities based on the final model estimate.

Chapter 6

Conclusions and Discussions

This dissertation undertook tasks to address two different but related topics for model based sequential design for dose-finding. First we developed a theoretical framework to build a two-stage likelihood CRM. Such design addresses the ethical concerns on the overly aggressive dose escalation at beginning of the trial of conventional one-stage Bayesian CRM design by pre-specifying sufficient number of patients are tested on lower dose levels. While it is desirable to escalate slowly to not overshoot the target dose level, overly conservative escalation will cause incoherent dose escalation upon transition into the model based design, i.e., the first model based dose assignment upon observing the first DLT will continue to escalate despite the previous patient has already experienced a toxicity at a lower dose level. To guard against such unethical dose escalation, we propose using the most conservative and coherent design, and proved the unique existence of the most conservative and coherent initial design. In practice, however, we do not always have to use the most conservative and coherent initial design. Rather, it can be used as a starting point and further pruned according to sample size constraint.

In the second topic, building upon the likelihood CRM design, we proposed a multi-stage design using a semi-parametric model to incorporate an external risk factor and identify patient specific MTD. The design uses likelihood method which is

computationally economical and easy to implement. The design allows the flexibility of using conventional CRM to identify a common MTD for homogeneous patient population when there is lack of risk effect, and switches into risk-adjusting design when risk effect is sufficient. While developed for the situations with continuous risk factor and discrete doses, the method can be easily generalized for categorical risk factor and continuous dose. The method was illustrated and compared with the conventional CRM design for homogeneous study population under various simulated scenarios. In the future, more evaluations will be conducted to compare our design to the existing methods for dose-finding studies with patient heterogeneity [21; 22; 14]. In addition, further study on the theoretical property of the proposed method is also warranted.

Bibliography

[1] Miriam Ayer, H.D.Brunk, G.M.Ewing, W.T. Reid, and Edward Silverman. An empirical distribution function for sampling with incomplete information. *The Annals of Mathematical Statistics*, 26(4):641–647, December 1955.

[2] James Babb, Andre Rogatko, and Shelemyahu Zacks. Cancer phase i clinical trials: Efficient dose escalation with overdose control. *Statistics in Medicine*, 17(10):1103–1120, May 1998.

[3] James S. Babb and Andre Rogatko. Patient specific dosing in a cancer phase i clinical trial. *Statistics in Medicine*, 20(14):2079–2090, July 2001.

[4] N.E. Breslow and N.E.Day. *Statistical Methods in Cancer Research Volumn 1- The Analysis of Case-control Studies*. World Health Organization, 1986.

[5] Ying Kuen Cheung. On the use of nonparametric curves in phase i trials with low toxicity tolerance. *Biometrics*, 58(1):237–240, March 2002.

[6] Ying Kuen Cheung. Coherence principles in dose-finding studies. *Biometrika*, 92(4):863–873, December 2005.

[7] Ying Kuen Cheung. *Dose Finding by the Continual Reassessment Method*. Chapman & Hall/CRC, boca Raton, Florida, 2011.

[8] Ying Kuen Cheung and Richard Chappell. A simple technique to evaluate model sensitivity in the continual reassessment method. *Biometrics*, 58(3):671–674, September 2002.

[9] Sylvie Chevret. The continual reassessment method in cancer phase i clinical trials: A simulation study. *Statistics in Medicine*, 12(12):1093–1108, June 1993.

[10] Mitchell S.V. Elkind, Ralph L, Sacco, Robert B. MacArthur, Daniel J. Fink, Ellinor Peerschke, Howard Andrews, Greg Neils, Josh Stillman, Tania Corporan, Dana Leifer, and Ken Cheung. The neuroprotection with statin therapy for acute recovery trials (neustart): an adaptive design phase i dose-escalation study of high-dose lovastatin in acute ischemic stroke. *Internaional Journal of Stroke*, 3(3):210–218, August 2008.

[11] Douglas Faries. Practical modifications of the continual reassessment method for phase i cancer clinical trials. *Journal of Biopharmaceutical Statistics*, 4(2):147–164, July 1994.

[12] Elizabeth Garrett-Mayer. The continual reassessment method for dose-finding studies: A tutorial. *Clinical Trials*, 3(1):57–71, February 2006.

[13] Steve N. Goodman, Marianna L. Zahurak, and Steven Piantadosi. Some practical improvements in the continual reassessment method for phase i studies. *Statistics in Medicine*, 14(11):1149–1161, June 1995.

[14] Anastasia Ivanova and Kai Wang. Bivariate isotonic design for dose-finding with ordered groups. *Journal of Biopharmaceutical Statistics*, 25(12):2018–2026, June 2006.

[15] Edward L. Korn, Douglas Midthune, T.Timothey Chen, Lawrence V. Rubinstein, Michaele C. Christian, and Richard M. Simon. A comparison of two phase i trial designs. *Statistics in Medicine*, 13(18):1799–1806, September 1994.

[16] Shing M Lee and Ying Kuen Cheung. Model calibration in the continual reassessment method. *Clinical Trials*, 6(3):227–238, June 2009.

[17] Shing M Lee and Ying Kuen Cheung. Calibration of prior variance in the bayesian continual reassessment method. *Statistics in Medicine*, 30(17):2081–2089, July 2011.

[18] Susanne Moller. An extension of the continual reassessment methods using a preliminary up-and-down design in a dose fiding study in cancer patients, in order to investigate a greater range of doses. *Statistics in Medicine*, 14(9):911–922, May 1995.

[19] John O'Quigley and Xavier Paoletti. Continual reassessment method for ordered groups. *Biometrics*, 59(2):430–440, June 2003.

[20] John O'Quigley, Margaret Pepe, and Lloyd Fisher. Continual reassessment method: A practical design for phase i clinical trials in cancer. *Biometrics*, 46:33–48, March 1990.

[21] John O'Quigley and Larry Z. Shen. Continual reassessment method" a likelihood approach. *Biometrics*, 52(2):673–684, June 1996.

[22] John O'Quigley, Larry Z. Shen, and Anthony Gamst. Two-sample continual reassessment method. *Journal of Biopharmaceutical Statistics*, 9(1):17–44, March 1999.

[23] Steven Piantadosi and Guanghan Liu. Improved designs for dose escalation studies using pharmacokinetic measurements. *Statistics in Medicine*, 15(15):1605–1618, August 1996.

[24] Mark J. Ratain, Deborah Collyar, Barton A. Kamen, Elizabeth Eisenhauer, Theodore Steven Lawrence, Carolyn Runowicz, Sam Turner, and james

L. Wade III. Critical role of phase i clinical trials in cancer treatment. *Journal of Clinical Oncology*, 24(1):206–208, January 1996.

[25] Andrew Rogatko, James S. Babb, Hao Wang, Michael J. Slifker, and Gary R. Hudes. Patient characteristics compete with dose as predictors of acute treatment toxicity in early phase clinical trials. *Clinical Cancer Research*, 10(14):4645–4651, July 2004.

[26] Daniela D. Rosa, John Harris, and Gordon C. Jayson. The best guess approach to phase i trial design. *Journal of Clinical Oncology*, 24(1):206–208, January 2006.

[27] Larry Z. Shen and John O'Quigley. Consistency of continual reassessment method under model misspecification. *Biometrika*, 83(2):395–405, June 1996.

[28] Barry E. Storer. Design and analaysis of phase i clinical trials. *Biometrics*, 45(3):925–937, September 1989.

[29] Peter F. Thall, Hoang Q. Nguyen, and Elihu H. Estey. Patient-specific dose finding based on bivariate outcomes and covariates. *Biometrics*, 64(4):1126–1136, December 2008.

[30] Jessica M. van der Bol, Ron H.J. Mathijssen, Geert-Jan M. Creemers, Andre S. Th. Planting, Walter J. Loos, A.C. Wiemer Erik, Lena E. Friberg, Jaap Verweij, Alex Sparreboom, and Floris A. de Jong. A cyp3a4 phenotype-based dosing algorithm for individualized treatment of irinotecan. *Clinical Cancer Research*, 16(2):736–742, January 2010.

[31] Guosheng Yin and Ying Yuan. Bayesian model averaging continual reassessment method in phase i clinical trials. *Journal of the American Statistical Association*, 104(487):954–968, September 2009.